



PB96-143961

**NTIS**  
Information is our business.

---

---

# CONSTRUCTION RELATED VIBRATIONS FIELD VERIFICATION OF VIBRATION INDUCED SETTLEMENT MODEL

NORTH CAROLINA STATE UNIV. AT RALEIGH

DEC 95



U.S. DEPARTMENT OF COMMERCE  
National Technical Information Service

---


PB96-143961



**CONSTRUCTION RELATED  
VIBRATIONS: FIELD VERIFICATION  
OF VIBRATION INDUCED  
SETTLEMENT MODEL**

by

**Roy H. Borden  
Lisheng Shao**

1. Report No. FHWA/NC/95-008		2. <b>P896-143961</b> 		3. Recipient's Catalog No.	
4. Title and Subtitle Construction Related Vibrations: Field Verification of Vibration Induced Settlement Model				5. Report Date December 1995	
				6. Performing Organization Code	
7. Author(s) Roy H. Borden and Lisheng Shao				8. Performing Organization Report No.	
9. Performing Organization Name and Address Center for Transportation Engineering Studies Department of Civil Engineering North Carolina State University Raleigh, NC 27695				10. Work Unit No. (TRAVIS)	
				11. Contract or Grant No. 23241-95-5	
12. Sponsoring Agency Name and Address North Carolina Department of Transportation Raleigh, NC 27611 Federal Highway Administration Raleigh, NC 27611				13. Type of Report and Period Covered Final Report July 1, 1994-June 30, 1995	
				14. Sponsoring Agency Code	
15. Supplementary Notes					
16. Abstract  <p>The objective of this research is to provide field verification of an analytical model for predicting ground surface settlement due to construction induced vibration. This model was proposed by Borden, Shao, and Gupta in the report "Construction Induced Vibrations" (1994) to NCDOT and FHWA.</p> <p>Three test sites with residual soil profile were investigated. At one of the sites, in Selma, North Carolina, both settlement of the residual soil profile and the characteristics of the vibration source, and the wave propagation behavior were monitored during pile driving. Laboratory resonant column and torsional shear tests were performed on samples obtained from the field test site. Based on a comparison between the measured field settlement at this site and that predicted based on laboratory test results, the proposed analytical model is shown to be somewhat conservative.</p> <p>Vibration attenuation with depth in the residual soil profile was investigated for the first time. The vibration time histories of the field test were analyzed and the peak velocities at various depths and surface distances were obtained. In addition, the ground vibration frequency and Rayleigh wave velocity were calculated. The Rayleigh wave attenuation function in the soil profile agreed well with the field tests records. The approach to evaluate the wave attenuation on the ground surface was confirmed to be conservative.</p>					
17. Key Words Construction vibrations, settlement, densification, cyclic loads, shear modulus, damping ratio, shear strain amplitude			18. Distribution Statement		
19. Security Classif. (of this report) Unclassified		20. Security Classif. (of this page) Unclassified		21. No. of Pages 197	22. Price

**CONSTRUCTION RELATED VIBRATIONS:  
FIELD VERIFICATION OF VIBRATION INDUCED  
SETTLEMENT MODEL**

by

**Roy H. Borden**

Professor

**Lisheng Shao**

Graduate Research Assistant

Department of Civil Engineering  
North Carolina State University

in Cooperation with  
The North Carolina Department of Transportation  
and  
The Institute for Transportation Research and Education

Center for Transportation Engineering Studies  
North Carolina State University  
Raleigh, North Carolina

December, 1995

PROTECTED UNDER INTERNATIONAL COPYRIGHT  
ALL RIGHTS RESERVED.  
NATIONAL TECHNICAL INFORMATION SERVICE  
U.S. DEPARTMENT OF COMMERCE

## DISCLAIMER

The contents of this report reflect the views of the authors who are responsible for the fact and accuracy of the data presented herein. The contents do not necessarily reflect the official views or policies of the North Carolina Department of Transportation or the Federal Highway Administration. This report does not constitute a standard, specification or regulation.

## ACKNOWLEDGMENTS

This research was sponsored by the North Carolina Department of Transportation (NCDOT) in cooperation with the US Department of Transportation, Federal Highway Administration (FHWA). A technical advisory committee chaired by Mr. William Moore, State Geotechnical Engineer and including Messrs. John Ledbetter, Soils and Foundations Unit, James Keene, Geotechnical Unit, Pat Strong and Mike Stanley of the Research and Development Unit aided in the coordination of the research, and is gratefully acknowledged.

Thanks are also due to

Mr. Richard Johnson of the NCDOT, for his assistance in selecting field test sites, performing field exploration, installation of experimental equipment, and sampling during this study;

Mr. Ned Perry of the NCDOT, for his assistance in selecting pile and pile driving energy, and his supervision of the driving performed during this study;

Professor Kenneth Stokoe, University of Texas, Austin, for providing reference information used to select geophones and perform field vibration measurements;

Professor Richard Woods, University of Michigan, for providing a bore hole 3-D geophone system with a pneumatic packer, and his valuable suggestions for field vibration measurement;

Mr. Ayushman Gupta, former graduate research assistant at NCSU, for his laboratory testing of soils reported in 1992 - 1994, and for his interpretation of dynamic settlement, shear modulus and damping ratio data for these residual soils;

Mr. Eric Wang, former graduate research assistant at NCSU, for his assistance in the installation of field test equipment, monitoring soil settlement and pile driving, and performing laboratory triaxial tests;

Mr. Ken Ivanetich, graduate research assistant at NCSU, for his assistance in recording of vibration attenuation during pile driving and performing laboratory tests to determine the engineering properties of samples obtained from the test site.

Special thanks are due to

Mr. William Dunleavy, Civil Engineering Department Electronics Technician, for his suggestions and assistance in implementing the computer control and data acquisition system for the field vibration measurements. His fabrication of electronic components as well as his insight into the development of LabView software was most important to the successful completion of the work performed.

## ABSTRACT

The objective of this research is to provide field verification of an analytical model for predicting ground surface settlement due to construction induced vibration. This model was proposed by Borden, Shao and Gupta in the report "Construction Induced Vibrations" (1994) to NCDOT and FHWA.

Three test sites with residual soil profile were investigated. At one of the sites, in Selma, North Carolina, both settlement of the residual soil profile and the characteristics of the vibration source, and the wave propagation behavior were monitored during pile driving. Laboratory resonant column and torsional shear tests were performed on samples obtained from the field test site. Based on a comparison between the measured field settlement at this site and that predicted based on laboratory test results, the proposed analytical model is shown to be somewhat conservative.

Vibration attenuation with depth in the residual soil profile was investigated for the first time. The vibration time histories of the field test were analyzed and the peak velocities at various depths and surface distances were obtained. In addition, the ground vibration frequency and Rayleigh wave velocity were calculated. The Rayleigh wave attenuation function in the soil profile agreed well with the field tests records. The approach to evaluate the wave attenuation on the ground surface was confirmed to be conservative.



## TABLE OF CONTENTS

TECHNICAL REPORT DOCUMENTATION PAGE (Form 1700.7) .....	i
DISCLAIMER .....	ii
ACKNOWLEDGMENTS .....	iii
ABSTRACT.....	v
TABLE OF CONTENTS .....	vi
LIST OF TABLES .....	ix
LIST OF FIGURES.....	xii
1. INTRODUCTION.....	1
2. BACKGROUND AND SUMMARY OF RESEARCH DURING 1992-1994.....	3
2.1 Literature Review.....	3
2.2 Research During 1992-1994.....	9
2.2.1 Data base of laboratory RC/TS tests .....	10
2.2.2 Modeling to evaluate vibration induced settlement .....	14
2.3 Scope of Present Study and Organization of Report .....	30
3. FIELD VERIFICATION EXPERIMENTAL PROGRAM.....	31
3.1 Site Details.....	31
3.2 Engineering Characteristics .....	40
3.3 Predicted Densification Using the Existing Model.....	43
3.4 Test Equipment.....	45

3.4.1	Extensometer.....	45
3.4.2	Geophones.....	47
3.4.3	Data acquisition system and computer software .....	48
3.5	Experimental Procedure .....	54
3.5.1	Site design.....	54
3.5.2	Installation of extensometer and geophone casing .....	58
3.5.3	Pile driving procedure.....	59
4.	RESULTS AND DISCUSSIONS OF FIELD EXPERIMENTS.....	61
4.1	Settlement Induced by Pile Driving Vibrations.....	61
4.2	Pile Driving Vibrations .....	61
4.2.1	Vibration attenuation on the ground surface.....	69
4.2.2	Vibration attenuation with depth in the soil profile .....	71
4.2.3	Characteristics of Rayleigh wave.....	75
5.	RESULTS OF LABORATORY TESTS.....	81
5.1	Resonant Column Tests.....	81
5.2	Torsional Shear Tests for Dynamic Densification.....	82
5.3	Shear Modulus Changes with Shear Strain Amplitude and Confining Pressure.....	88
6.	MODELING .....	91
6.1	Attenuation of Construction Induced Vibration in Soil Profile.....	91
6.2	Modification of Models for Shear Modulus and Material Damping .....	95
6.2.1	Modeling of maximum shear modulus .....	96

6.2.2 Shear modulus as a function of confining pressure, shear strain amplitude and soil types .....	101
6.2.3 Comparison with other studies .....	104
6.2.4 Modeling of material damping .....	106
6.3 Modification of the Dynamic Densification Model .....	111
6.4 Comparison between Experimental Results and Model Predictions .....	115
7. CONCLUSIONS AND RECOMMENDATIONS .....	118
8. IMPLEMENTATION AND TECHNOLOGY TRANSFER .....	120
9. REFERENCES .....	132
 APPENDIX A1: LABORATORY EXPERIMENT RESULTS .....	 A-1
A1.1 Data Summary of Resonant Column Tests Results .....	A-2
A1.2 Data Summary of Torsional Shear Tests Results .....	A-6
APPENDIX A2: ORIGINAL PROJECT AUTHORIZATION WORK PLAN .....	A-13

## LIST OF TABLES

Table #		Page #
2.1	Site Details of the Specimens Tested .....	11
2.2	Engineering Properties of the Specimens Tested.....	12
2.3	USCS Classification of Each Specimen Tested .....	13
2.4	Test Conditions for Each Specimen Tested.....	15
2.5	Factors for Dynamic Soil Densification Modeling .....	27
2.6	Guidelines for Tolerable Foundation Settlement .....	29
3.1	Soil Profile of Selma Site .....	36
3.2	Soil Profile of Trenton Road Site .....	37
3.3a	Soil Profile of Edward Mill Road Extension Site (Sta. 5+00).....	38
3.3b	Soil Profile of Edward Mill Road Extension Site (Sta. 7+00).....	39
3.4	Specimens Characteristics of Site 1 (Selma, NC) .....	40
3.5	Soil Particle Size Distribution, Atterberg Limits, and USCS Classification of Soils from Site 1 .....	42
3.6	Engineering Properties of Specimens from Site 2.....	42
3.7	Comparison of Engineering Properties between Site 1 and the Data Base.....	43
3.8	Prediction of Dynamic Settlement on Site 2 (Trenton Road, Raleigh) .....	45
3.9	Geophone Parameters .....	48
4.1	Extensometer Records at Site 1 (Selma, NC) .....	62

4.2	Elevation Changes of Magnet Targets .....	64
4.3	Records of Pile Driving Vibrations .....	66
4.4	Statistic Results of Peak Particle Velocity Recorded by the 3-D Surface Geophone, S3.....	69
4.5	Frequency Analysis on the Time History of Pile B .....	79
5.1	Shear Wave Velocity and Shear Modulus from Resonant Column Tests .....	82
5.2	Parameters Investigated in Torsional Shear Tests for Specimens Obtained from Site 1 (Selma, NC).....	83
5.3	Relationship between Shear Modulus and Shear Strain Amplitude.....	89
6.1	Maximum Shear Modulus and Minimum Damping on the Basis of Soil Types.....	97
6.2	Values of the Constants and Square of Coefficient of Regression for the model of $G_{max}$ .....	101
6.3	Values of the Constants and Square of Coefficient of Regression for the Model of Normalized Shear Modulus .....	104
6.4	Modeling of Dynamic Settlement for Samples Obtain from Site 1 (Selma, NC).....	115
6.5	Calculation of Dynamic Settlement on Site 1 (Selma, NC).....	116
8.1	Values of the Constants and Square of Coefficient of Regression for the Normalized Shear Strain Modulus Model (Reprint of Table 6.3).....	126

---

8.2	Table 8.2 Values of the Constants and Square of Coefficient of Regression for the Model of Gmax (Reprint of Table 6.2) .....	127
8.3	Factors for the Dynamic Soil Densification Modeling (Reprint of Table 2.5) .....	129
8.4	Guidelines for Tolerable Foundation Settlement (Reprint of Table 2.6).....	130

## LIST OF FIGURES

Figure #		Page #
2.1	Relative Intensities of Construction Vibrations (Wiss, 1981) .....	4
2.2	Wave Motion Record (10 Mg Truck, Speed 60 km/hour, 18 mm Bump, Vertical Component) (Taniguchi and Sawada, 1979).....	5
2.3	Fourier Spectra (10 Mg Truck, Speed 60 km/hour, 18 mm Bump, Vertical Component) (Taniguchi and Sawada, 1979).....	5
2.4	Plot of $\tau/\tau_{\max}$ vs. N at $\tau=0.65$ (Seed et al., 1975) .....	7
2.5	Equivalent Numbers of Uniform Stress Cycles Based on Strong Component of Ground Motion (Seed et al., 1975).....	7
2.6	Comparison of Peak Particle Velocity at the Ground Surface and on a Buried Pipe Line (Dowding, 1991).....	8
2.7	Wave Attenuation Profile for a Loaded Truck (20 Mg) over a 18 mm Thick Plank at 60 km/hour (Calculated from the Field Test Data Reported by Taniguchi and Sawada, 1979).....	19
2.8	Distribution of Displacement Waves from a Circular Footing on a Homogeneous, Isotropic, Elastic Half-Space (after Woods, 1968).....	19
2.9	Variation of the Horizontal and Vertical Vibration Amplitudes of Raleigh Waves with Depth (Poisson's Ratio = 0.25) (Das, 1983).....	21

2.10	Relationship Between Rayleigh Wave Velocity, Shear Wave Velocity, and Poisson's Ratio.....	21
2.11	The Flow Chart for Calculating the Shear Strain Amplitude.....	22
2.12	Effect of Soil Type on Dynamic Settlement (1000 Cycles).....	25
2.13	Comparison Between Dynamic Volumetric Strain as a Function of Shear Strain Amplitude for Dry Sand (Youd, 1972) and Residual Soils for 1000 Cycles.....	25
2.14	Comparison between Measured and Predicted Volumetric Strain. (Test results for specimen 3ST#11B are shown by points. The results from the model are shown by the curves) .....	26
3.1	Location of the Piedmont Province and Test Sites(After Sowers,1954) .....	32
3.2	Detailed Map of Test Site 1 (Selma, NC) .....	33
3.3	Detailed Map of Test Site 2 and Site 3 (Rayleigh, NC).....	34
3.4	Soil Particle Size Distribution of Specimens Tested .....	41
3.5	Magnet Extensometer System .....	46
3.6	Computerized Data Acquisition and Analysis System .....	49
3.7	Front Panel of the Data Acquisition Program .....	53
3.8	Field Test Design at Site 1 (Selma, NC) .....	55
3.9	Design of Extensometer and Bore Hole Geophone System.....	56
3.10	Picture of 3-D Surface Geophone and the Geophone Casing .....	57
3.11	Picture of the Access Tube, Reference Ring and Spider Magnet of the Extensometer.....	57



3.12	Installation of Geophone Casing.....	60
3.13	Picture of Field Test Site 1 (Selma, NC).....	60
4.1	Vibration Time Histories on the Ground Surface Recorded by Geophone S3 .....	68
4.2	Vibration Attenuation on the Ground Surface.....	70
4.3	Vibration Attenuation along with Depth for Pile A .....	72
4.4	Vibration Attenuation along with Depth for Pile B .....	73
4.5	The Front Panel of Wave Analytical Software, SASW.VI.....	77
5.1	The Volumetric Strain Changes with Cyclic Number and Shear Strain Amplitude at Each Confining Pressure for Specimen 6ST#2.....	84
5.2	The Volumetric Strain Changes with Cyclic Number and Shear Strain Amplitude at Each Confining Pressure for Specimen 6ST#2A .....	85
5.3	The Volumetric Strain Changes with Cyclic Number and Shear Strain Amplitude at Each Confining Pressure for Specimen 6ST#4.....	86
5.4	Normalized Shear Modulus as a Function of Shear Strain for Samples Obtained from Selma, NC .....	90
6.1	Comparison of Vibration Attenuation on the Ground Surface between Field Tests and Literature Reports.....	93
6.2	Modeling of $G_{max}$ as a Function of Confining Pressure for Four Types of Residual Soil.....	99
6.3	Summary of $G_{max}$ Model on the Basis of Soil Type .....	100

6.4	Modeling of Normalized Shear Modulus as a Function of Shear Strain Amplitude under Different Confining Pressures for Four Types of Residual Soil.....	103
6.5	Comparison of All the Test Results in this Study with Other Studies in the Literature .....	105
6.6	Damping Values Obtained at Various Shear Strain Amplitudes on the Basis of Soil Type.....	107
6.7	Modeling of the Relationship between Damping Ration and Normalized Shear Modulus .....	109
6.8	The Relationship between Normalized Shear Modulus and Damping Obtained from this Study and that Reported in the Literature .....	110
6.9	Modeling of Dynamic Volumetric Strain as a Function of Shear Strain Amplitude and Number of Cycles for Specimen 6ST#2 .....	112
6.10	Modeling of Dynamic Volumetric Strain as a Function of Shear Strain Amplitude and Number of Cycles for Specimen 6ST#2A.....	113
6.11	Modeling of Dynamic Volumetric Strain as a Function of Shear Strain Amplitude and Number of Cycles for Specimen 6ST#4 .....	114
6.12	Dynamic Volumetric Strain Versus Shear Strain Amplitude at 1000 Cycles for Specimen 6ST#2A.....	114
8.1	Relative Intensities of Construction Vibrations (Wiss, 1981) (Reprint of Figure 2.1).....	121

8.2 Comparison of Vibration Attenuation on the Ground Surface between  
Field Tests and Literature Reports (Reprint of Figure 6.1)..... 122

8.3 The Flow Chart of Calculating the Shear Strain Amplitude. (Reprint of  
Fig. 2.11)..... 125

**CONSTRUCTION RELATED VIBRATIONS:  
FIELD VERIFICATION OF VIBRATION INDUCED SETTLEMENT MODEL**

**CHAPTER 1  
INTRODUCTION**

The research program described in this report was undertaken to provide field verification of an analytical model developed to predict ground surface settlement due to construction induced vibrations. In order to accomplish this verification, three test sites with residual soil profile were investigated. At one of the sites, in Selma, North Carolina, settlement of the residual soil profile was monitored during pile driving. The characteristics of the vibration source and the propagating waves were recorded. Utilizing the database of resonant column/torsional shear data developed at NCSU and a knowledge of the intended vibration sources and site geometry, pre-test predictions of settlement versus number of vibration source events (i.e. pile strikes) were made. Based on a comparison of predicted and measured particle velocity and settlement as a function of depth below the loaded footings, the existing model was modified.

In response to the need for a quantitative basis for evaluating the potential settlement of structures as the result of soil densification due to construction vibrations, a two-year investigation, Highway Research Project 93-7, was performed from July 1, 1992 to June 30, 1994 (Borden, Shao and Gupta, 1994). The objective of this 2-year project on "Construction Related Vibrations" was to develop a procedure for evaluating soil response

to both impulse and steady state construction induced vibrations. Resonant column and torsional shear tests on a wide range of soils including silty and clayey sands were performed to develop an experimental data base. The settlement potential of these soils was evaluated based on both frequency and amplitude response. Analytical modeling techniques were developed to predict ground-surface settlement as a function of soil type and vibration source characteristics and location.

In May, 1994, an additional phase of research was approved by NCDOT to provide verification of the analytical methods developed on actual construction projects from July 1, 1994 to June 30, 1995. This report provides a detailed description of the accomplishments of the project.

## CHAPTER 2

### BACKGROUND AND SUMMARY OF RESEARCH DURING 1992-1994

#### 2.1 Literature Review

Construction vibrations are of three different types: (1) transient or impact vibration; (2) steady-state or continuous; and (3) pseudo-steady-state vibrations. Examples of transient construction vibrations are those that occur from blasting with explosives, impact pile driving, demolition, and wrecking balls. Steady-state vibrations may be generated by vibratory pile drivers, large pumps used in jacking underground pipes, and compressors. Pseudo-steady-state vibrations are so called because they are of a random nature or a series of impact vibrations that are at short enough intervals to approach essentially a steady-state condition. Examples of these are jackhammers, pavement breakers, trucks, and scrapers. The relative intensities of construction vibration are shown in Fig. 2.1. (Wiss, 1981)

Some typical vibration data characteristics of vehicular induced ground motion in a sandy gravel profile were given by Barneich (1985) and Taniguchi (1979). The vibration amplitude and frequency are dependent on wheel base, speed of vehicle and road roughness. Frequencies are generally in the 3 to 30 Hz range with most data in the range of 10 to 30 Hz. The time history and Fourier spectra of a truck induced vibration are shown in Fig. 2.2 and Fig. 2.3 respectively. Horizontal vibration amplitude is one-half to two-thirds of vertical amplitude in the same frequency range.

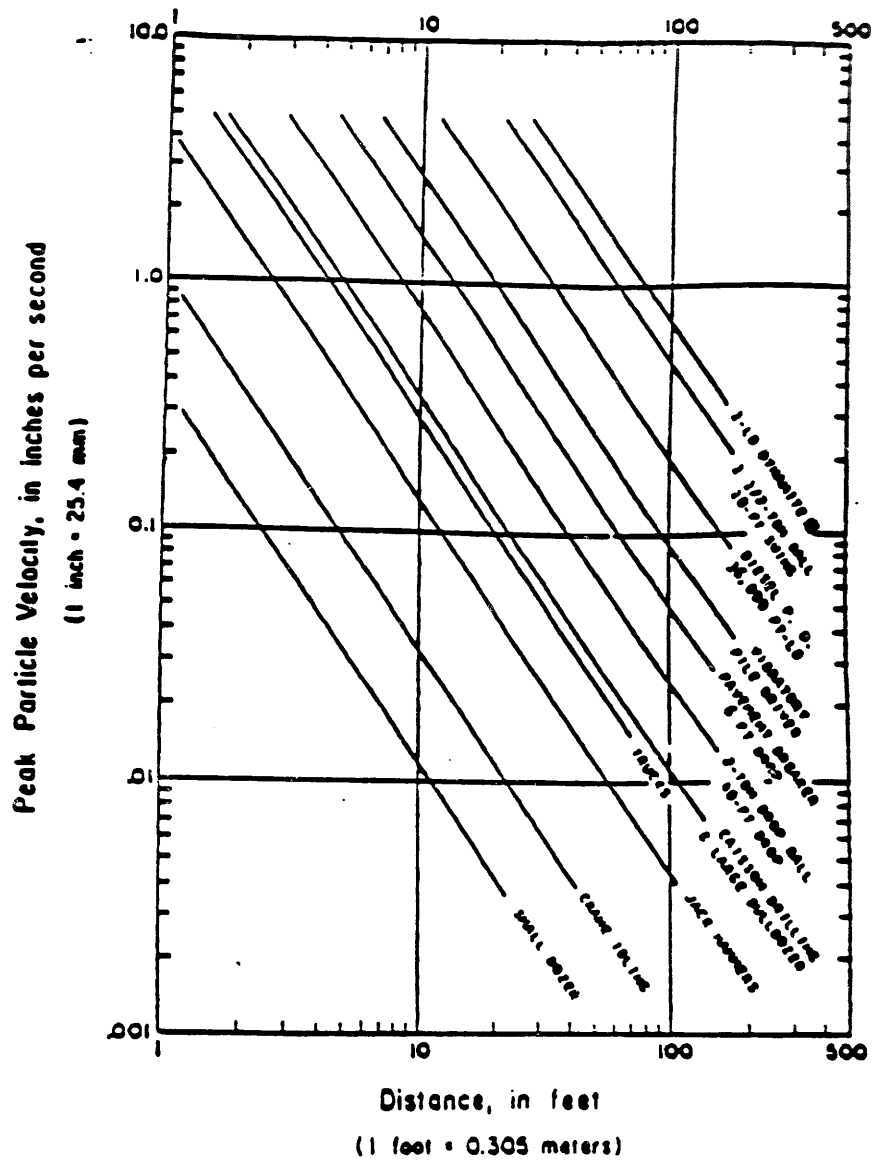


Figure 2.1 Relative Intensities of Construction Vibrations (Wiss, 1981)

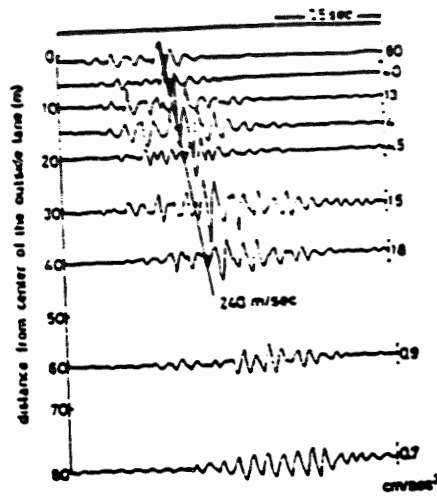


Figure 2.2 Wave Motion Record (10 Mg Truck, Speed 60 km/hour, 18 mm Bump, Vertical Component) (Taniguchi and Sawada, 1979)

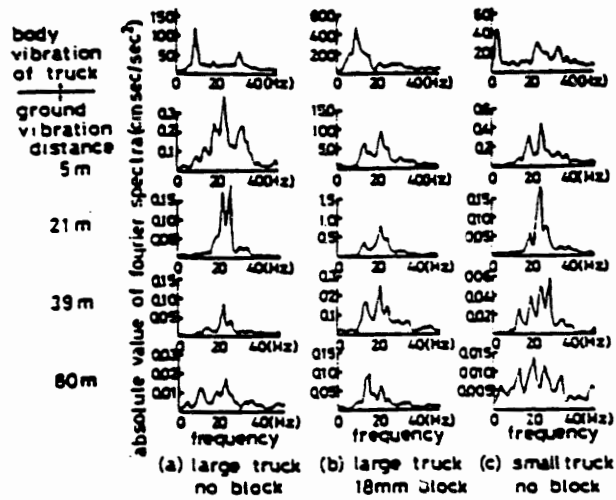


Figure 2.3 Fourier Spectra (10 Mg Truck, Speed 60 km/hour, 18 mm Bump, Vertical Component) (Taniguchi and Sawada, 1979)



Dowding (1991) gave a comprehensive evaluation of pile driving vibrations. The dominant frequency of impact motion is dependent upon driving conditions and the pile and hammer properties, but will range between 10 and 50 Hz for typical hammers. Vibratory hammers produce ground motions at the hammer frequency, which typically is in the range between 15 to 30 Hz.

The above data are needed in the field verification phase to enable proper selection of vibration monitoring instrumentation, i.e. geophones and data acquisition system characteristics

In the study of soil settlement during vibration, it becomes necessary to determine the equivalent number of significant uniform stress or strain cycles for construction vibrations that have an irregular time history. The effect of the stress or strain history on a given soil deposit should be same as the equivalent number of uniform cycles. The basic procedure included in developing the equivalent stress cycle method has been described by Seed et al (1975,1976,1979) from the point of view of soil liquefaction during earthquake. Fig. 2.4 is generated using the results of the soil liquefaction study by simple shear tests. Equivalent numbers of uniform stress cycles for several earthquakes with magnitudes of 5.3 - 7.7 are shown in Fig. 2.5. Similar relations need to be developed to evaluate construction induced vibrations at different energy levels as explained above .

As shown in Fig. 2.6, vibratory ground motion during pile driving can be as high as 100 mm/sec within 1.5 m of the pile, but decreases rapidly to 25 mm/sec at 3 m. Dowding (1991) found that densification can extend approximately as far as the piling is long. Dowding (1991) noted that densification and thus settlement results from a complex

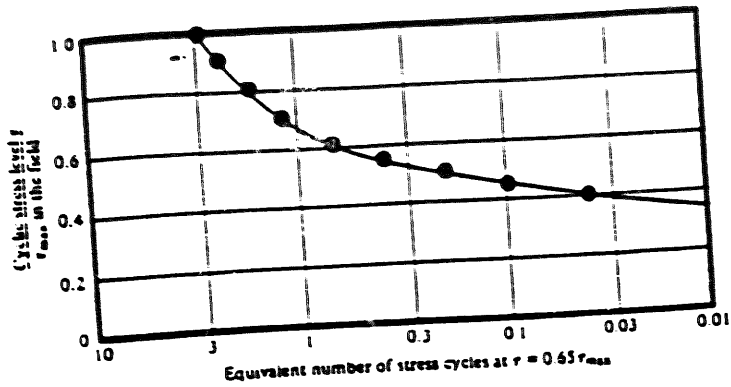


Figure 2.4 Plot of  $\tau/\tau_{max}$  vs.  $N$  (Seed et al., 1975)

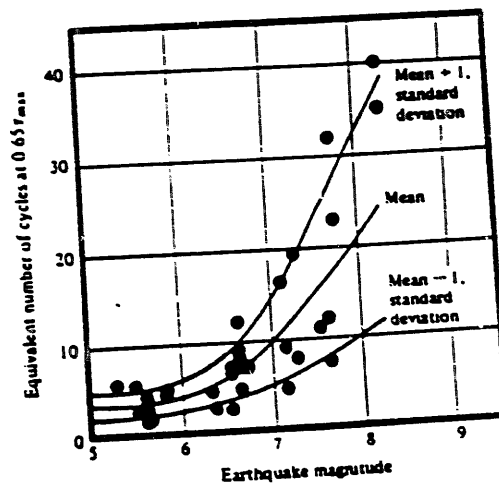


Figure 2.5 Equivalent Numbers of Uniform Stress Cycles Based on Strong Component of Ground Motion (Seed et al., 1975)

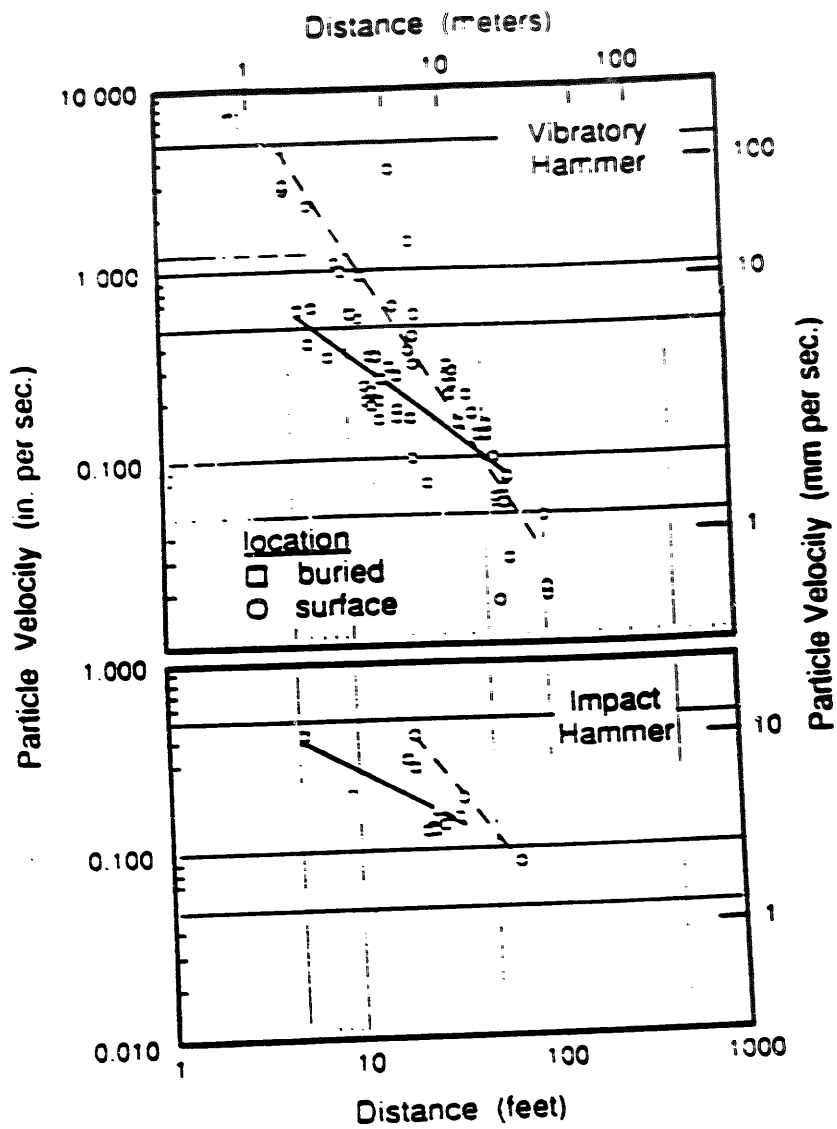


Figure 2.6 Comparison of Peak Particle Velocity at the Ground Surface and on a Buried Pipe Line (Dowding, 1991)

combination of vibration amplitude, number of repetitions, soil properties, and position of the water table. "The number of repetitions or pulses depends upon the number of piles, their length, and the number of blows or vibratory cycles required per unit penetration." Even though the magnitude of single or short term vibration is not enough to result in a considerable settlement, long-term accumulative vibration effects may result in settlement causing damage to adjacent buildings and therefore must be investigated in order to establish safe design guidelines. In addition, the ground motion attenuates very rapidly with distance from source. As a consequence, the differential settlement caused by differential ground motion is much more dangerous for building. It is needed to emphasize that all of the above cases concentrated on the settlement of sand. There is no published data describing the response of silty or clayey sandy, residual soils or slightly cemented soils under construction vibrations.

## **2.2 Research During 1992-1994**

From July 1, 1992 to June 30, 1994, a two year project on "Construction Related Vibrations" (Borden, Shao and Gupta, 1994) developed a procedure for evaluating soil response to both impulse and pseudo-steady-state construction induced vibrations. The settlement potential of 33 residual soil specimens obtained from 8 different sites was evaluated by resonant column and torsional shear tests. These tests included an evaluation of the effect of confining pressure from 25 kPa to 100 kPa, shear strain amplitude from  $1 \times 10^{-4} \%$  to  $1 \times 10^{-1} \%$ , frequency of vibration from 0.2 to 10 Hz and number of cycles up to 1 million on the dynamic densification of residual soil. This research also studied the

influence of confining pressure, shear strain amplitude, and number of cycles on the shear modulus and damping ratio of residual soil specimens. The dynamic settlement of the residual soil tested was observed to be small, especially in comparison to that reported in the literature for sands.

### **2.2.1 Data base of laboratory RC/TS tests**

Residual soil samples were collected from eight different sites in North Carolina. The Shelby tube samples from these sites were supplied by NCDOT. The site details of the specimens tested, their engineering properties, and USCS classification are listed in Table 2.1, Table 2.2 and Table 2.3, respectively.

Vibration induced settlement tests was investigated by resonant column and torsional shear tests which concentrated on the influence of:

- number of cycles (for a given confining stress and amplitude of shear strain);
- amplitude of shear strain ( for a given value of normal stress and number of cycles);
- confining pressure ( for a given amplitude of shear strain and number of cycles);
- soil samples with different grain size distribution and densities recovered from different sites and at different depths;
- cyclic frequency; and,
- degree of soil saturation.

Table 2.1 -Site Details of the Specimens Tested

Site No.	County	NCDOT Project No.	Specimen No.	Station	Depth (ft)	GWT (ft)	SPT (N)
<i>Phase I</i>							
I-1	Franklin/Vance	6.399001T	RC-1	344+00 105' RT	2.7 - 4.2	Dry	-
			RC-2	344+00 105' RT	2.7 - 4.2	Dry	-
I-2	Franklin/Vance	6.399001T	RC-3	330+00 163' RT	3.0 - 5.0	Dry	-
			RC-4	330+00 163' RT	3.0 - 5.0	Dry	-
			RC-5	330+00 163' RT	3.0 - 5.0	Dry	-
I-3	Guilford	8.1570601	TS-1	320+00 140' LT	9.0 - 11.2	27	-
			TS-2	320+00 140' LT	9.0 - 11.2	27	-
			TS-3	320+00 140' LT	9.0 - 11.2	27	-
<i>Phase II</i>							
II-1	Rockingham	5.5151	1ST#4	13+90 -L- 31' LT	13.3 - 15.3	Dry	6
II-2	Wake	4.6321302 (M - 220)	2ST#1	22+92 -L- 31' LT	3.0 - 5.0	N/A	10
			2ST#2	22+95 -L- 31' LT	3.0 - 5.0	N/A	10
			2ST#3	22+95 -L- 31' LT	3.0 - 5.0	N/A	10
			2ST#5	81+00 -L- C. L.	5.0 - 7.0	N/A	15
			2ST#7	81+00 -L- C. L.	5.0 - 7.0	N/A	15
			2ST#8	81+00 -L- C. L.	7.0 - 9.0	N/A	15
			2ST#9	22+95 -L- 32' LT	3.0 - 5.0	N/A	10
			2ST#10	22+95 -L- 32' LT	3.0 - 5.0	N/A	10
			2ST#11	22+95 -L- 31' LT	3.0 - 5.0	N/A	10
			II-3	Wake	6.409003T	3ST#2	4+50 72' LT
3ST#2L	4+50 72' LT	4.1 - 6.1				N/A	14
3ST#3	4+50 72' LT	7.7 - 9.0				N/A	14
3ST#4	4+50 75' LT	4.8 - 6.8				N/A	14
3ST#5L	4+00 60' LT	4.0 - 6.0				N/A	11
3ST#6	4+00 60' LT	6.0 - 8.0				N/A	12
3ST#8	4+00	4.1 - 6.0				N/A	11
3ST#9	4+00	2.9 - 4.9				N/A	-
3ST#10L	4+00	3.3 - 5.3				N/A	-
3ST#11A	4+00	5.8 - 7.8				N/A	-
3ST#11B	4+00	5.8 - 7.8				N/A	-
3ST#12	4+00	3.8 - 5.8				N/A	-
II-4	Wake	8.T401704	4ST#1	143+00 250' LT	13.2 - 15.2	11	9
			4ST#4	143+00 250' LT	15.4 - 17.4	11	9
II-5	Wake	8.U401710	5ST#2	627+00 C. L.	11.0 - 13.0	1.0	5

Table 2.2 Engineering Properties of the Specimens Tested

Specimen No.	Water Content (%)	Initial Void Ratio	Specific Gravity	Saturation (%)	Initial Length (in)	Initial Diameter (in)
RC-1	24.6	0.89	2.74	75	5.81	2.87
RC-2	30.5	1.00	2.74	84	5.88	2.87
RC-3	39.2	1.25	2.81	88	5.96	2.87
RC-4	40.7	1.31	2.81	87	5.91	2.87
RC-5	41.9	1.35	2.81	87	5.83	2.87
TS-1	37.8	1.50	2.69	68	5.99	2.85
TS-2	36.8	1.42	2.69	70	5.92	2.85
TS-3	29.6	1.18	2.69	67	5.94	2.86
1ST#4	20.7	0.60	2.67	92	5.91	2.88
2ST#1	33.5	1.41	2.79	66.0	5.87	2.86
2ST#2	33.1	1.43	2.85	65.9	5.88	2.86
2ST#3	38.9	1.64	2.79	66.2	5.79	2.88
2ST#5	14.8	0.79	2.60	48.4	5.71	2.85
2ST#7	12.6	0.84	2.60	39.1	5.67	2.83
2ST#8	15.0	0.87	2.60	45.0	5.82	2.83
2ST#9	26.2	1.01	2.69	69.8	5.72	2.86
2ST#10	29.6	1.12	2.75	72.9	5.82	2.86
2ST#11	29.6	1.14	2.71	70.6	5.89	2.86
3ST#2	23.9	1.32	2.75	49.7	5.89	2.85
3ST#2L	22.9	1.24	2.75	50.6	5.58	2.85
3ST#3	26.8	1.14	2.67	63.0	5.78	2.87
3ST#4	23.6	1.17	2.66	53.6	5.72	2.86
3ST#5L	18.4	1.16	2.69	42.7	5.72	2.87
3ST#6	19.5	0.93	2.75	57.5	5.84	2.92
3ST#8	22.8	1.24	2.72	50.2	5.57	2.87
3ST#9	15.3	0.86	2.74	48.8	5.84	2.85
3ST#10L	34.8	1.42	2.76	67.5	5.86	2.85
3ST#11A	50.3	1.78	2.74	77.6	5.78	2.86
3ST#11B	36.6	1.48	2.74	67.7	5.75	2.87
3ST#12	35.6	1.43	2.72	67.7	5.87	2.85
4ST#1	16.6	0.49	2.81	96.1	5.78	2.88
4ST#4	24.7	0.72	2.79	96.6	5.80	2.90
5ST#2	50.9	1.48	2.86	98.7	5.79	2.88

Table 2.3 USCS Classification of Each Specimen Tested

Specimen No.	Gravel Size > #4 (> 4.75 mm)	Coarse Sand Size #4 to #10 (2 to 4.75 mm)	Medium Sand Size #10 to #40 (0.42 to 2 mm)	Fine Sand Size #40 to #200 (0.074 to 0.42 mm)	Silt Size (0.074 to 0.002 mm)	Clay Size (< 0.002 mm)	LL	PL	PI	USCS
RC-1	0	0	15.5	36.5	25	23	48	40	8	SM-ML
RC-2	0	0	15.5	36.5	25	23	48	40	8	SM-ML
RC-3	0	0	1.8	8.5	61.7	28	57	43	14	MH
RC-4	0	0	1.8	8.5	61.7	28	57	43	14	MH
RC-5	0	0	1.8	8.5	61.7	28	57	43	14	MH
TS-1	0	0	15.5	26.5	44	14	44	34	10	ML
TS-2	0	0	15.5	26.5	44	14	44	34	10	ML
TS-3	0	0	15.5	26.5	44	14	44	34	10	ML
1ST#4	0	0	3	46	31	20	30	19	11	SC-CL
2ST#1	0	0	0.6	22	47.4	30	75	46	29	MH
2ST#2	0	0	1	15.4	53.6	30	75	48	27	MH
2ST#3	0	0	0.5	27.2	44.3	28	92	61	31	MH
2ST#5	0	0	15	54.6	19.4	11	-	-	-	NP SM
2ST#7	0	0	14	60.3	19.7	6	-	-	-	NP SM
2ST#8	0	0	14	56.6	18.4	11	-	-	-	NP SM
2ST#9	0	0	0	35.6	40.4	24	-	-	-	NP SM-ML
2ST#10	0	0	2	41.6	41.4	15	-	-	-	NP SM-ML
2ST#11	0	0	0.5	35.5	44	20	-	-	-	NP SM-ML
3ST#2	0	0	4	42.8	48.2	5	29	-	-	NP SM-ML
3ST#2L	0	0	4	42.8	48.2	5	29	-	-	NP SM-ML
3ST#3	0	0	3	27.2	67.8	2	34	-	-	NP ML
3ST#4	0	0	1	31.9	65.1	2	35	-	-	NP ML
3ST#5L	0	0	1	35.2	62.8	1	37	-	-	NP ML
3ST#6	0	0	1	28.1	69.9	1	33	-	-	NP ML
3ST#8	0	0	0.8	34.2	61.9	3.1	36	-	-	NP ML
3ST#9	0	0	6	16.3	69.7	8	35	30	5	ML
3ST#10L	0	0	2.2	13.5	75.3	9	52	46	6	MH
3ST#11A & B	0	0	0.6	5.2	84.2	10	78	56	22	MH
3ST#12	0	0	1.5	18	72.5	8	56	43	13	MH
4ST#1	0	0	10	70.4	18.1	1.5	-	-	-	NP SM
4ST#4	5.3	6.9	6.9	74.6	9.8	0.2	-	-	-	NP SP-SM
5ST#2	0	0	0.4	8.5	86.1	5	59	45	14	MH

\* NP = Nonplastic



Table 2.4 lists detailed test conditions for each of the 33 specimens. In addition to investigating the settlement potential of the specimens, the shear modulus and damping ratios are obtained in the resonant column and torsional shear tests. Table 2.4 provides maximum shear modulus and basic soil properties of all the specimens tested.

### **2.2.2 Modeling to evaluate vibration induced settlement**

The modeling of vibration induced settlement includes three major steps. First, the vibration amplitude and number of cycles based on characteristics of the sources need be determined. Secondly, it is necessary to assess the peak particle velocity, and therefore, shear strain amplitude in the soil profile which is influenced by the attenuation of vibration waves. And, finally, the resulting soil densification as a function of the soil properties, confining pressure, shear strain amplitude, and number of cycles can be evaluated.

To evaluate the potential settlement of a foundation under construction induced vibration, it is very difficult to describe the characteristics of sources. For example, the dump truck induced vibration depends on the trucks weight, wheel base, type of suspension, tire pressure, road condition, speed, soil properties, etc. Therefore, we proposed a simplified method to estimate the equivalent number of cycles for a moving line source (i.e., truck or bulldozer). The detailed procedures are presented in the report "Construction Related Vibration" by Borden, Shao and Gupta, 1994. It is necessary to emphasize that construction induced vibrations are very complicated and depend on type of equipment, road condition, operating condition of equipment, and soil profile. The best way to estimate the equivalent number of cycles is from field measurement and the above

Table 2.4 Test Conditions for Each Specimen Tested

Specimen No.	Confining Pressure* (kPa)	Estimated Shear Strain Amplitude** (%)	Number of Cycles***	Cyclic Frequency**** (Hz)
<i>Phase I</i>				
RC-1	25	0.001 - 0.25	-	Resonant
	50	0.0005 - 0.1	-	Resonant
	100	0.0005 - 0.075	-	Resonant
RC-2	25	0.001 - 0.25	-	Resonant
	50	0.0005 - 0.1	-	Resonant
	100	0.001 - 0.1	-	Resonant
RC-3	25	0.0025 - 0.25	-	Resonant
	50	0.001 - 0.25	-	Resonant
	100	0.00075 - 0.25	-	Resonant
RC-4	25	0.0015 - 0.25	-	Resonant
	50	0.0015 - 0.15	-	Resonant
	100	0.0015 - 0.15	-	Resonant
RC-5	25	0.0015 - 0.25	-	Resonant
	50	0.001 - 0.15	-	Resonant
	100	0.00075 - 0.1	-	Resonant
TS-1	25	0.001 - 0.15	100	0.2
	50	0.0075 - 0.075	100	0.2
	100	0.0075 - 0.075	100	0.2
TS-2	25	0.0075 - 0.1	100	0.2
	50	0.0075 - 0.1	100	0.2
	100	0.0005 - 0.075	100	0.2
TS-3	100	0.0005 - 0.1	100	0.2
<i>Phase II</i>				
1ST#4	25	0.001, 0.0025, 0.005, 0.01, 0.025, 0.05, 0.1	1000	1
	50	0.001, 0.0025, 0.005, 0.01, 0.025, 0.05	1000	1
	100	0.001, 0.0025, 0.005, 0.01, 0.025	1000	1
2ST#1	50	0.0025, 0.005, 0.01, 0.025, 0.05	1000	1
2ST#2	100	0.005, 0.01, 0.025, 0.05, 0.075	1000	1
2ST#3	25	0.0025, 0.005, 0.01, 0.025, 0.05, 0.1	1000	1
	50	0.005, 0.01, 0.025, 0.05, 0.075	1000	1
	100	0.005, 0.01, 0.025, 0.05	1000	1
2ST#5	50	0.0025, 0.005, 0.01, 0.025, 0.05	1000	1
	100	0.005, 0.01, 0.025	1000	1
2ST#7	25	0.005, 0.01, 0.025, 0.05, 0.1	1000	1
	50	0.005, 0.01, 0.025, 0.05, 0.075	1000	1
	100	0.005, 0.01, 0.025, 0.05	1000	1
2ST#8	100	0.005, 0.01, 0.025, 0.05	1000	1
	50	0.005, 0.01, 0.025, 0.05	1000	1

\* Confining pressures were applied in the order as presented here

\*\* Attempt was made to apply these shear strains

\*\*\* Number of cycles for each shear strain amplitude at the given confining pressure

\*\*\*\* Cyclic frequency for each test

Table 2.4 (Continued)

Specimen No.	Confining Pressure* (kPa)	Estimated Shear Strain Amplitude** (%)	Number of Cycles***	Cyclic Frequency**** (Hz)
2ST#9	25	0.0025, 0.005, 0.01, 0.025, 0.05, 0.1	1000	1
	50	0.0025, 0.005, 0.01, 0.025, 0.05	1000	1
	100	0.005, 0.01, 0.025, 0.05	1000	1
	25	0.005, 0.01, 0.025, 0.05	1000	1
2ST#10	100	0.0025, 0.005, 0.01, 0.025	1000	1
2ST#11	50	0.0025, 0.005, 0.01, 0.025	1000	1
	50	0.05	420000	1
3ST#2	25	0.005, 0.01, 0.025, 0.05, 0.1	1000	1
	50	0.005, 0.01, 0.025, 0.05	1000	1
	100	0.005, 0.01, 0.025, 0.05, 0.075	1000	1
3ST#2L	25	0.075	180000	1
3ST#3	50	0.005, 0.01, 0.025, 0.05, 0.1	1000	1
	100	0.005, 0.01, 0.025, 0.05, 0.075	1000	1
3ST#4	25	0.005, 0.01, 0.025, 0.05, 0.1	1000	1
	50	0.005, 0.01, 0.025, 0.05, 0.1	1000	1
	100	0.005, 0.01, 0.025, 0.05, 0.075	1000	1
3ST#5L	25	0.1	180000	1
3ST#6	50	0.005, 0.01, 0.025, 0.05, 0.1	1000	1
	100	0.005, 0.01, 0.025, 0.05, 0.075	1000	1
3ST#8	25	0.005, 0.01, 0.025, 0.05, 0.1	1000	1
	50	0.005, 0.01, 0.025, 0.05, 0.1	1000	1
	100	0.005, 0.01, 0.025	1000	1
3ST#9	50	0.005, 0.01, 0.025, 0.05, 0.1	1000	1
	100	0.005, 0.01, 0.025, 0.05	1000	1
3ST#10L	25	0.1	1050	1
3ST#11A	25	0.01, 0.025, 0.05	1000	10
	25	0.1	1000000	10
3ST#11B	25	0.01, 0.025, 0.05, 0.1	1000	10
	50	0.01, 0.025, 0.05, 0.1	1000	10
	100	0.01, 0.025, 0.05	1000	10
	100	0.1	1000000	10
3ST#12	25	0.005, 0.01, 0.025, 0.05, 0.1	1000	1
	50	0.005, 0.01, 0.025, 0.05, 0.1	1000	1
	100	0.005, 0.01, 0.025, 0.05, 0.075	1000	1
	50	0.05, 0.1	1000	1
4ST#1	50	0.005, 0.01, 0.025, 0.05, 0.1	1000	1
	100	0.005, 0.01, 0.025, 0.05, 0.1	1000	1
4ST#4	50	0.005, 0.01, 0.025, 0.05, 0.1	1000	1
	100	0.005, 0.01, 0.025, 0.05, 0.1	1000	1
5ST#2	50	0.01, 0.025, 0.05	1000	10
	50	0.1	1000000	10

\* Confining pressures were applied in the order as presented here

\*\* Attempt was made to apply these shear strains

\*\*\* Number of cycles for each shear strain amplitude at the given confining pressure

\*\*\*\* Cyclic frequency for each test

simplified method only provides a preliminary estimate when field records are not available.

Vibrations lose energy during wave propagation through the ground. The decay of amplitude of vibrations with distance can be attributed to geometrical damping and material damping. From the evaluation of wave propagation theory and the field tests reported in the literature, it has been concluded that for surface vibration sources such as trucks, heavy equipment and dynamic compaction, Rayleigh waves dominate the energy transfer in the ground. For a point source, like pile driving near the ground surface, the surface vibration amplitude can be expressed as :

$$A = A_1 \left( \frac{r_1}{r} \right)^{1/2} \exp[-\alpha(r - r_1)] \quad (2.1)$$

where  $A$  is the amplitude of particle velocity at a distance  $r$  from the source,  $A_1$  is the amplitude of particle velocity at a reference point, at a distance  $r_1$ , from the source, and  $\alpha$  denotes the coefficient of material damping. The coefficient of material damping,  $\alpha$ , can be obtained from field measurements or can be calculated by :

$$\alpha = \frac{2\pi f \eta}{V_R} \quad (2.2)$$

where  $f$  is the vibration frequency,  $V_R$  is the Rayleigh wave velocity and  $\eta$  is the material damping ratio, which can be obtained from resonant column/torsional shear tests. Frequency of traffic-induced vibrations is mainly determined by soil conditions.

Equation 2.1 is the wave attenuation expression for a point source. However, bulldozers, pans and trucks are finite line sources for which the point source equation is

not strictly valid. For this case, no exact solutions are available. Wahls (1981), developed the following approximate analysis method in 1981 based on geometric damping and energy conservation theory :

$$A = A_1 \sqrt{\frac{\frac{L}{\pi} + r_1}{\frac{L}{\pi} + r}} \exp[-\alpha (r - r_1)] \quad (2.3)$$

where  $L$  is the length of the source.

The preponderance of experimental studies reported in the literature here concentrated on wave propagation along the ground surface in sand or clay profiles. Only one report (Taniguchi and Sawada, 1979) provided the vibration amplitude distribution with depth in the sandy gravel profile as shown in Fig. 2.7. As this is the only data of its kind known to be in the literature, the substantiation of this function should be a significant component of field verification

The attenuation of construction induced vibrations as a function of depth below the ground surface depends on type of soil and vibration amplitude. The peak particle velocity distribution can be calculated by Rayleigh wave propagation theory. Taniguchi and Sawada (1979) concluded that the Rayleigh wave is dominant in the traffic-induced vibration. They measured the soil particle velocity at different surface distance and two depths. From the theoretical analysis of wave propagation in an elastic half-space, the Rayleigh wave carries 67% of total vibration energy, as shown in Fig. 2.8. The attenuation of Rayleigh waves is much slower than S-waves and P-waves. Therefore, for practical purposes, the Rayleigh wave controls the shear strain amplitude distribution in

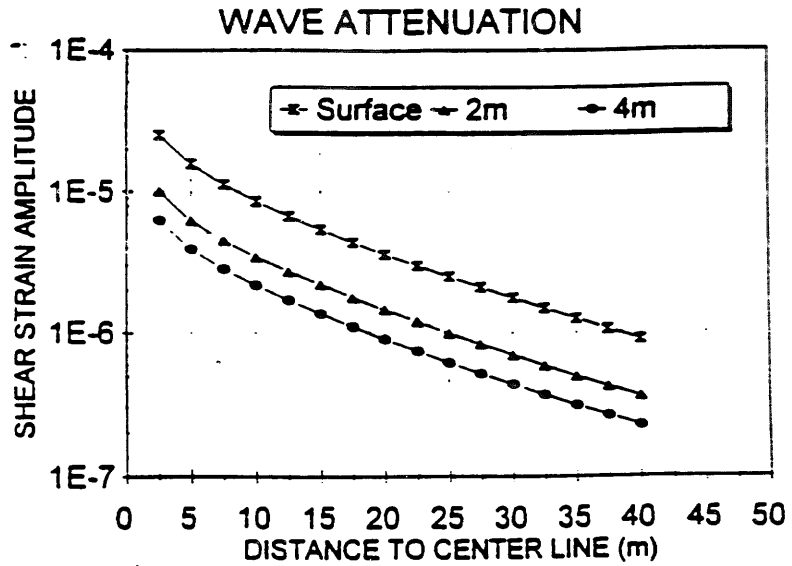


Figure 2.7 Wave Attenuation Profile for a Loaded Truck (20 Mg) over a 18 mm Thick Plank at 60 km/hour (Calculated from the Field Test Data Reported by Taniguchi and Sawada, 1979)

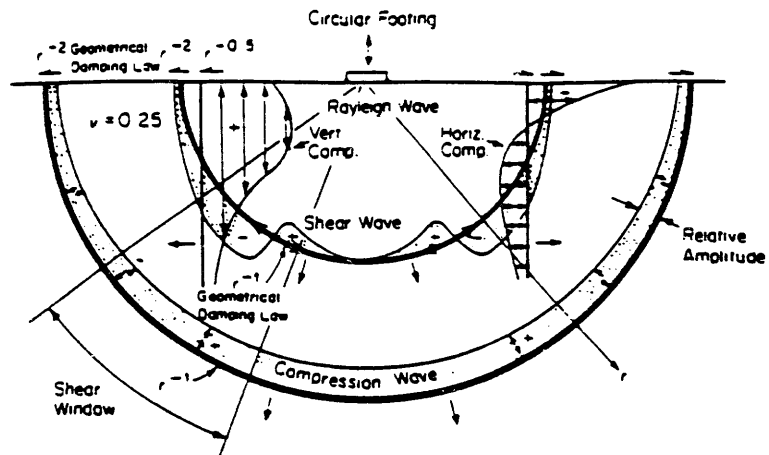


Figure 2.8 Distribution of Displacement Waves from a Circular Footing on a Homogeneous, Isotropic, Elastic Half-Space (after Woods, 1968)

the ground. The attenuation of Rayleigh waves as a function of depth can be calculated by wave propagation theory. For a homogeneous soil profile and Poisson's ratio equal to 0.25, the attenuation of the vertical component of a Rayleigh wave can be expressed as :

$$\frac{A_z}{A_{z=0}} = 1.366 \left( -e^{-1.695\pi\frac{z}{\lambda}} + 1.732e^{-0.786\pi\frac{z}{\lambda}} \right) \quad (2.4)$$

where  $A_z$  is the vertical amplitude at depth  $z$ , and  $\lambda$  is the wave length of the Rayleigh wave (see Fig. 2.9). To simplify the calculation, we conservatively estimate the attenuation of peak particle velocity with depth by the equation for the vertical component. The peak particle velocity decreases rapidly with depth. When the depth equals one Rayleigh wave length, the particle velocity amplitude is only 10% ~20% of the ground surface amplitude. Below this depth, the magnitude of vibration induced settlement is unlikely to be significant. For example, the ground vibration frequency caused by a loaded truck is in the range of 15 Hz to 30 Hz. The Rayleigh wave length of a residual soil profile is around 5m ~ 8m for this frequency range. For this reason, the cyclic torsional shear tests were performed using confining pressures of no more than 100 kPa.

After the peak particle velocity profile is obtained, the shear strain amplitude profile can be calculated as :

$$\gamma = \frac{A}{V_R} \quad (2.5)$$

The Rayleigh wave velocity,  $V_R$ , can be calculated as a function of shear wave velocity and Poisson's ratio as shown in Fig. 2.10. The shear wave velocity,  $V_s$ , can be obtained from

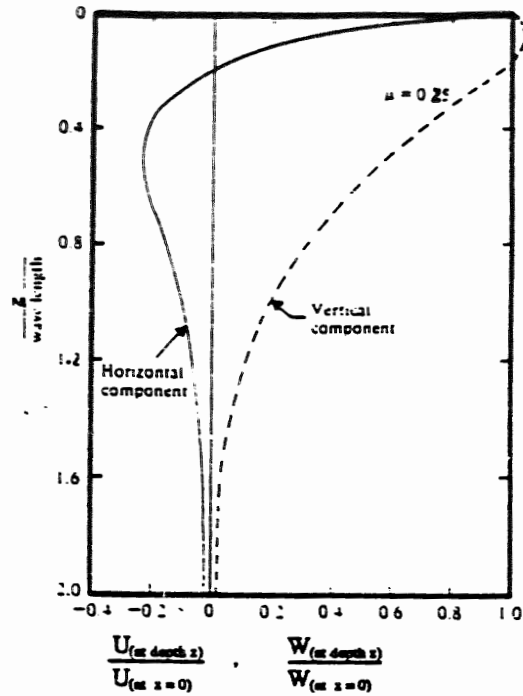


Figure 2.9 Variation of the Horizontal and Vertical Vibration Amplitudes of Raleigh Waves with Depth (Poisson's Ratio = 0.25) (Das, 1983)

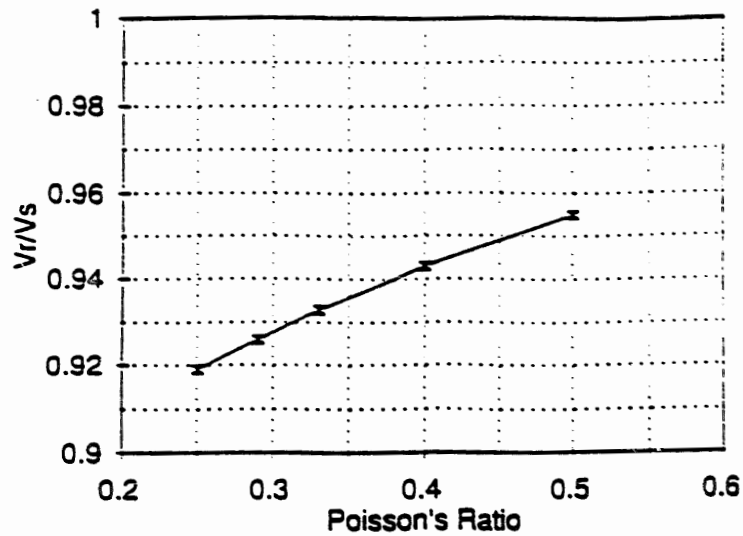


Figure 2.10 Relationship Between Rayleigh Wave Velocity, Shear Wave Velocity, and Poisson's Ratio



field measurement or calculated from shear modulus by  $V_s = (G/\rho)^{1/2}$  and the shear modulus,  $G$ , can be found from laboratory test results as a function of shear strain amplitude and confining pressure. By using an iteration procedure to obtain convergence of the relationship between  $\gamma \sim V_R \sim V_s \sim G \sim \gamma$  as shown in Fig. 2.11, the correct shear strain amplitude is obtained.

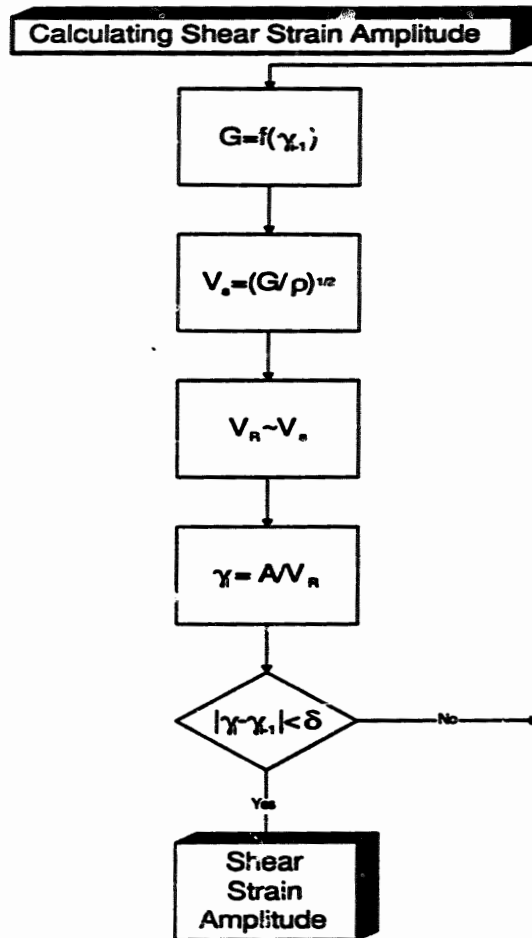


Fig. 2.11 The Flow Chart of Calculating the Shear Strain Amplitude

After the peak particle velocity as a function of horizontal and vertical distance is obtained as previously described, the soil profile can be divided into several layers and shear strain amplitude can be calculated as a function of depth. The resultant ground surface settlement will be calculated as the cumulative settlement of each of the layers. The relationship between densification and shear strain amplitude, number of cycles, and confining pressure are determined from the data base obtained from resonant column and torsional shear tests.

From the torsional shear test results, the volume change caused by static isotropic consolidation and that resulting from dynamic torsional shear are considered separately. This relation can be modeled by regression analysis as :

$$\Delta \varepsilon_{vol} = c(\log N)^b \quad (2.6)$$

where  $\Delta \varepsilon_{vol}$  is the dynamic volumetric strain under  $N$  cycles of torsional shear,  $b$  is the constant which depends only on the confining pressure and type of soil, and  $c$  is the parameter controlled by the shear strain amplitude, confining pressure and type of soil.

The factor  $c$  is a function of shear strain amplitude. The relationship between  $c$  and shear strain amplitude can be modeled by regression analysis as:

$$c = a(\gamma - \gamma_c) \quad (2.7)$$

where the factor  $a$  is only influenced by type of soil and confining pressure,  $\gamma_c$  is the threshold shear strain amplitude (in %) of the specimen at each confining pressure and  $\gamma$  is the current shear strain amplitude (in %). If the shear strain amplitude is below  $\gamma_c$ , dynamic settlement is unlikely. Combining Eq. 2.6 and 2.7, one can obtain :

$$\Delta \varepsilon_{vol} = a(\gamma - \gamma_c)(\log N)^b \quad (2.8)$$

This model for dynamic settlement incorporates the influence of shear strain amplitude, number of cycles, empirically determined factors  $a$  and  $b$ , and threshold shear strain amplitude, which is a function of confining pressure and soil type. By using the model (Eq. 2.8), one can predict the settlement caused by cyclic shear strain.

For the same kind of dynamic load (shear strain amplitude and number of cycles), the dynamic settlement is a function of the soil properties and confining pressure. The finer the particle size, the smaller is the settlement observed. Figure 2.12 provides the best fit lines for the dynamic volumetric strain at 1000 cycles for MH, ML SM-ML, and SM soils. Table 2.5 lists factors  $a$ ,  $b$ , and  $\gamma_c$  for different classifications of residual soil under confining pressures of 25 kPa, 50 kPa, and 100 kPa. When site-specific data is not available, one can match the soil at different depths to Table 2.5 by the nearest soil classification and grain size distribution, and then select values for factors  $a$ ,  $b$ , and  $\gamma_c$ . By using Eq. 2.8, an estimate of potential settlement induced by construction vibration can be made.

Figure 2.13 compares the dynamic settlement for the tests results on dry sand obtained by Youd (1972) and the residual soils tested in this project. It is clear that the residual soil tested densified much less than dry sand. Figure 2.14 shows the comparison of the dynamic volumetric strain between the test data of specimen 3ST#11B and the results from the model.

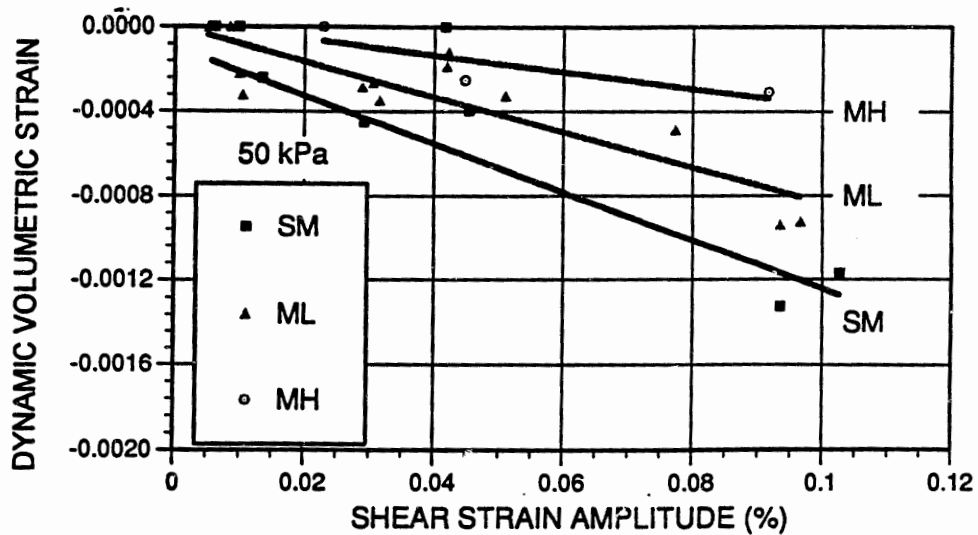


Figure 2.12 Effect of Soil Type on Dynamic Settlement (1000 Cycles)

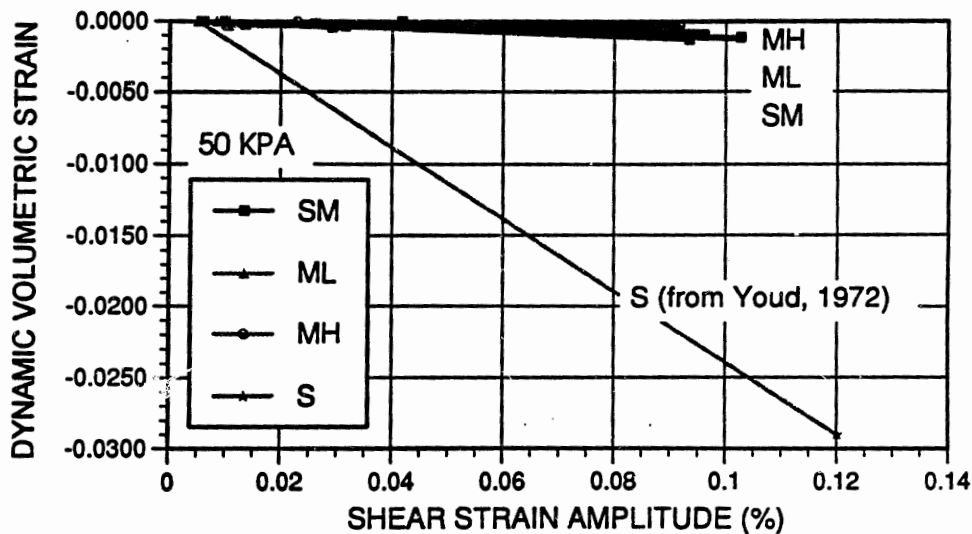


Figure 2.13 Comparison between Dynamic Volumetric Strain as a Function of Shear Strain Amplitude for Dry Sand (Youd, 1972) and Residual Soils for 1000 Cycles

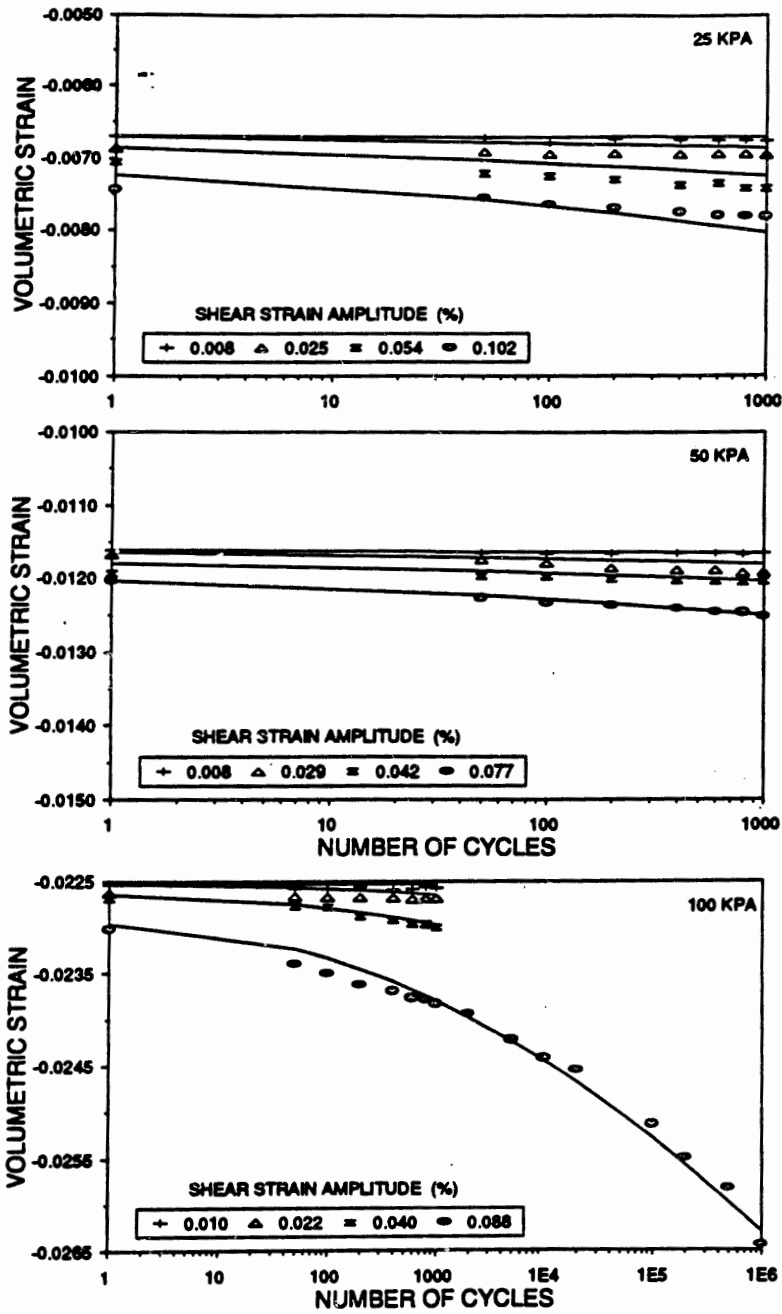


Figure 2.14 Comparison between Measured and Predicted Volumetric Strain (Test results for specimen 3ST#11B are shown by points. The results from the model are shown by curves)

Table 2.5 Factors for Dynamic Soil Densification Modeling

Type of Soil	SM			ML			ML		
Specimen Number	4ST#4			3ST#3			3ST#8		
Factors	a	b	rc (%)	a	b	rc (%)	a	b	rc (%)
Confining Pressure (Kpa)									
25							0.002812	1	0.00683
50	0.00344	1.3	0.0052	0.00597	1.75	0.00725	0.00113	1.5	0.00375
100	0.00333	1.7	0.0023	0.00242	2.5	0.003			

Type of Soil	ML			MH			MH		
Specimen Number	2ST#3			3ST#11B			5ST#2		
Factors	a	b	rc (%)	a	b	rc (%)	a	b	rc (%)
Confining Pressure (Kpa)									
25	0.00534	1.5	0.0071	0.00144	1.6	0.00705			
50	0.00232	1.8	0.003	0.00111	1.6	0.00449	9.9E-05	3.5	0.01692
100	0.00112	3	0.0121	0.0012	2	0.0109			

Type of Soil	SM-ML		ML	
Specimen Number	RC-1,2		RC-3,4,5	
Factors	G1	rg (%)	G1	rg (%)
Confining Pressure (Kpa)				
25	0.382	0.00136	0.416	0.00412
50	0.400	0.00134	0.400	0.00405
100	0.409	0.00192	0.384	0.00448

27

In the above sections, the attenuation of construction induced vibrations, the evaluation of equivalent number of cycles, and the modeling of dynamic settlement and shear modulus of residual soil from NCSU experimental data base were discussed. Based on these considerations, we can evaluate the construction vibration induced settlement using the following procedure :

1. Determine the source characteristics of the construction induced vibration from field measurement or literature, such as presented in Fig. 2.1;
2. Determine the peak particle velocity on the ground surface at the site of the building foundation by field measurement, or surface wave attenuation theory from Eq. 2.1 or 2.3;
3. Estimate the equivalent number of cycles of each event by field time history records or by the simplified method;
4. Calculate the particle velocity amplitude at different depths (for example, 1.5 m, 3.0 m and 6.0 m) by the Rayleigh wave attenuation theory;
5. Find the shear strain amplitude at different depths;
6. Calculate the dynamic settlement by Eq. 2.8 for the equivalent number of cycles for the appropriate shear strain amplitude in each layer; and finally,
7. Obtain the total vibration induced settlement by adding the settlement from each layer.

Wahls (1994) has presented a comprehensive review of criteria for tolerable movements of buildings and bridges. There are basically three criteria which have to be

satisfied when considering limiting settlements: (i) visual appearance, (ii) serviceability or function, and (iii) stability.

The popularly used recommendations on allowable differential settlement of structures were initially proposed by Skempton and MacDonald (1956) and later systematically reviewed by Burland et al. (1977). Table 2.6 is provided following their recommendations. It needs to be emphasized that the tolerable foundation settlement in this table is total settlement, i.e., settlement during and after construction. The construction vibration induced settlement is just one mechanism potentially responsible for the post-construction settlement and therefore, the design criteria for determining tolerable levels for this component must be based on engineering judgment.

Table 2.6 Guidelines for Tolerable Foundation Settlement

	Sands	Clayey Soils
<b>Isolated Foundation:</b>		
Total Settlement	40 mm	65 mm
Differential Settlement	25 mm	40 mm
Relative Rotation	1/500	1/500
Tilt	Determined in Design	Determined in Design
<b>Raft Foundation:</b>		
Total Settlement	40 - 65 mm	65 mm - 100 mm



### **2.3 Scope of Present Study and Organization of Report**

Chapter 3 presents the field verification test program. It includes the site geometry, soil's properties, test equipment and procedure, as well as settlement predictions by using the existing model.

Chapter 4 provides results and discussions of field experiments. The records of settlement and vibration amplitude were reported. The measured vibration attenuation along surface distance and with depth were compared with analytical results.

Chapter 5 shows the laboratory resonant column and torsional shear test results. From these test data, the vibration induced settlement and shear modulus of specimens were obtained as a function of confining pressure, shear strain amplitude, and number of cycles.

Chapter 6 provides the wave attenuation function, a modified model for predicting shear modulus and damping ratio, and the dynamic densification model. The analytical results were verified with that obtained in the field tests.

Finally, the conclusions and recommendations are made in Chapter 7 and the implementation and technology transfer are provided in Chapter 8.

## CHAPTER 3

### FIELD VERIFICATION EXPERIMENTAL PROGRAM

#### 3.1 Site Details

Three field test sites were selected for potential verification of the construction vibration induced settlement model previously described. It was determined that the test sites should be in residual soil with profiles deeper than 10 meters, have undisturbed ground surfaces and be easily accessible by heavy equipment. A deep ground water table (more than 10 m) although not required, would make easy installation of the monitoring system.

At one of the tests sites, in Selma, North Carolina, (Fig. 3.1 and Fig. 3.2) settlement of the residual soil profile was monitored during pile driving. The characteristics of the vibration source and the propagating waves were investigated. Resonant column / torsional shear tests were performed on Shelby samples obtained from this site. The results from this test site were compared with those previously obtained from laboratory tests and predicted by the NCSU analytical model.

At two other tests sites in Raleigh, NC (Fig. 3.1 and Fig. 3.3), exploration bore holes were drilled up to 9m, and SPT tests were performed. Split spoon samples were obtained from these sites, and their Atterberg limits and particle size distribution were determined. By comparing their engineering properties with those of soils in our data base and using our analytical model, we predicted that no measurable settlement would occur

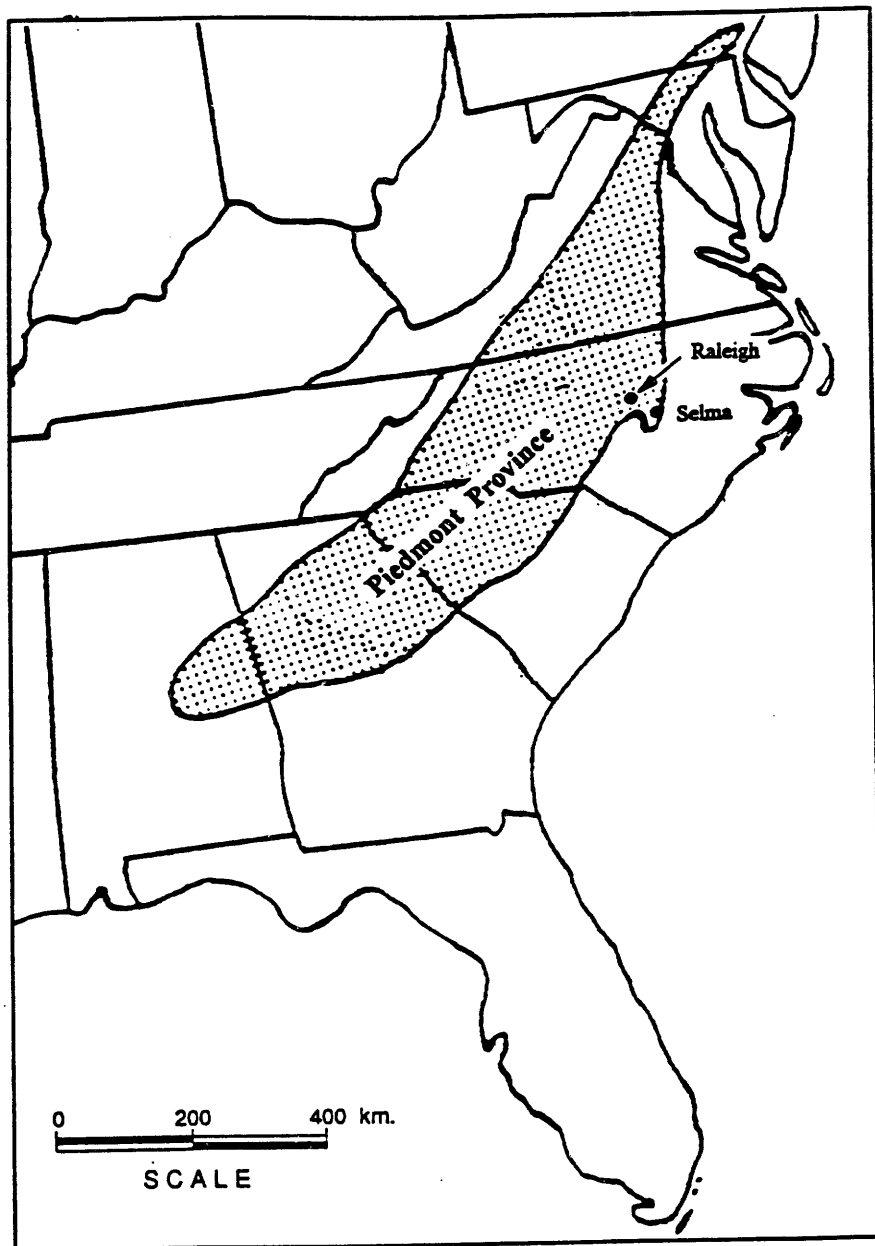


Figure 3.1 Location of the Piedmont Province and Test Sites (After Sowers, 1954)

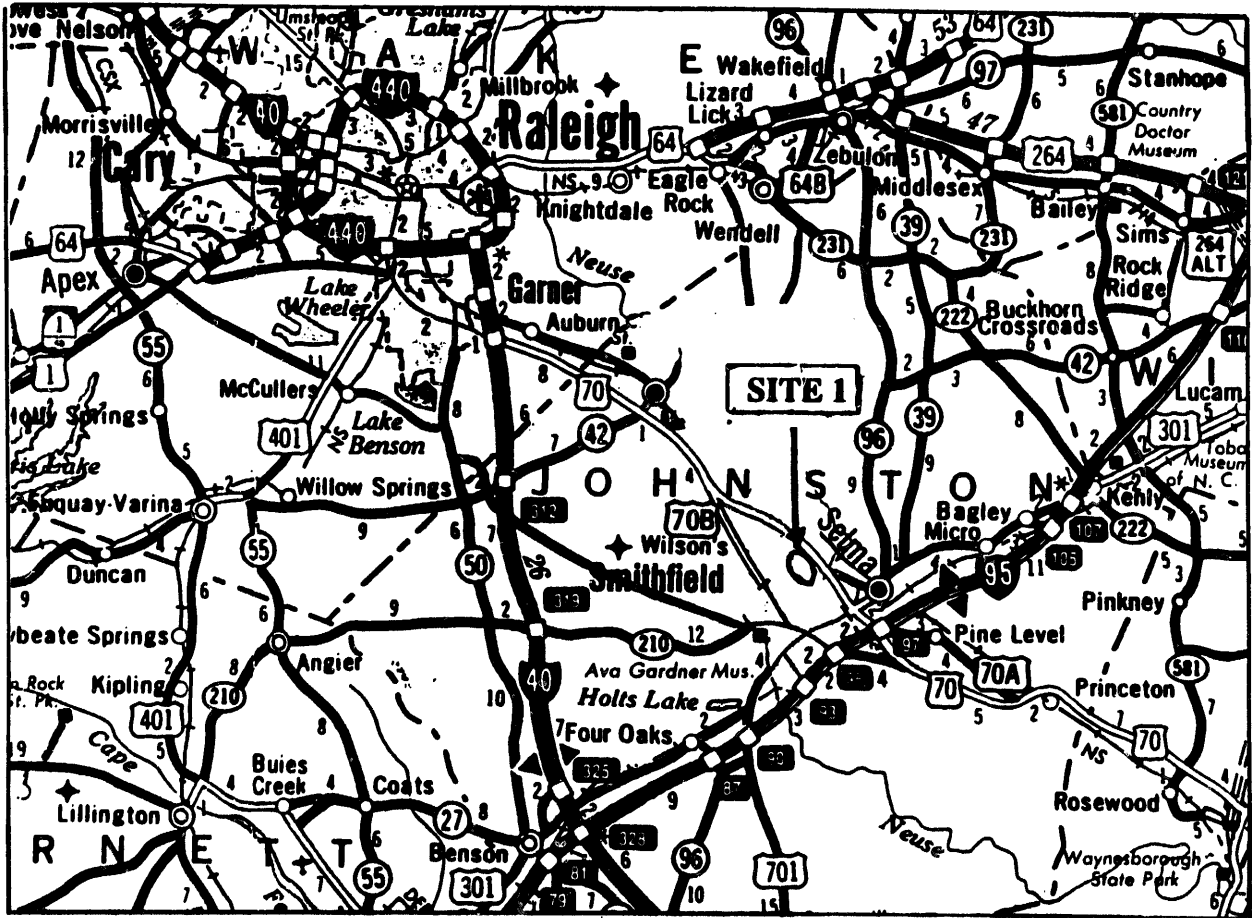


Figure 3.2 Detailed Map of Test Site 1 (Selma, NC)

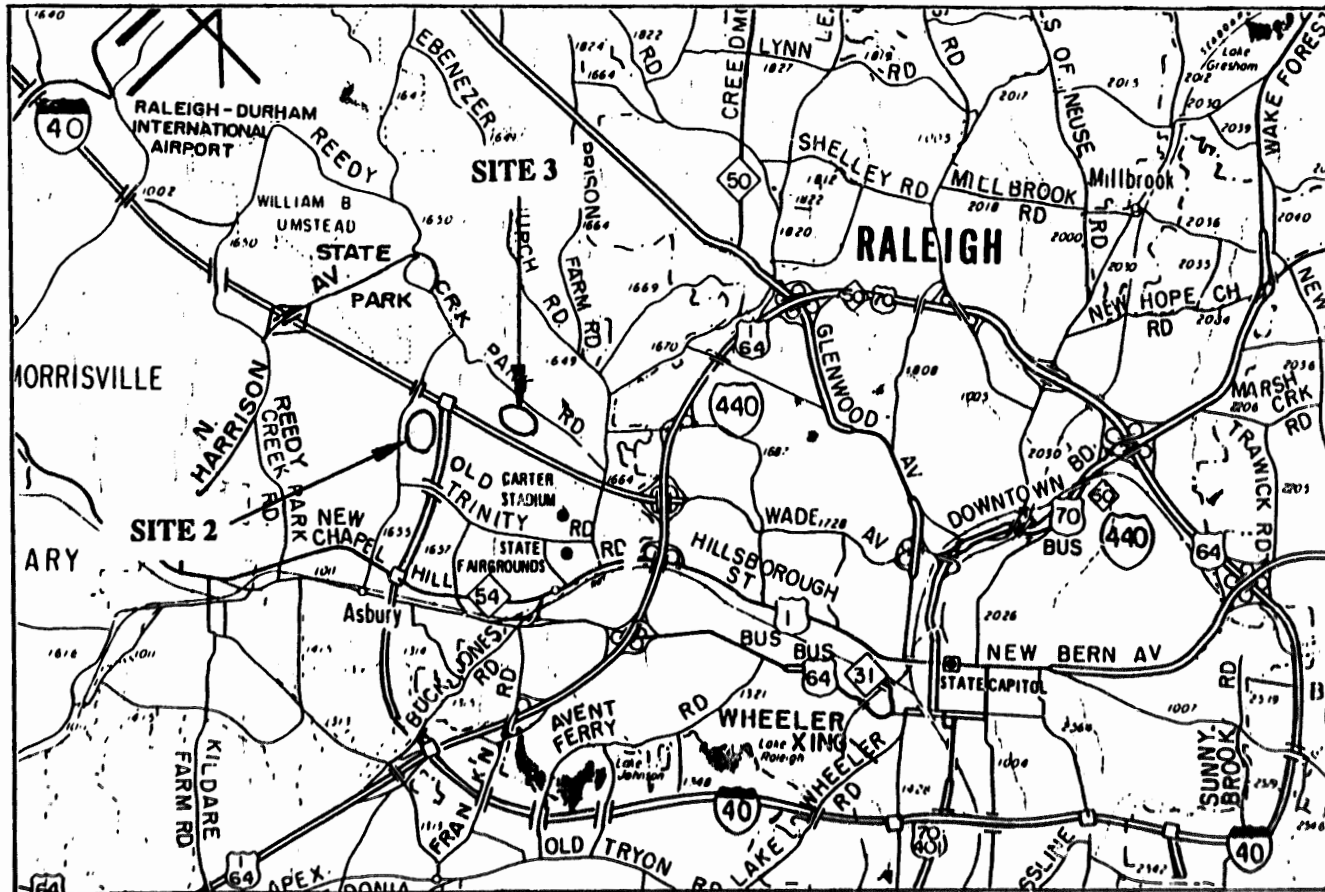


Figure 3.3 Detailed Map of Test Site 2 and Site 3 (Rayleigh, NC)

under construction vibrations. Therefore, dynamic vibration tests were not performed at these two sites:

As shown in Fig. 3.1, site 1 is located in the NCDOT bridge maintenance yard near Selma, Johnston County, North Carolina. This site is at the edge of what is commonly mapped as the Piedmont area. Figure 3.2 shows in detail that the test site is two miles west of Selma along NC-70A and 2.5 miles from the intersection of Interstate 95 and NC-70A. The boring log is shown in Table 3.1. The ground surface is covered with grass. Below the surface to 0.5 m is a sand and gravel layer. From 0.5 to 1.0 m depth, the soil is stiff fine sandy clay with SPT number 9. From 1.0 m to 3.0 m, the soil is stiff fine sandy silt with SPT number around 15. Below 3.0 m, there is very stiff sandy silt and slightly weathered rock. (The SPT N-value exceed 100) The ground water table at the time of testing in March was found at a depth of 9.7 m.

The boring log for test site 2, located on Trenton Road, Raleigh, near the intersection of Interstate 40 and Wade Avenue (Fig 3.3), is shown in Table 3.2. The geologic history and soil profile are the same as that at North Carolina State University (NCSU) Research Farm, 500 m away from the test site, and described by Hertz (1986), Wilson (1988), and Wang (1995). The top 2m of the soil is silty clay with SPT N-value around 10. From depth 2.0 m to 3.0 m, the soil is clayey silt with SPT number around 12. Below 3m, the soil is mainly sandy silt with some rock fragments. The ground water table is deep and the bore hole remained dry for 24 hours later.

Test site 3 is located on the planned Ramp A of the intersection of Edward Mill Road Extension and Wade Avenue (Fig. 3.3). Two bore holes were drilled at a separation

Table 3.1 Soil Profile of Selma Site

Field Verification Test in Selma, North Carolina

Project No. : NCSU                      County : Johnston                      Geologic Province: Piedmont  
 Test Site: NCS  
 Boring Location (Sta.): Salt Bin Yard, Johnston Co. Maint.  
 Boring No.: SPT                      Geologist: C. D. Pender  
 Date started: 3-13-95                      Drill Equipment: BK-51, Hollow Stems, SPT  
 Total Depth: 9m (29.6ft)                      Date completed: 3-13-95

Depth (m)	Depth (ft)	Sample No.	Soil Description
0.75	2.5	6ST#2	sandy, silty clay
1.50	5.0	6ST#2A	sandy silt
2.25	7.5	SS-3	
		ST-2	
3.00	10.0	SS-4	sandy silt
		ST-3	
4.11	13.7		sandy silt
5.61	18.7	WR	SWR
7.11	23.7	WR	SWR
8.61	28.7	WR	

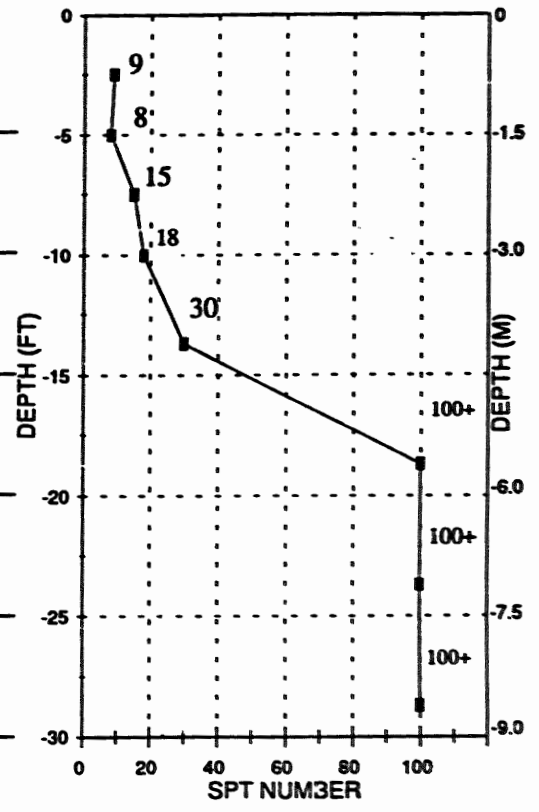
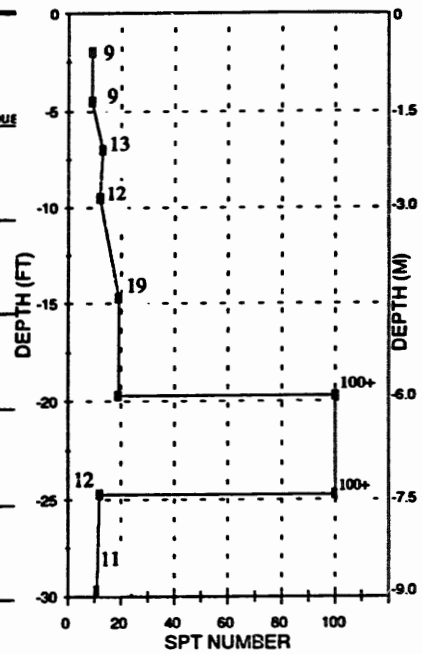


Table 3.2 Soil Profile of Trenton Road Site

Field Verification Test in Raleigh, North Carolina

Project No.: NCSU      County: Wake      Geologic Province: Piedmont  
 Test Site: Vibration Study      Raleigh Belt  
 Boring Location (Sta.): Trenton Road  
 Boring No.: SPT      Geologist: T. L. Vargason      GWT: Dry @24.2 Hrs  
 Date started 6-9-95      Drill Equipment: CME 550, Hollowstems, SPT, Automatic Hammer  
 Total Depth: 9.3m (31.2ft)      Date completed: 6-9-95

Depth (m)	Depth (ft)	Sample No.	Soil Description
0.60	2.0	SS-1	Stiff brown clayey silt, micaceous
		SS-2	gray sand lens 27"-28", qtz gravel
1.35	4.5	SS-3	Stiff tan silty clay (saprolitic, micaceous
		M-3	w/ some qtz gravel
2.10	7.0	SS-4	Stiff tan & grey clayey silt (saprolitic, high micaceous)
2.85	9.5	SS-5	Stiff tan & brown silt w/ thin (0.001ft) fine sand layers
4.41	14.7	SS-6	Med. dense tan silty fine sand w/ 0.05' qtz layers
5.91	19.7		Tan fine grain SWR (granitic) w/ rock fragments of granite
7.41	24.7	SS-7	Stiff tan fine sandy silt qtz gravel layer 0.1' @ 25.8'
8.91	29.7	SS-8	Stiff brown silt (highly micaceous), wet
			Boring terminated @ 31.2'





**Table 3.3a Soil Profile of Edward Mill Road Extension Site (Sta. 5+00)**

**Field Verification Test in Raleigh North Carolina**

Project No. : 8.2402801      County : Wake      Geologic Province: Piedmont  
 Test Site: Ramp A, Edwards Mill Rd. Extension / Wade Ave.  
 Boring Location (Sta.) 5+00      Offset: 40+/-  
 Boring No.: SB1      Geologist: O. B. Oti      GWT: Dry @25.5 Hrs  
 Date started: 7-17-95      Drill Equipment: BK-51, Hollotems, SPT  
 Total Depth: 9m (29.8ft)      Date completed: 7-17-95

Depth (m)	Depth (ft)	Sample No.	Soil Description
0.99	3.3	SS-1	Tan-brown micaceous sandy silt, sap.
2.49	8.3	SS-2	Tan-brown micaceous sandy silt, sap.
3.99	13.3	SS-3	Tan-brown micaceous sandy silt, sap. w/ qtz minor lense
5.49	18.3	SS-4	Tan brown sandy silt w/ trace of micaceous, sap.
6.99	23.3	SS-5	Red-tan-brown micaceous sandy silt, sap.
8.49	28.3	SS-6	Red-tan-brown micaceous sandy silt, sap.

Boring terminated @ 29.8'

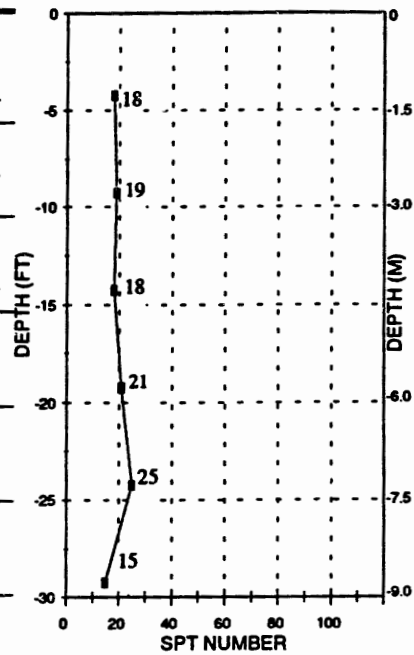
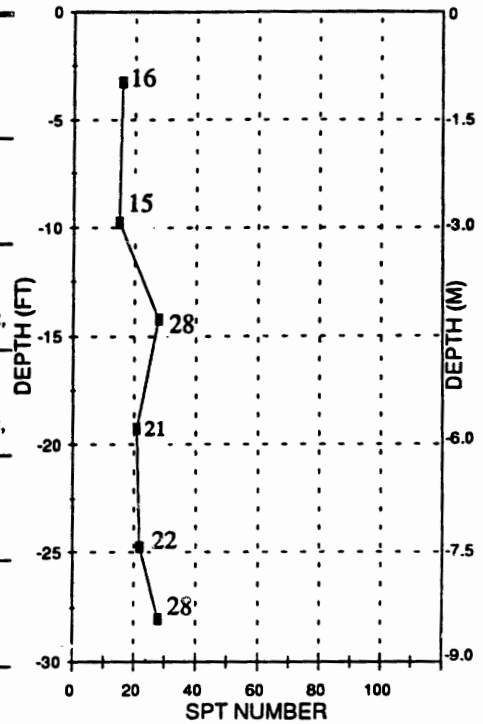


Table 3.3b. Soil Profile of Edward Mill Road Extension Site (Sta. 7+00)

Field Verification Test in Raleigh, North Carolina

Project No. : 8.2402801      County : Wake      Geologic Province: Piedmont  
 Test Site: Ramp A, Edwards Mill Rd. Extension / Wade Ave.  
 Boring Location (Sta.): 7+00      Offset: 40+/-  
 Boring No.: SB2      Geologist: O. B. Oti      GWT: Dry @26 Hrs  
 Date started: 7-17-95      Drill Equipment: BK-51, Hollostems, SPT  
 Total Depth: 9m (29.6ft)      Date completed: 7-17-95

Depth (m)	Depth (ft)	Sample No.	Soil Description
0.93	3.1	SS-7	Red-brown sandy silty clay, residual
2.43	8.1	SS-8	Tan-brown micaceous sandy silt, sap.
3.93	13.1	SS-9	Tan-brown micaceous sandy silt, w/ qtz lense, sap.
5.43	18.1	SS-10	Tan-brown micaceous sandy silt, w/ qtz lense, sap.
6.93	23.1		Tan-brown sandy silt, w/ trace of mica, sap.
8.43	28.1		Yello-tan sandy silt, w/ trice of mica, very sap. Boring terminated @ 29.6'



distance of 65 m. The soil profiles at these two locations are very similar, as shown in Table 3.3a and Table 3.3b, respectively. There is a 1 m thick silty clay cap near the surface, and below that is sandy silt. The SPT number is between 15 and 30. Because of the high SPT number and some quartz particles, Shelby tube sampling would be difficult.

### 3.2 Engineering Characteristics

The engineering properties of the soils at test Site 1 (Selma, NC) were evaluated, which included: initial water content, void ratio, degree of saturation, and specimen dimensions, as shown in Table 3.4. These values were obtained from sample trimmings before RC/TS tests. Specific gravity and grain size analyses were performed on test specimens after RC/TS tests. Table 3.5 gives the percentage of gravel, sand, silt, and clay size particles, the Atterberg limits, and the USCS soil classification for each specimen tested. The soil particle size distribution is also shown in Fig. 3.4.

Table 3.4 Specimens Characteristics of Site 1 (Selma, NC)

Specimen No.	Water Content (%)	Initial Void Ratio	Specific Gravity	Saturation (%)	Initial Length (in)	Initial Diameter (in)
6ST#2	22.4	0.70	2.71	87	5.82	2.87
6ST#2A	22.4	0.75	2.69	80	5.80	2.89
6ST#4	24.8	0.74	2.78	93	5.76	2.90

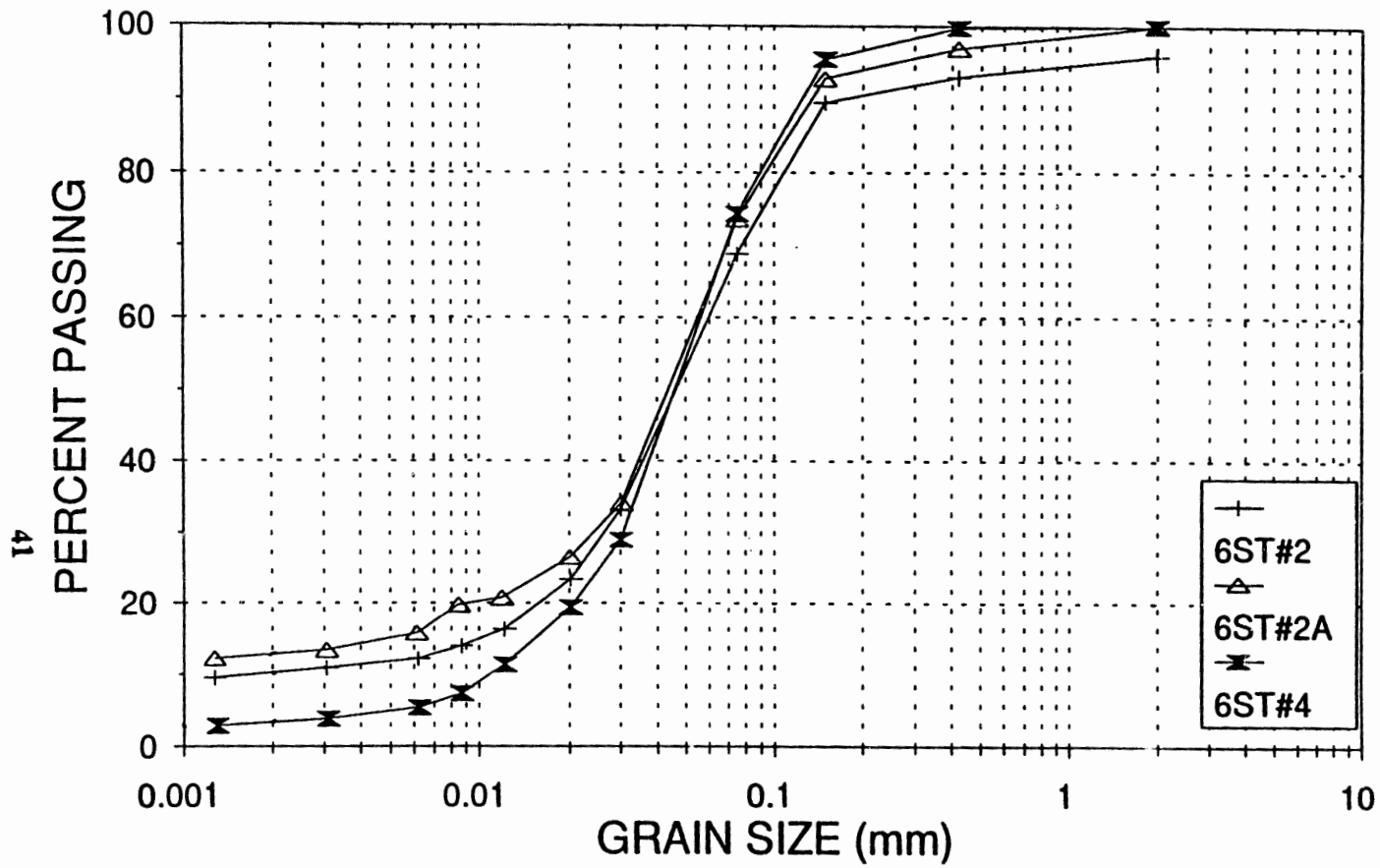


Figure 3.4 Soil Particle Size Distribution of Specimens Tested

Table 3.5 Soil Particle Size Distribution, Atterberg Limits, and USCS Classification of Soils from Site 1

Specimen No.	Gravel > # 4 > 4.75 mm	Coarse # 4 to # 10 2 - 4.75 mm	Medium # 10 to # 40 0.42 - 2 mm	Fine Sand # 40 to # 200 0.074 - 0.42 mm	Silt .074-.002	Clay <.002m	Atterberg			USCS
							LL	PL	PI	
6ST#2	0	4	3	24	59	10	34	35	NP	ML
6ST#2A	0	0	3	23	62	12	38	35	NP	ML
6ST#4	0	0	0	26	72	3	34	33	NP	ML

\*NP = Nonplastic

The Atterberg Limits, the soil particle size distribution, and AASHTO classification of the specimens from Site 2 are listed in Table 3.6. The data provided in Table 3.6 were provided by NCDOT. Predicted dynamic densification of the soil at Site 2 is analyzed in the Section 3.3. The intended dynamic field test was canceled because the predicted settlement was so small and it did not exceed our equipment resolution.

Table 3.6 Engineering Properties of Specimens from Site 2.

Sample No.	SS-1	SS-2	SS-3	SS-4	SS-5	SS-6	SS-7	SS-8
Depth	0.73	0.96	1.60	2.36	3.12	4.71	7.76	9.28
Coarse Sand #60 (%)	14.1	10.6	5.3	3.1	6.5	28.7	14.9	12.6
Fine Sand #270 (%)	38.7	19.6	26.1	45.8	47.3	48.5	46.5	52.5
Silt 0.05-0.005 mm (%)	18.6	16.9	20.2	26.7	36.0	18.7	32.5	28.7
Clay <0.005 mm (%)	28.6	53.0	48.5	24.4	10.2	4.1	6.1	6.1
LL	40	65	65	46	48	27	32	38
PI	19	34	29	16	9	NP	NP	NP
AASHTO	A-6(6)	A-7-5(25)	A-7-5(24)	A-7-5(8)	A-5(4)	A-2-4(0)	A-4(0)	A-4(0)

### 3.3 Predicted Densification Using the Existing Model

Before the field test at Site 1 (Selma, NC), the preliminary site exploration was performed by NCDOT. Based on the information provided, including soil classification, particle size distribution and Atterberg limits, anticipated ground surface settlement due to construction vibration was predicted by the existing model. By matching the engineering properties, specimen 3ST#8 in the NCSU data base was found to be the soil most close to that at the Selma site (Table 3.7).

Table 3.7 Comparison of Engineering Properties between Site 1 and the Data Base

Site 1 (Selma, NC)		Data Base 3ST#8	
Coarse Sand #60	7.6%	0.42-2 mm	0.8%
Fine Sand #270	21.1%	0.074-0.42 mm	34.2%
Silt 0.05-0.005 mm	53.1%	0.074-0.002 mm	61.9%
Clay <0.005 mm	18.1%	<0.002 mm	3.1%
LL=44	PI=8	LL=36	PI= ---

The dynamic properties of specimen 3ST#8 can be obtained from Chapter 5 of the report "Construction Related Vibrations" (Borden, Shao and Gupta, 1994). It was assumed that the further tests would use a pile driving energy on the order of 24.4 KJ (18,000 ft\*lb) with 1000 blows; the peak particle velocity resulted on the ground surface would be 50.8 mm/sec; and that the dominant frequency would be 30 Hz. To produce a

conservative estimate, it was assumed that there was no load on the ground surface and that the residual soil profile was as deep as 10 meters. By using the computer program, CVIS (Construction Vibration Induced Settlement), the settlement of the ground surface was predicted to be 1.7 mm.

In order to maximize the measurable settlement, it was decided that the model footing on the ground surface would not be necessary. From the previous study by Borden, Shao and Gupta (1994), it is clear that dynamic settlement is reduced by increasing confining pressure. At the Selma test site, the predicted ground settlement was very small, so there was no loading on the ground surface in the field test design.

Following the same procedure just outlined for Site 1, the dynamic settlement at Site 2 (Trenton Road, Raleigh) was predicted only 0.6 mm. It was again assumed that the pile driving energy would be 24.4 KJ (18,000 ft\*lb) with 1000 blows; the peak particle on the ground surface would be 50.8 mm/sec; and that the dominant frequency is 30 Hz. The analysis assumed no load on the ground surface and that the soil profile was divided to three layers as shown in Table 3.8. The top layer is basically a silt clay, which is unlikely densified under dynamic load. Because the predicted settlement is less than the resolution of the extensometer, the dynamic verification tests at this site were not performed.

Table 3.8 Prediction of Dynamic Settlement on Site 2 (Trenton Road, Raleigh)

	Layer 1	Layer 2	Layer 3
Depth (m)	0.0-2.0	2.0-4.5	4.5-7.5
Sample No.	SS-3	SS-5	SS-7
Data Base	5ST#2	3ST#8	4ST#4
Shear Strain Amplitude (%)	0.040	0.017	0.0027
Settlement (mm)	0.27	0.31	0.07

### 3.4 Test Equipment

In the field tests, the settlement in the soil profile is observed by an extensometer. The vibration time history is monitored by geophones on the ground surface and in a bore hole. The vibration signal is recorded by a computerized data acquisition system. Each of these systems are discussed in the following sections.

#### 3.4.1 Extensometer

The extensometers used in this study can measure the settlement at different depths below the ground surface. As the vibration amplitude and over burden pressure vary with depth, the dynamic densification through out the soil profile should be expected to vary. As shown schematically in Fig. 3.5, the extensometer has spider magnets fixed in the bore hole at desired depths. These spider magnets are free to move with the soil as consolidation or densification occurs. A PVC access tube sits on the datum, which is placed at a location where no settlement is anticipated below this depth. Inside the access tube, a magnet reed switch probe can give the elevation when it passes through the spider



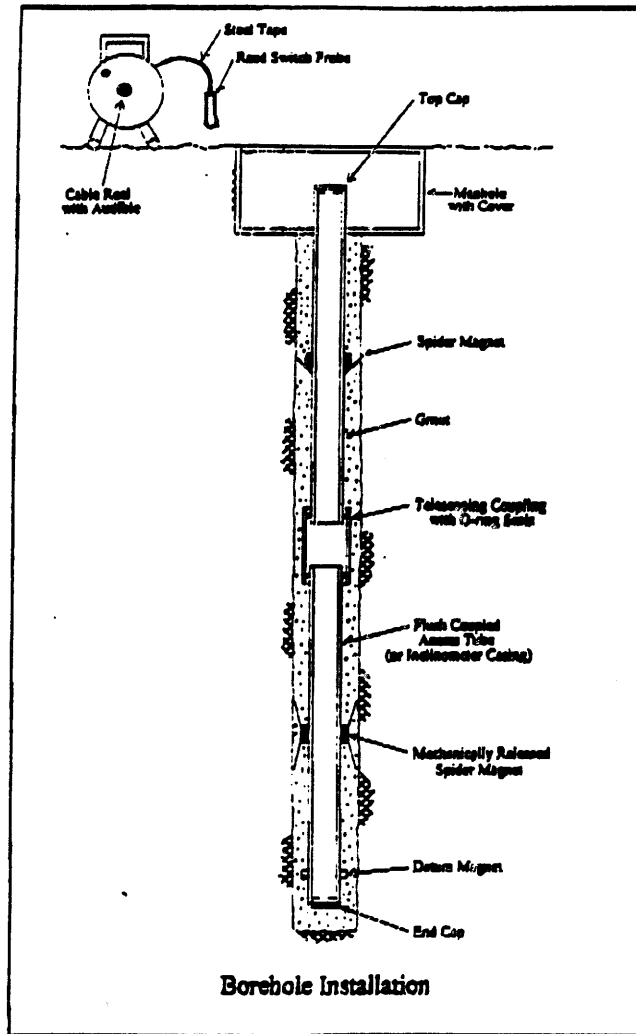


**Figure 3.5 Magnet Extensometer System**

magnet. By monitoring the elevation of spiders before and after construction activities, one can calculate the dynamic settlement at different depths. The resolution of this device is 2 mm, proved by the manufacturing company. The extensometer can measure the settlement both above and below the ground water table.

### 3.4.2 Geophones

A total of eight geophones were used to measure vibrations in the soil profile. They are made by Mark Product and West Atlas Inc. Among them, one three dimensional land geophone package and two vertical land geophones were used to evaluate the construction wave propagation along the ground surface, and one 3-D bore hole geophone package was used to record vibrations within the soil profile.

Geophones with a natural frequency of 4.5 Hz were selected to measure vibrations on the ground surface. They have linear response outputs within the frequency ranges of construction induced vibrations. The calibration curves of 4.5 Hz geophones have constant factor values in the frequency range larger than 10 Hz. One three dimensional borehole geophone system with pneumatic packer includes three geophones (two horizontal and one vertical) with 10 Hz natural frequency. The pneumatic packer can be inflated by compressed air and push the geophone case against the wall of the bore hole. The parameters of geophones used in the field test are listed in Table 3.9.

Table 3.9 Geophone Parameters

Geophone	Model	Natural Frequency	Sensitivity V/mm/s (V/in/s)	Channel
1-D Surface Geophone	Mark Product L-10B Vertical	4.5 Hz	0.0312 (0.793)	0
	Western Atlas SM-6B Vertical	4.5 Hz	0.0288 (0.730)	1
3-D Surface Geophone	Western Atlas SM-6B Vertical	4.5 Hz	0.0288 (0.730)	2
	Western Atlas SM-6B Horizontal	4.5 Hz	0.0288 (0.730)	3
	Western Atlas SM-6B Horizontal	4.5 Hz	0.0288 (0.730)	4
3-D Bore Hole Geophone	Mark Product Model 410 Vertical	10.0 Hz	0.0220 (0.560)	5
	Mark Product Model 410 Vertical	10.0 Hz	0.0220 (0.560)	6
	Mark Product Model 410 Horizontal	10.0 Hz	0.0220 (0.560)	7

### 3.4.3 Data acquisition system and computer software

To record and analyze construction induced vibrations, a computerized data acquisition system was developed in the Department of Civil Engineering, NCSU. This system includes a Toshiba 486-DX4 notebook computer, National Instrument DAQCard-700 data acquisition card, and LabView software package as shown in Fig. 3.6.

The Toshiba notebook computer provides the platform to drive the data acquisition card, to record data, and to analyze the vibration wave forms. It has an Intel

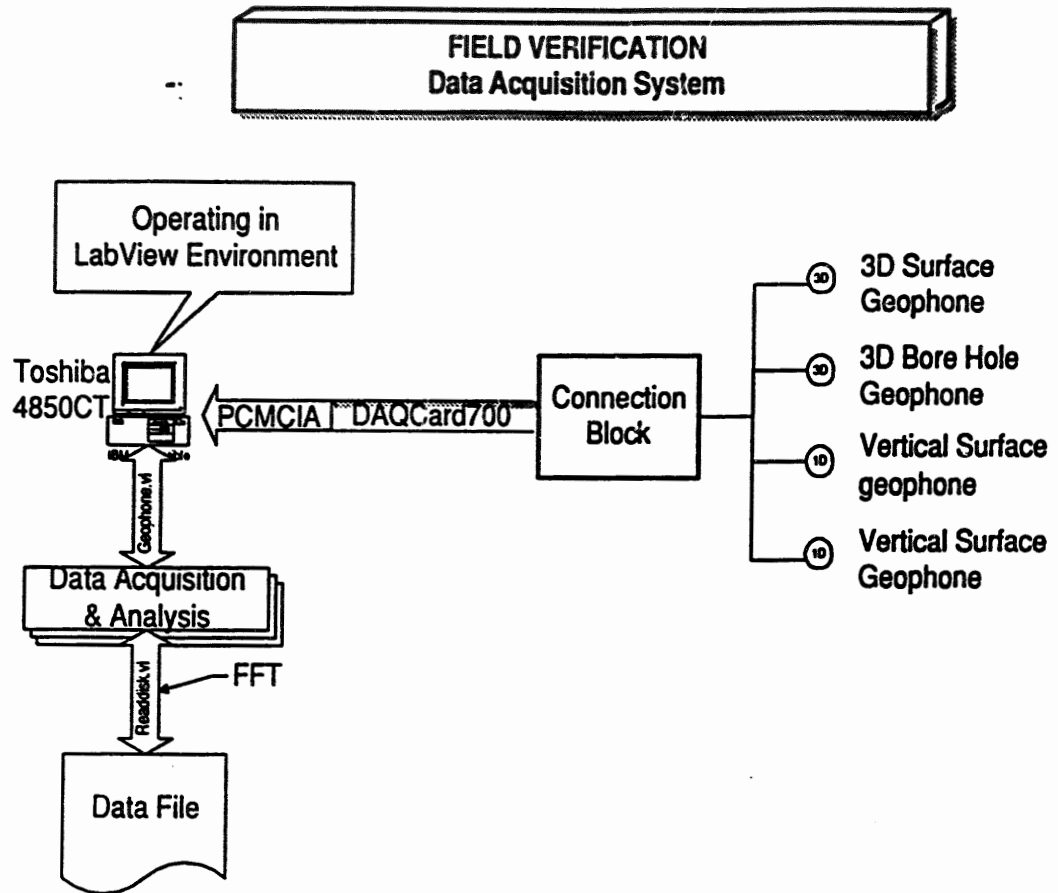


Fig. 3.6 Computerized Data Acquisition and Analysis System

486-DX4 75 MHz CPU, 8MB RAM, 520MB hard disk, 29 cm active matrix LCD monitor, and PCMCIA slots.

National Instrument DAQCard 700 is a Type II PCMCIA multi-function I/O board for notebook computer. It has a 12-bit ADC with 16 single-ended or 8 differential analog inputs, an 8-bit TTL-compatible digital input port, an 8-bit TTL-compatible digital output, and two 16-bit counter/timer channels for timing I/O. The PCMCIA interface has 16-bit data paths with interrupt generation circuitry.

In the field tests, 8 differential input channels were used. With differential input, each input had its own ground reference. Noise errors could be reduced because the common-mode noise picked up by the leads was canceled. We found that the AC power supply generated considerable noise to the data acquisition system. During the test, the AC power supply were turned off and the computer was only powered by its internal battery.

An internal multiplexer of the data acquisition card provides the capacity to measure 8 channels with a single ADC. The maximum sampling rate of DAQCard 700 is 100 K/Sec. Because the same ADC is sampling many channels instead of one, the effective rate of each individual channel is inversely proportional to the number of channels sampled. When all the eight channels are used, the maximum sampling rate reduces to 12.5 K/Sec. The frequency of the construction induced vibration is in the range of 20 - 50 Hz, therefore, a sampling rate larger than 1 KHz is considered enough to record peak vibration amplitude. Higher sampling rate is desired for frequency analysis. A 512-word FIFO (First In First Out) buffers the data during multiple A/D conversions to prevent data loss due to bus latency of the host notebook computer. The inter-channel delay can be calculated as:

$$\text{Inter Channel Delay} = \frac{\text{Sampling Period}}{\text{Number of Channels}} \quad (3.1)$$

Before the field tests, the sampling rate and the inter-channel delay are measured and calibrated in the lab.

The ranges of analog input signal are software selectable to  $\pm 10\text{V}$ ,  $\pm 5\text{V}$ ,  $\pm 2.5\text{V}$ . The gain is always one for all channels. The output of geophones is usually in the range of  $\pm 2.5\text{V}$ . The vibration signal can be connected to the data acquisition card directly without any amplification or conditioning. The range, resolution, and gain on a DAQ card determine the smallest detectable change in voltage. This change in voltage represents 1 LSB of the digital value, which is often called the code width. In the range of  $\pm 2.5\text{V}$ , the ideal code width of the 12-bit DAQ card is:

$$1 \text{ LSB} = \frac{\pm 2.5 \text{ V}}{2^{12}} = \pm 0.61 \text{ mV} \quad (3.2)$$

The relative accuracy of DAQCard 700 is  $\pm 1$  LSB typical and  $\pm 1.5$  LSB maximum. The nonlinearity deviation (DNL) is  $\pm 0.5$  LSB typical and  $\pm 1.0$  LSB maximum. Conservatively, the accuracy of the input signal sampled is considered as  $\pm 1.5$  LSB typical ( $\pm 0.92 \text{ mV}$  in the range of  $\pm 2.5\text{V}$ ), and  $\pm 2.5$  LSB maximum ( $\pm 1.53 \text{ mV}$ ). Also, because the input impedance of the data acquisition card is  $1 \text{ G}\Omega$ , there is little interference between the geophones and the input ports of the card. Compared with the geophones output signal range, DAQCard 700 provides satisfactory resolution.

The data acquisition system is controlled by the program, GEOPHONE.VI, which is written in G language under the LabView environment. It can config hardware, set up ranges for each input channel, select sampling frequency, and record data. It uses software to assemble programmable hardware instruments to function as a digital oscilloscope, operational amplifiers, and disk drivers, etc. The user can set up trigger channel and trigger voltage, and the computer can save data automatically if the input

signal exceed the threshold value. The data file is written in the spread sheet format and saved in the user defined name and directory. After the test, the data file can be easily processed in LabView working environment or by other spread sheet programs. GEOPHONE.VI is a graphical based interactive program. The front panel of the program has a multi-channels digital oscilloscope, which shows vibration wave forms for each channel (Fig. 3.7). All the parameters can be adjusted during data acquisition session and the operation is very straight forward. Because the LabView is a window based software package, all the data and figures in the GEOPHONE.VI program can be transferred through any window based software. The user can copy and paste data and figures to desired word processing or spread sheet programs.

MS DOS and MS Window (V3.1) operating systems have a 55 ms barrier to response control signals. To solve this problem, GEOPHONE.VI uses an advanced computer technique, multi-buffers, to record data at high speed. The FIFO buffer in the DAQCard 700 and the computer cache prevent data loss due to bus latency. To accelerate the data recording speed, the data acquisition function and the data analysis function are performed in separate programs. GEOPHONE.VI records the incoming voltage signals from eight channels. READWAVE.VI, PREANA.VI and SASW.VI can view the data, convert voltage signals into vibration velocities, pick up peak vibration amplitude, and perform FFT and cross power spectrum analysis.

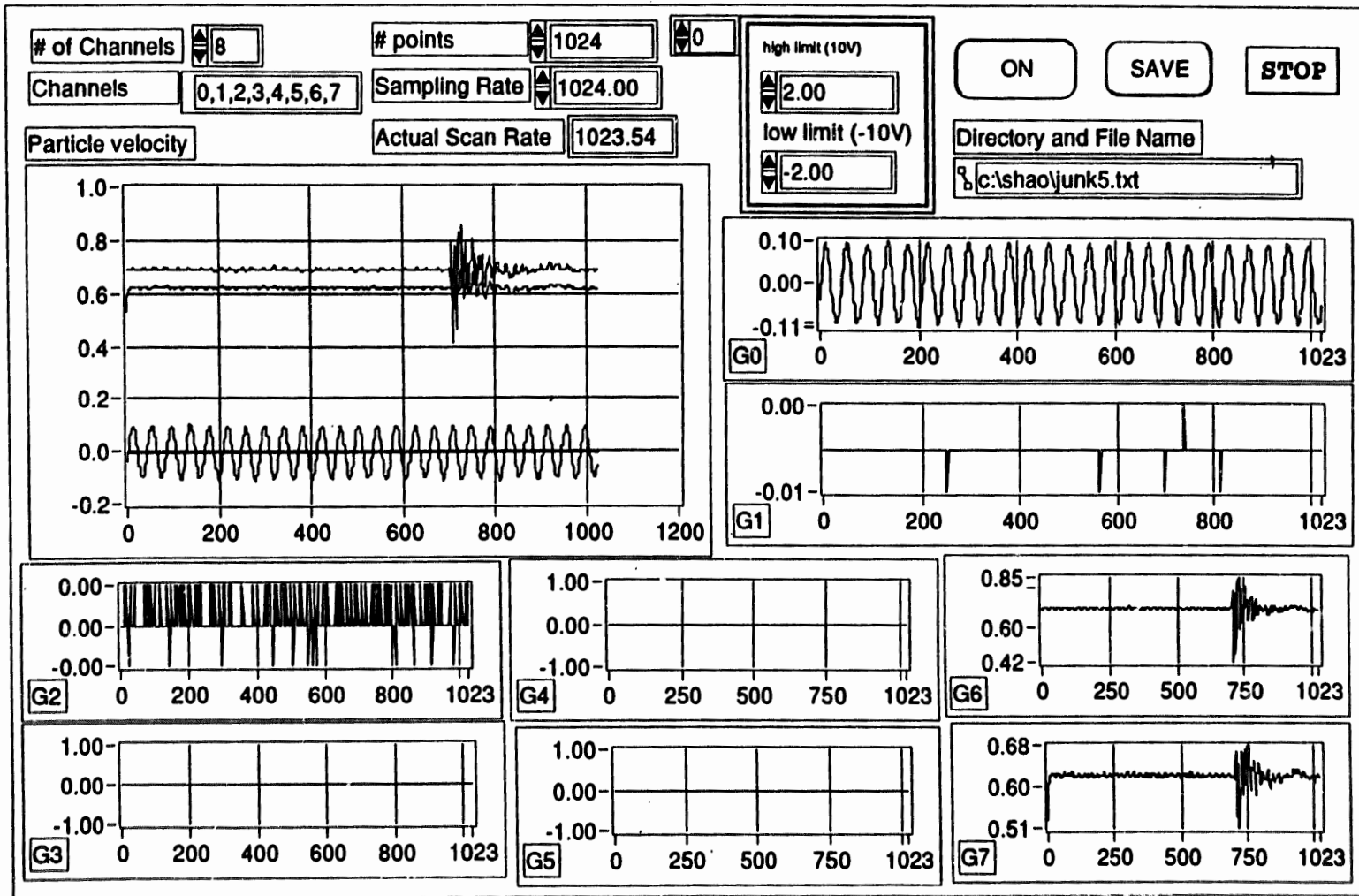


Figure 3.7 Front Panel of the Data Acquisition Program



### **3.5 Experimental Procedure**

The procedure of the field verification test included the field exploration (SPT, split spoon sampling, etc.), Shelby tube sampling, installation of the extensometer and geophones casing, pile driving, vibration time history recording, and settlement monitoring.

#### **3.5.1 Site design**

The test site in Selma located in a open field behind the salt dome in the NCDOT bridge maintenance yard in Johnston County. Two piles, Pile A and Pile were driven at 3.66 m (12 ft) and 2.44 m (8ft), respectively, from the extensometer. As shown in Fig. 3.8 and Fig. 3.9, the geophone hole and the extensometer hole located on a circle, on which the distance from piles to the geophone hole and the extensometer hole were the same. The vibration amplitude at these two holes were considered identical. The 3-D bore hole geophone package was placed in the geophone hole to record vibration time history inside soil profile. A 3-D surface geophone (marked as S3 in Fig. 3.8) was placed on the same circle, on which geophone hole and extensometer hole were located (Fig. 3.10). Two vertical surface geophones, MV and WV, were placed at different distance from the piles. Pile A and Pile B were 10.67 m and 10.36m long timber piles, respectively, and 23 cm in diameter at the tip, and 40.4 cm at the end.

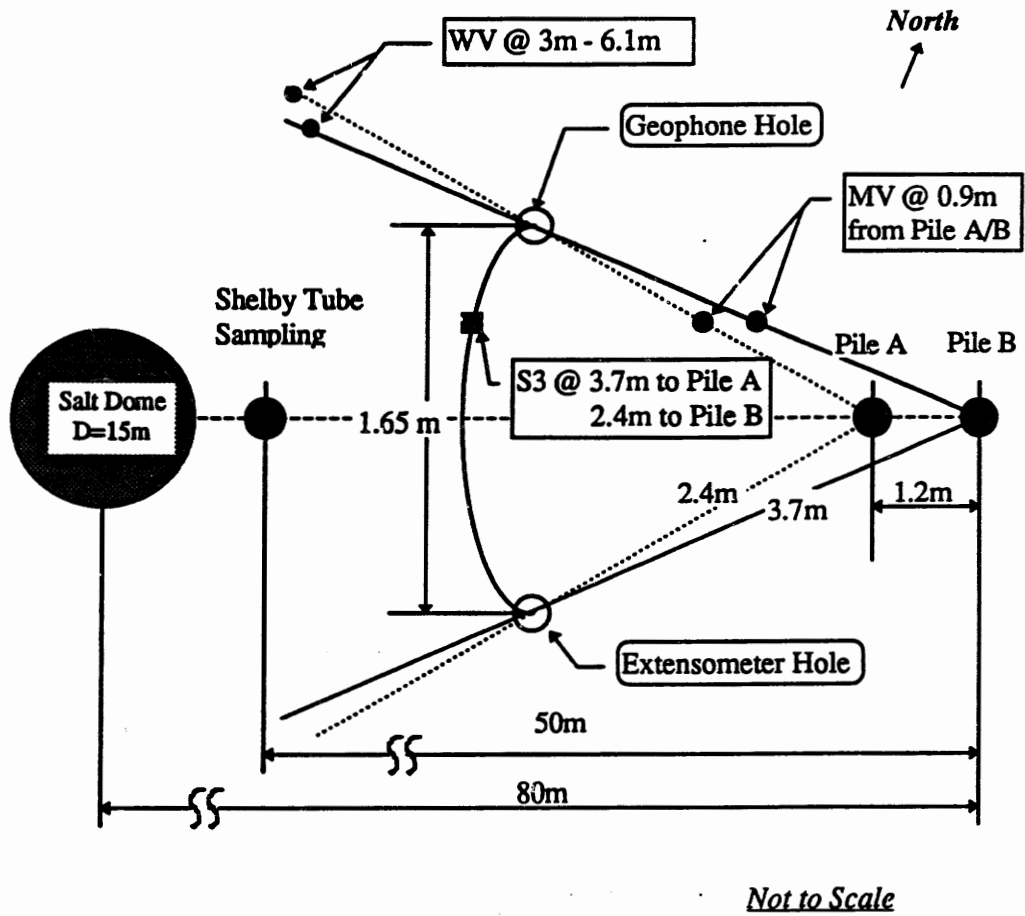


Figure 3.8 Field Test Design at Site 1 (Selma, NC)

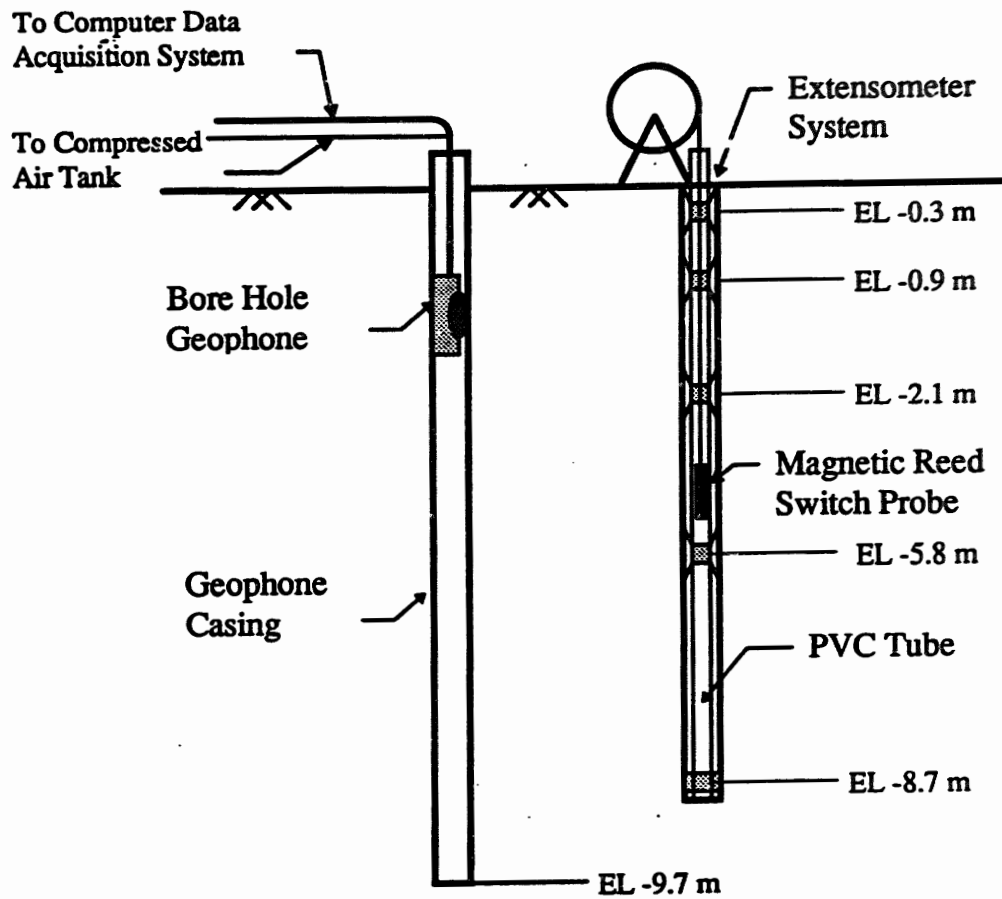


Figure 3.9 Design of Extensometer and Bore Hole Geophone

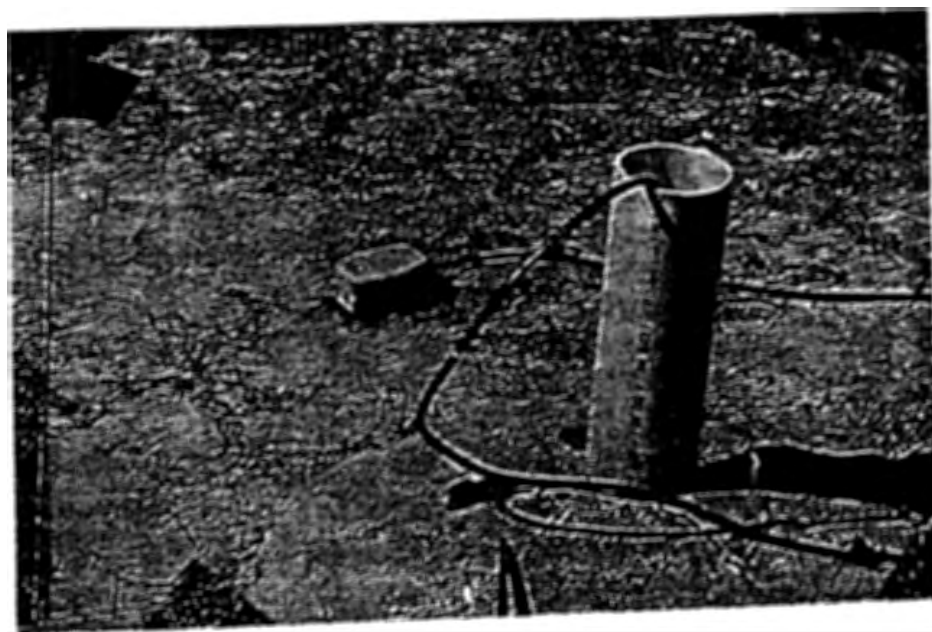


Figure 3.10 Picture of 3-D Surface Geophone and the Geophone Casing



Figure 3.11 Picture of the Access Tube, Reference Ring and Spider Magnet of the Extensometer

### **3.5.2 Installation of extensometer and geophone casing**

The extensometer hole was drilled to 10.3 m deep by a 10.0 cm diameter( 4 inch) auger. Due to cave in of soil, the final depth of the bore hole was 10.0 m. The access tube was assembled from six 1.5 m PVC tube sections. At the end of each section, there were flush coupling connections. An end cap was affixed to the bottom length of access tubing using PVC cement. One datum ring was installed 30 cm from the tube bottom and one reference ring installed 15 cm from the top with PVC cement and screws. Four spider magnets were positioned along the access tubing at depths of 0.3 m, 0.9 m, 2.1 m, and 5.8 m. They were temporarily secured by masking tape and all the leaf springs were wrapped by wire loops which attached to a trigger cable. The access tube sections and spider magnets were lowered down into the bore hole along with a grouting tube. After the access tube settled firmly on the bore bottom, the elevation of each spider magnet was verified by the reed probe. The leaf springs were release by pulling out the trigger cable, so they could firmly hold the sidewall of the boring and support the magnet. The bore hole was grouted from bottom up with cement / bentonite slurry while the grouting tube was pulled up carefully. The grouting slurry was prepared with a slurry pump using 82.6% of water, 12.4% of cement and 5.0% of bentonite by weight. The picture of the access tube, the reference ring and a spider magnet are shown in Fig. 3.11. This picture was taken after the field test was completed and the equipment was excavated.

The geophone bore hole was drilled with a 12.5-cm (5 inch) auger to the depth of 10.30 m (31 ft) and the real depth measured was 9.70 m (29 ft) due to cave in of soil. Two sections of PVC tube (inside diameter, 10 cm) were connected as a 10-m (30 ft)

length geophone casing. An end cap was affixed to the bottom length of the tube using PVC cement. After half of the bore hole was filled with thick cement slurry, the casing was pushed into the bore hole by the drilling equipment (Fig 3.12). The gap between the bore hole and the casing was filled with grout slurry to provide required continuity between the geophone inside the casing and adjacent soil.

### 3.5.3 Pile driving procedure

Two timber piles were driven at the Selma site. As shown in Fig. 3.13, the pile driving equipment is mounted on a heavy crane. A 1350 kg (3000 lb.) steel hammer was lifted by the crane to the height of 1.83m (6 ft) for the pile A, 3m (10 ft) for the pile B, and then released to strike the pile cap. Because the height of the hammer lifted was estimated by the crane driver and the impact location on the pile cap was variable, the pile driving energy varied for each blow. Therefore, the ground vibration amplitude was also not constant. The settlement in the soil profile was measured after desired number of blows and the vibration time histories on the ground surface and in the soil profile were recorded.

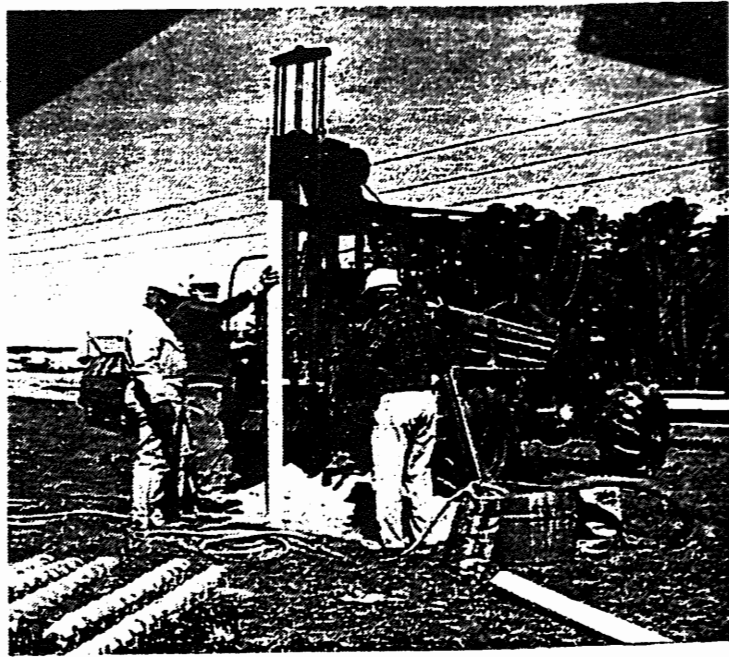


Figure 3.12 Installation of Geophone Casing

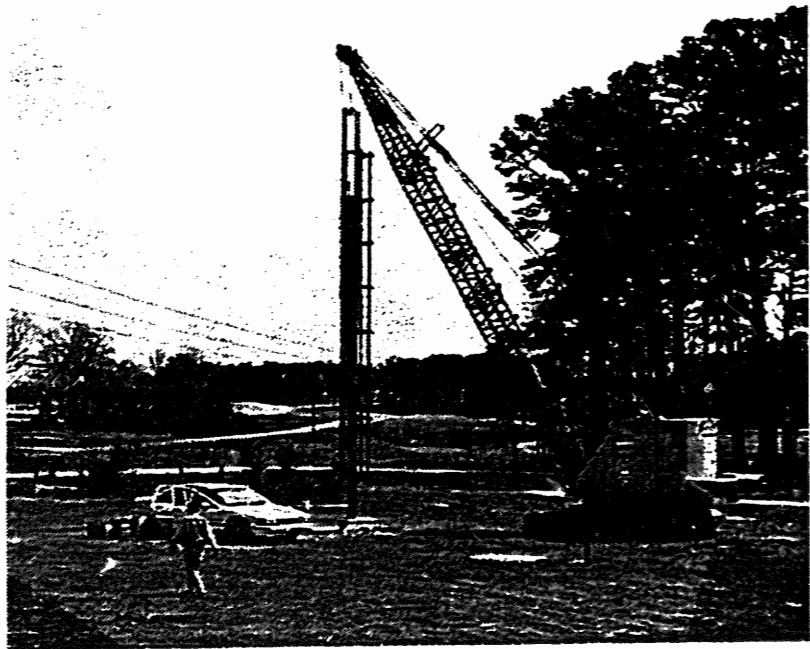


Figure 3.13 Picture of Field Test Site 1 (Selma, NC)

## CHAPTER 4

### RESULTS AND DISCUSSION OF FIELD EXPERIMENT

#### 4.1 Settlement Induced by Pile Driving Vibrations

At the field test Site 1 (Selma, NC), the settlement of the soil profile during pile driving was measured using the extensometer system previously described. Four spider magnets were installed at depths of 0.3m, 0.9m, 2.1m, and 5.8m. The location of each magnet was measured by a reed probe after installation of the extensometer, before pile drilling, during pile driving, and after pile driving. Table 4.1 shows the elevation readings of each spider magnet. There are two magnetic rings in each spider magnet, which result in two elevation readings from the upper ring and the lower ring, respectively. The average of the upper and lower reading gives the elevation of the spider magnet. The elevation of each spider magnet was measured twice to prove the accuracy of the data.

As shown in Table 4.1, there was no measurable settlement due to the vibrations caused by pile driving. The average elevation of each spider magnet and their corresponding standard deviation are listed in Table 4.2. The variation of elevations is less than 2 mm, which is within the resolution of the extensometer system.

#### 4.2 Pile Driving Vibrations

The pile driving induced vibrations were monitored by geophones. The sensitivity and channel connection of each geophone is presented in Table 3.9. The geophone locations are shown in Fig. 3.7. The location of a 3-D surface geophone system (marked



Table 4.1 Extensometer Records at Site 1 (Selma, NC)

Location	Before Trigger Released 3/10/95						After Trigger Released 3/10/95						3/13/95			3/17/95				
	lower		upper		average	lower		upper		average	lower		upper		average	lower		upper		average
M1 @ 0.3m (1ft)	0.290	0.290	0.282	0.282	0.286	0.279	0.279	0.271	0.271	0.275	0.264	0.263	0.255	0.254	0.259	0.263	0.263	0.254	0.254	0.259
M2 @ 0.9m (3ft)	0.958	0.958	0.950	0.949	0.954	0.954	0.955	0.948	0.946	0.951	0.942	0.942	0.937	0.937	0.940	0.943	0.943	0.933	0.934	0.938
M3 @ 2.1m (7ft)	2.163	2.162	2.154	2.153	2.158	2.162	2.161	2.153	2.153	2.157	2.154	2.153	2.145	2.145	2.149	2.153	2.154	2.144	2.144	2.149
M4 @ 5.8m (19ft)	5.870	5.870	5.861	5.861	5.866	5.870	5.870	5.862	5.862	5.866	5.865	5.864	5.855	5.855	5.860	5.864	5.864	5.855	5.855	5.860
Datum @ 8.7m (29ft)	8.740	8.740	8.732	8.732	8.736	8.738	8.738	8.731	8.731	8.735	8.739	8.739	8.730	8.730	8.735	8.740	8.740	8.732	8.732	8.736

62

Location	Before Pile Drving 3/20/95						1st Pile 1Blows						1st pile 5 Blows						1st Pile 10 Blows					
	Upper		Lower		average	Upper		Lower		average	Upper		Lower		average	Upper		Lower		average				
M1 @ 0.3m (1ft)	0.254	0.254	0.264	0.263	0.259	0.254	0.254	0.263	0.263	0.259	0.256	0.256	0.265	0.265	0.261	0.256	0.255	0.265	0.264	0.260				
M2 @ 0.9m (3ft)	0.934	0.933	0.943	0.943	0.938	0.934	0.933	0.943	0.942	0.938	0.935	0.934	0.944	0.942	0.939	0.934	0.935	0.943	0.943	0.939				
M3 @ 2.1m (7ft)	2.146	2.146	2.155	2.155	2.151	2.145	2.145	2.154	2.154	2.150	2.147	2.145	2.156	2.155	2.151	2.146	2.146	2.155	2.155	2.151				
M4 @ 5.8m (19ft)	5.857	5.856	5.866	5.865	5.861	5.856	5.855	5.865	5.865	5.860	5.857	5.856	5.867	5.866	5.862	5.855	5.856	5.866	5.865	5.861				
Datum @ 8.7m (29ft)	8.733	8.732	8.742	8.741	8.737	8.732	8.731	8.741	8.740	8.736	8.734	8.733	8.742	8.741	8.738	8.733	8.732	8.742	8.741	8.737				

Location	1st Pile 20 Blows						1st Pile 50 Blows						1st pile 100 Blows						1st Pile 200 Blows					
	Upper		Lower		average	Upper		Lower		average	Upper		Lower		average	Upper		Lower		average				
M1 @ 0.3m (1ft)	0.256	0.255	0.264	0.264	0.260	0.255	0.255	0.265	0.264	0.260	0.256	0.255	0.264	0.265	0.260	0.255	0.254	0.264	0.263	0.259				
M2 @ 0.9m (3ft)	0.935	0.934	0.944	0.943	0.939	0.934	0.933	0.943	0.942	0.938	0.934	0.935	0.944	0.943	0.939	0.934	0.933	0.943	0.942	0.938				
M3 @ 2.1m (7ft)	2.146	2.146	2.155	2.155	2.151	2.146	2.145	2.155	2.154	2.150	2.146	2.147	2.155	2.156	2.151	2.146	2.145	2.155	2.154	2.150				
M4 @ 5.8m (19ft)	5.857	5.856	5.866	5.865	5.861	5.856	5.856	5.866	5.865	5.861	5.857	5.858	5.866	5.867	5.862	5.856	5.855	5.865	5.864	5.860				
Datum @ 8.7m (29ft)	8.734	8.732	8.741	8.741	8.737	8.733	8.732	8.741	8.740	8.737	8.735	8.733	8.741	8.741	8.738	8.732	8.732	8.741	8.740	8.736				

Table 4.1 Continued

Location	1st Pile 303 Blows					2nd Pile 18Blow					2nd pile 5 Blows					2nd Pile 10 Blows				
	Upper		Lower		average	Upper		Lower		average	Upper		Lower		average	Upper		Lower		average
M1 @ 0.3m (1ft)	0.255	0.256	0.264	0.264	0.260	0.254	0.254	0.264	0.263	0.259	0.255	0.256	0.265	0.264	0.260	0.255	0.254	0.264	0.263	0.259
M2 @ 0.9m (3ft)	0.934	0.934	0.943	0.943	0.939	0.933	0.933	0.942	0.942	0.938	0.934	0.933	0.943	0.942	0.938	0.934	0.933	0.942	0.942	0.938
M3 @ 2.1m (7ft)	2.146	2.146	2.154	2.155	2.150	2.145	2.145	2.154	2.154	2.150	2.145	2.146	2.154	2.155	2.150	2.145	2.145	2.154	2.154	2.150
M4 @ 5.8m (19ft)	5.856	5.857	5.865	5.866	5.861	5.856	5.855	5.865	5.865	5.860	5.857	5.856	5.866	5.865	5.861	5.856	5.855	5.865	5.865	5.860
Datum @ 8.7m (29ft)	8.734	8.732	8.741	8.741	8.737	8.732	8.732	8.740	8.740	8.736	8.732	8.733	8.741	8.741	8.737	8.732	8.732	8.740	8.740	8.736

Location	2nd Pile 20 Blows					2nd Pile 50 Blows					2nd pile 100 Blows					4 days after pile driving 3/24/95				
	Upper		Lower		average	Upper		Lower		average	Upper		Lower		average	Upper		Lower		average
M1 @ 0.3m (1ft)	0.255	0.255	0.265	0.264	0.260	0.255	0.254	0.264	0.263	0.259	0.255	0.255	0.264	0.264	0.260	0.256	0.256	0.264	0.264	0.260
M2 @ 0.9m (3ft)	0.934	0.934	0.943	0.943	0.939	0.933	0.933	0.942	0.942	0.938	0.933	0.933	0.943	0.942	0.938	0.934	0.934	0.943	0.943	0.939
M3 @ 2.1m (7ft)	2.145	2.146	2.154	2.155	2.150	2.145	2.145	2.154	2.154	2.150	2.145	2.145	2.155	2.155	2.150	2.146	2.145	2.155	2.155	2.150
M4 @ 5.8m (19ft)	5.856	5.856	5.865	5.865	5.861	5.856	5.855	5.865	5.865	5.860	5.857	5.856	5.866	5.866	5.861	5.857	5.857	5.866	5.866	5.862
Datum @ 8.7m (29ft)	8.733	8.733	8.741	8.741	8.737	8.732	8.732	8.740	8.740	8.736	8.733	8.732	8.741	8.740	8.737	8.733	8.733	8.741	8.741	8.737

**Table 4.2 Elevation Changes of Magnet Targets**

Location	3/10/1995 B	3/10/1995 A	03/13/95	03/17/95	Before Pile Dr. 3/20/95
M1 @ 0.3m (1ft)	0.286	0.275	0.259	0.259	0.259
M2 @ 0.9m (3ft)	0.954	0.951	0.940	0.938	0.938
M3 @ 2.1m (7ft)	2.158	2.157	2.149	2.149	2.151
M4 @ 5.8m (19ft)	5.866	5.866	5.860	5.860	5.861
Datum @ 8.7m (29ft)	8.736	8.735	8.735	8.736	8.737

Location	PA 1B.	PA 5 B.	PA 10 B.	PA 20B.	PA 50B.
M1 @ 0.3m (1ft)	0.259	0.261	0.260	0.260	0.260
M2 @ 0.9m (3ft)	0.938	0.939	0.939	0.939	0.938
M3 @ 2.1m (7ft)	2.150	2.151	2.151	2.151	2.150
M4 @ 5.8m (19ft)	5.860	5.862	5.861	5.861	5.861
Datum @ 8.7m (29ft)	8.736	8.738	8.737	8.737	8.737

Location	PA 100 B.	PA 200 B.	PA 303 B	2PB 1B.	PB 5B.
M1 @ 0.3m (1ft)	0.260	0.259	0.260	0.259	0.260
M2 @ 0.9m (3ft)	0.939	0.938	0.939	0.938	0.938
M3 @ 2.1m (7ft)	2.151	2.150	2.150	2.150	2.150
M4 @ 5.8m (19ft)	5.862	5.860	5.861	5.860	5.861
Datum @ 8.7m (29ft)	8.738	8.736	8.737	8.736	8.737

Location	PB 10B.	PB 20 B.	PB 50 B.	PB 100 B	4 days after, 3/24/95	AVG	STD
M1 @ 0.3m (1ft)	0.259	0.260	0.259	0.260	0.260	0.260	0.0006
M2 @ 0.9m (3ft)	0.938	0.939	0.938	0.938	0.939	0.938	0.0005
M3 @ 2.1m (7ft)	2.150	2.150	2.150	2.150	2.150	2.150	0.0004
M4 @ 5.8m (19ft)	5.861	5.861	5.860	5.861	5.862	5.861	0.0005
Datum @ 8.7m (29ft)	8.737	8.737	8.736	8.737	8.737	8.737	0.0005

as S3 in Fig. 3.6) was fixed during pile driving. A vertical geophone (marked as MV) was always 0.91m (3 ft) from the pile being struck. Another vertical geophone (marked as WV) was placed at different distance from the pile to evaluate the wave attenuation on the ground surface. The 3-D bore hole geophone package was positioned at different depths within the profile to evaluate the wave attenuation with depth. The location of these geophones, pile blowing number, peak particle velocity, and file names are listed in Table 4.3.

In each file, the vibration time histories of eight geophones are recorded at a time step of 1/1024 second. One typical vibration time history on the ground surface is shown in Fig. 4.1. Channel 2, 3, and 4 represent Z, X, and Y directions, respectively, of the 3-D surface geophone system (S3). Based on these vibration time histories, we can use our data processing software developed in the LabView environment was used to calculate the peak particle velocity.

The 3-D surface geophone system (S3), the bore hole geophone, and the extensometer were located on the same radius from the pile as shown Fig. 3.7. On this circle, the vibration time history should be essentially the same. Therefore, the vibration time history recorded by S3 is considered as the ground surface vibration at the extensometer position. In addition, the data recorded by bore hole geophone system (H3) is considered to be representative of the vibration experienced within the extensometer profile, at same depth..

The position of S3 was unchanged during pile driving. Table 4.4 lists the statistical result of peak particle velocities recorded by S3. The 3-D value is calculated from the

Table 4.3 Records of Pile Driving Vibrations

Date: 3/20/95 Pile: A Energy 24.2 KJ

Blow Number	Pile Depth(m)	Location of Geophones (m)				Peak Partical Velocity (mm/Sec)							Vector Sum of 3D Geophone				
		Mv	Wv	S3	H3	C 0	C 1	C 2	C 3	C 4	C 5	C 6	C 7	S3 A	S3 H	H3 A	H3 H
5		0.914	5.486	3.658	0.305	51.38	2.06	5.18	4.98	3.48	4.27	3.99	3.05	5.56	5.00	4.55	5.18
21	1.067	0.914	3.048	3.658	0.305	79.76	6.32	5.77	6.38	5.99	5.44	5.44	7.44	8.13	7.24	7.59	8.74
25		0.914	3.048	3.658	1.524	79.76	7.14	5.92	6.60	5.82	5.08	6.12	4.17	8.74	7.67	6.25	7.87
26		0.914	3.048	3.658	1.524	79.76	6.48	6.22	7.32	6.15	5.03	6.22	4.57	8.38	7.82	6.45	8.18
29	1.524	0.914	3.048	3.658	6.096	79.76	7.72	6.55	9.12	6.15	1.27	0.91	2.54	9.75	9.37	2.57	2.82
30		0.914	3.048	3.658	6.096	79.76	8.15	6.96	8.15	6.32	1.22	0.74	2.49	9.09	8.46	2.49	2.79
50	1.829	0.914	3.048	3.658	3.962	79.76	10.97	9.02	10.19	9.22	2.82	2.01	4.98	13.82	13.61	5.13	5.46
51		0.914	3.048	3.658	3.962	79.76	10.44	9.04	10.62	10.41	3.00	2.26	5.54	15.01	14.86	5.59	5.84
103		0.914	2.438	3.658	3.962	79.76	22.12	10.64	14.05	13.64	2.95	3.07	6.71	17.35	17.35	6.73	7.09
104		0.914	2.438	3.658	3.962	79.76	20.85	11.00	14.02	11.35	3.23	3.45	6.07	16.59	15.49	6.12	6.27
105		0.914	5.486	3.658	1.524	79.76	4.50	10.80	14.96	11.94	7.09	10.26	5.03	18.34	16.10	10.26	11.53
106		0.914	5.486	3.658	1.524	79.76	5.18	10.80	14.48	12.34	8.08	10.34	5.18	17.20	15.93	10.44	12.04
107		0.914	5.486	3.658	0.610	51.41	1.80	3.23	8.66	4.27	3.81	2.36	9.30	9.91	9.65	9.47	9.93
108		0.914	5.486	3.658	0.610	52.04	1.78	3.02	7.14	4.24	3.53	2.54	8.08	8.28	8.03	8.18	8.56
110		0.914	2.438	3.658	7.620	79.76	24.46	9.25	17.40	11.96	1.55	1.04	3.48	20.19	18.31	3.51	3.61
200	3.200	0.914	2.438	3.658	7.620	79.76	27.66	10.62	22.17	16.54	1.68	1.45	3.99	27.48	25.70	3.99	4.01
203		0.914	5.486	3.658	0.610	79.76	4.06	11.63	21.13	16.00	9.30	12.83	9.83	26.39	24.84	15.57	15.70
204		0.914	5.486	3.658	0.610	79.76	4.62	11.23	21.23	17.30	8.94	14.10	9.30	24.66	23.24	16.89	17.09
207		0.914	5.486	3.658	3.962	79.76	4.67	11.58	22.28	16.00	4.34	3.05	7.85	27.94	26.44	7.95	8.36
208		0.914	5.486	3.658	3.962	79.76	4.42	11.51	20.62	14.76	4.17	3.71	7.57	25.35	24.05	7.62	8.03
209	3.231	0.914	5.486	3.658	6.096	79.76	4.62	11.73	25.86	18.06	2.59	3.35	6.71	30.84	28.63	7.11	7.57
210		0.914	5.486	3.658	6.096	79.76	4.50	11.02	22.58	17.75	2.54	2.87	6.22	27.25	25.48	6.60	7.01
303	3.556	0.914	2.438	3.658	0.305	22.71	7.62	3.07	8.20	5.38	5.36	6.76	8.13	8.53	8.48	9.86	9.88

Table 4.3 Continued

Date: 3/20/95 Pile: B Energy 39.7 KJ

Blow Number	Pile Depth(m)	Location of Geophones (m)				Peak Partical Velocity (mm/Sec)								Vector Sum of 3D Geophones			
		Mv	Wv	S3	H3	C 0	C 1	C 2	C 3	C 4	C 5	C 6	C 7	S3 A	S3 H	H3 A	H3 H
1	0.274	0.914	3.048	2.438	0.305	79.76	4.98	9.12	13.67	6.20	8.53	10.26	6.53	16.03	14.17	11.51	13.00
2		0.914	3.048	2.438	0.305	51.74	6.22	13.77	19.20	7.54	8.84	13.97	8.71	20.27	19.89	16.33	17.96
3		0.914	3.048	2.438	0.610	58.85	7.06	14.61	20.24	6.78	8.36	8.53	7.72	21.62	20.83	10.72	10.82
5	0.762	0.914	3.658	2.438	1.524	14.76	1.52	1.32	3.10	1.57	0.99	1.55	1.17	3.12	3.10	1.55	1.63
6	0.274	0.914	3.658	2.438	3.962	79.76	6.10	15.54	20.68	10.97	1.68	1.55	2.36	22.58	20.70	2.77	2.87
8	0.274	0.914	3.658	2.438	6.096	30.96	7.16	17.20	14.86	7.16	1.22	1.04	1.40	21.13	15.09	1.47	1.50
13		0.914	6.096	2.438	6.096	39.50	2.92	20.42	21.51	11.63	1.73	2.36	3.05	24.56	23.19	3.05	3.05
15		0.914	6.096	2.438	3.962	41.48	2.90	19.94	20.22	10.64	5.99	16.87	10.52	23.85	22.02	19.51	19.69
20		0.914	6.096	2.438	0.610	42.90	2.74	17.58	17.91	9.35	8.71	5.72	8.20	21.59	19.96	9.07	11.13
21	1.067	0.914	6.096	2.438	0.305	49.48	2.36	18.92	15.77	7.98	10.11	6.30	7.21	21.82	17.65	7.24	10.13
41		0.914	6.096	2.438	0.305	29.11	2.44	5.05	9.47	7.52	5.77	8.20	9.75	12.12	11.73	11.35	12.04
42		0.914	6.096	2.438	0.305	29.34	2.51	4.22	10.16	7.72	4.85	8.84	10.34	12.04	11.61	11.58	11.79
47	2.438	0.914	6.096	2.438	0.305	77.75	3.40	20.19	19.25	17.91	15.34	18.92	13.87	23.50	20.78	19.25	20.73
48		0.914	6.096	2.438	0.305	38.25	1.02	6.55	12.07	8.46	5.99	8.03	9.58	14.73	14.48	12.12	12.17
49		0.914	6.096	2.438	0.610	79.65	2.95	20.73	26.70	21.89	13.84	11.07	10.29	31.55	26.70	11.25	15.06
50		0.914	6.096	2.438	0.610	33.27	6.20	7.16	10.92	6.15	5.84	6.53	10.26	12.01	11.25	10.90	10.90
51		0.914	6.096	2.438	1.524	79.65	3.61	19.08	19.63	16.54	10.21	28.17	10.39	21.97	19.94	28.22	28.80
52		0.914	6.096	2.438	1.524	79.76	3.58	18.92	22.68	17.75	9.70	14.73	11.53	24.54	22.91	16.43	18.85
53		0.914	6.096	2.438	3.962	79.76	3.66	19.20	19.10	18.24	4.32	5.26	5.54	23.47	19.63	7.37	7.49
55		0.914	6.096	2.438	6.096	79.76	3.28	21.62	20.24	20.90	3.86	2.59	3.00	26.82	21.77	3.86	4.22
56		0.914	6.096	2.438	7.620	79.76	3.51	22.38	21.74	20.22	2.77	1.91	2.95	26.87	22.35	2.95	4.04
57		0.914	6.096	2.438	7.620	79.76	1.91	7.98	18.92	7.34	1.32	0.99	1.50	19.43	18.92	1.50	1.80
98		0.914	3.048	2.438	0.305	47.45	3.02	6.38	10.80	6.78	6.63	11.25	6.22	11.40	11.20	11.25	11.76
100	2.996	0.914	3.048	2.438	1.524	23.16	3.23	4.70	8.64	5.26	5.31	2.31	2.67	8.97	8.84	3.05	6.12

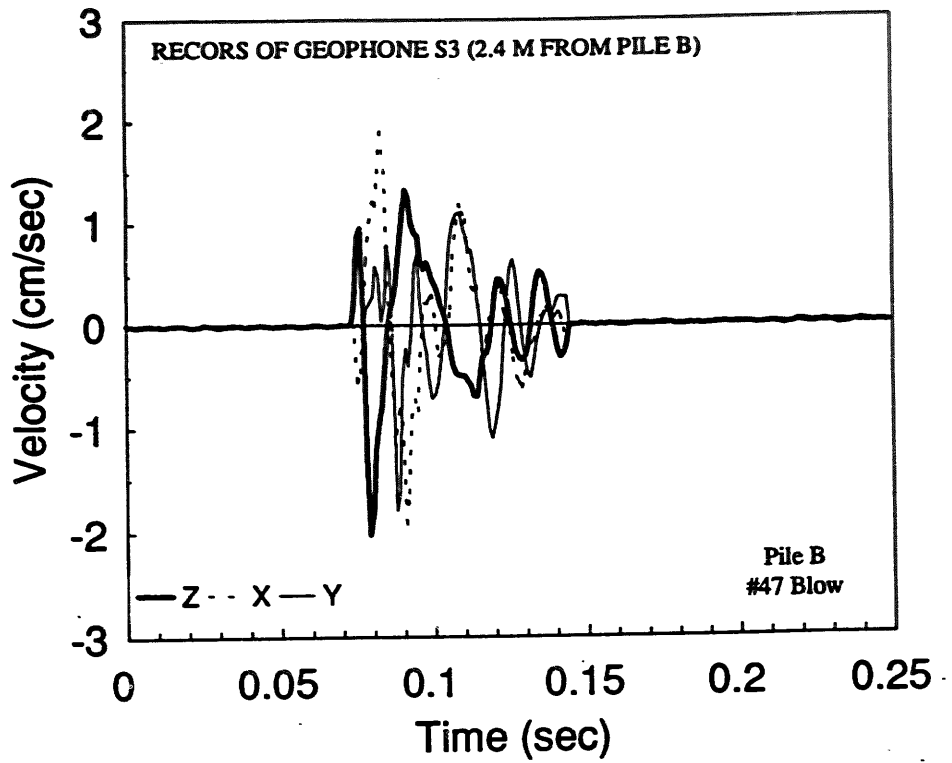


Figure 4.1 Vibration Time Histories on the Ground Surface Recorded by Geophone S3

vectors sum of three directional velocities at every time step. From this table, it can be seen that the standard derivation (STD) is relatively large. This is reasonable because the pile driving energy varied for each blow and the hammer impact position on the pile cap was variable. During field tests, the input range of the data acquisition system was set to  $\pm 2.5$  volt for all channels. The surface vertical geophone, MV, which is 0.91 m (3 ft) from the pile, sometimes experienced very high vibration velocity (larger than 79.8 mm/sec), and its output signal surpassed the voltage range. Thus, input channel 1 was saturated and outputted as 2.5 volt.

Table 4.4 Statistic Results of Peak Particle Velocity Recorded by the 3-D Surface Geophone, S3

Location	Peak Particle Velocity (mm/sec)					
	3D	STD	Vertical	STD	Horiz.	STD
Pile A @ 3.66m	15.11	8.69	7.67	3.63	14.20	8.13
Pile B @ 2.44m	18.19	7.59	12.93	7.16	16.36	6.48

#### 4.2.1 Vibration attenuation on the ground surface

As with all vibrations, those induced by pile driving attenuate with distance. By comparing the vertical vibration amplitude recorded with geophones MV, WV, and S3 on the ground surface, the attenuation curves are plotted in Figures 4.2A and 4.2B for Pile A



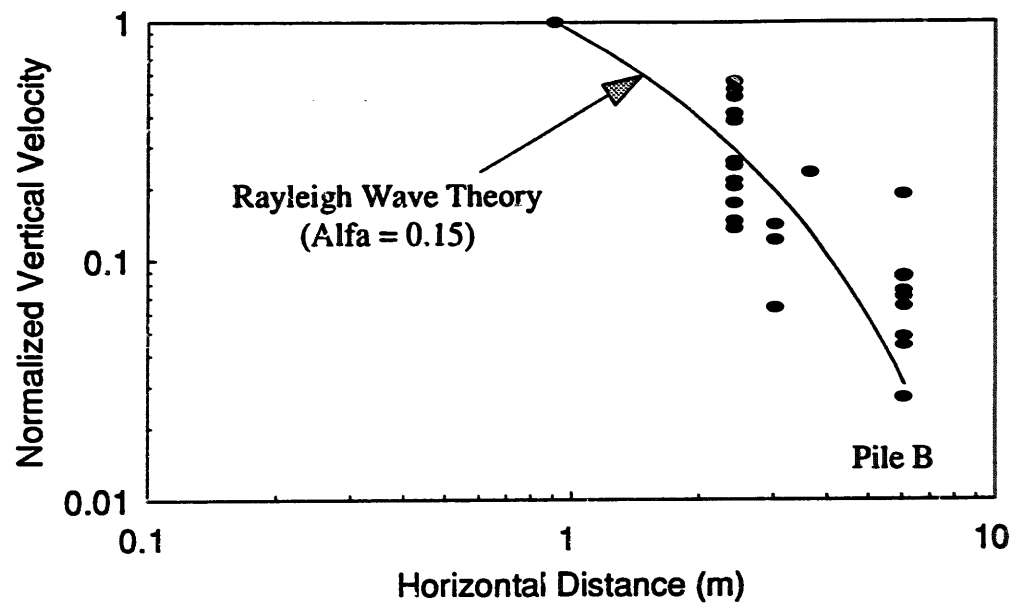
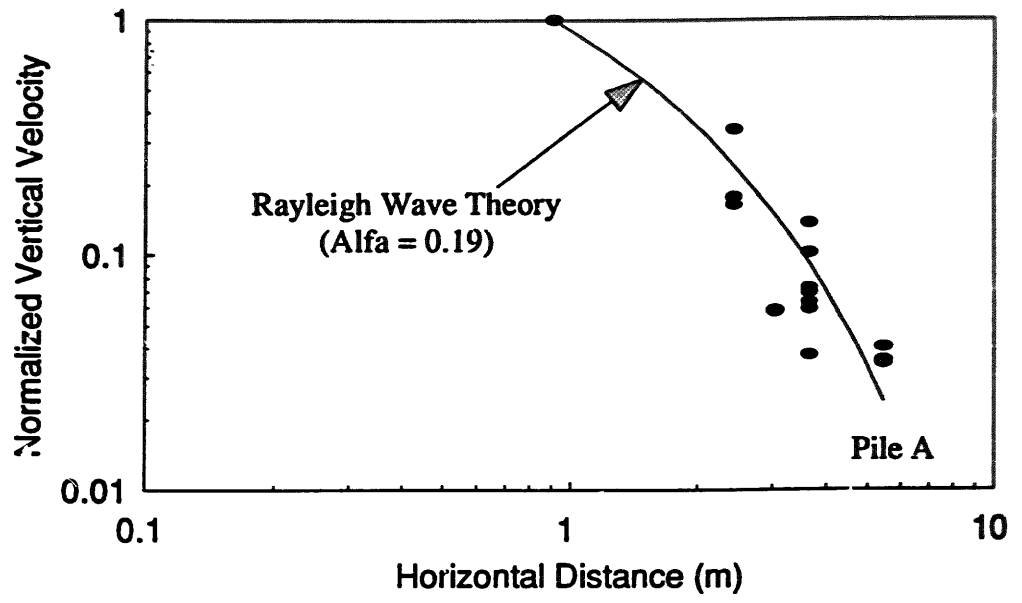


Figure 4.2 Vibration Attenuation on the Ground Surface

and Pile B, respectively. Because the pile driving energy is not constant for each blow, the vertical velocity amplitude was normalized. The vibration amplitude recorded at different distances from the pile was divided by that amplitude recorded by geophone MV, 0.19m (3 ft) from the pile. As stated above, the geophone (MV) closest to the pile, produced an output that sometimes saturated the channel. These saturated signals were neglected in calculating the normalized ground surface vibration amplitude.

The vertical vibration amplitude is seen to attenuate much faster than that shown in Fig 2.1 and that calculated from Equation 2.1. This is because Equation 2.1 and Fig. 2.1 are based on Rayleigh wave theory in a linear elastic half space. The reference geophone is 0.91m (3 ft) from the pile, which is much shorter than the Rayleigh wave length. At this distance, the Rayleigh wave is not well developed and the soil's behavior is nonlinear. This field test proves that Fig 2.1 and Equation 2.1 based on Rayleigh theory is conservative, especially when the reference point is near the vibration source.

#### **4.2.2 Vibration attenuation with depth in soil profile**

The vibration amplitude also attenuates with depth in the soil profile. The bore hole geophone package was positioned at different depths during pile driving and the vibration time history recorded in three directions. The wave attenuation with depth is shown in Fig. 4.3 and Fig 4.4 for Pile A and Pile B driving, respectively. In these two figures, the vertical and horizontal velocity components are normalized by the corresponding components recorded by the reference surface geophone, S3. In addition, the attenuation of both vertical and horizontal components were calculated by Rayleigh

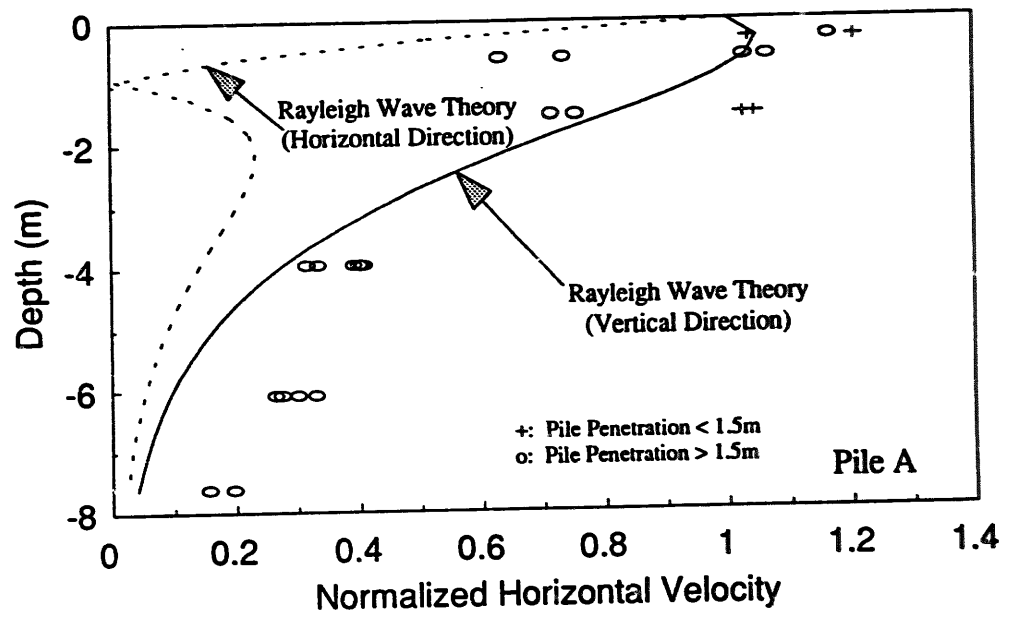
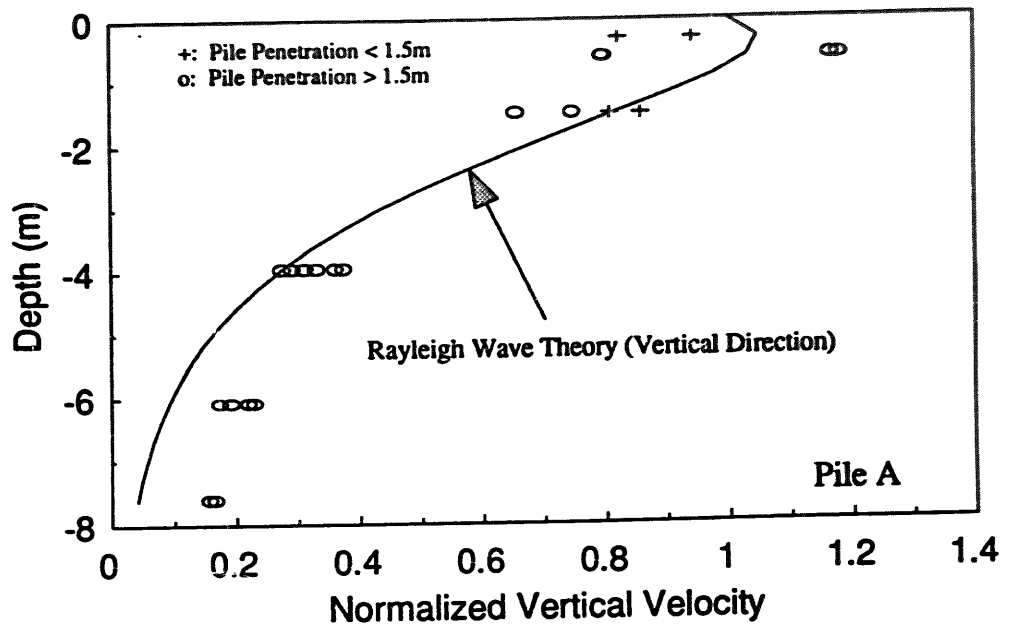


Figure 4.3 Vibration Attenuation along with Depth for Pile A

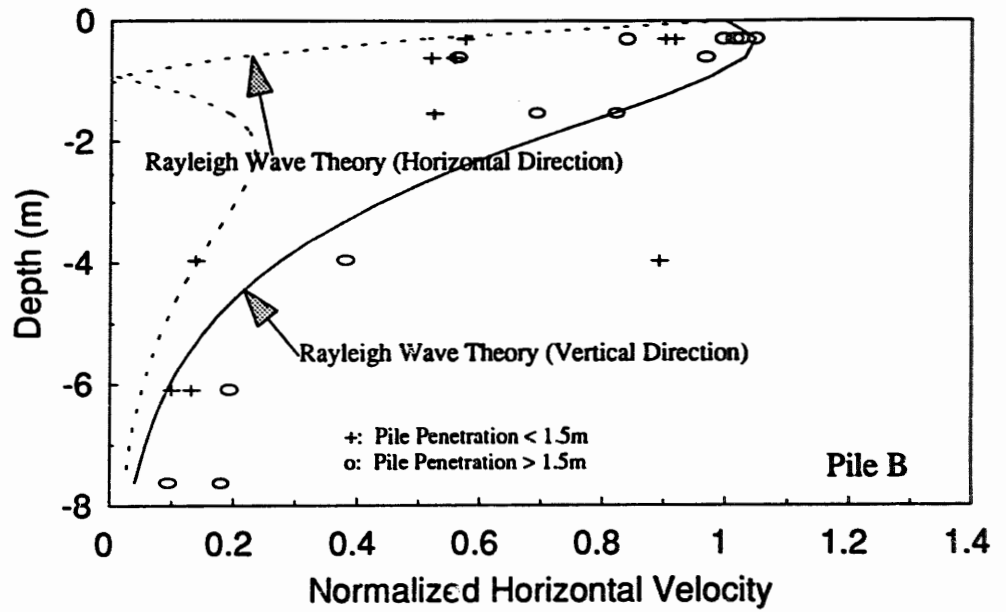
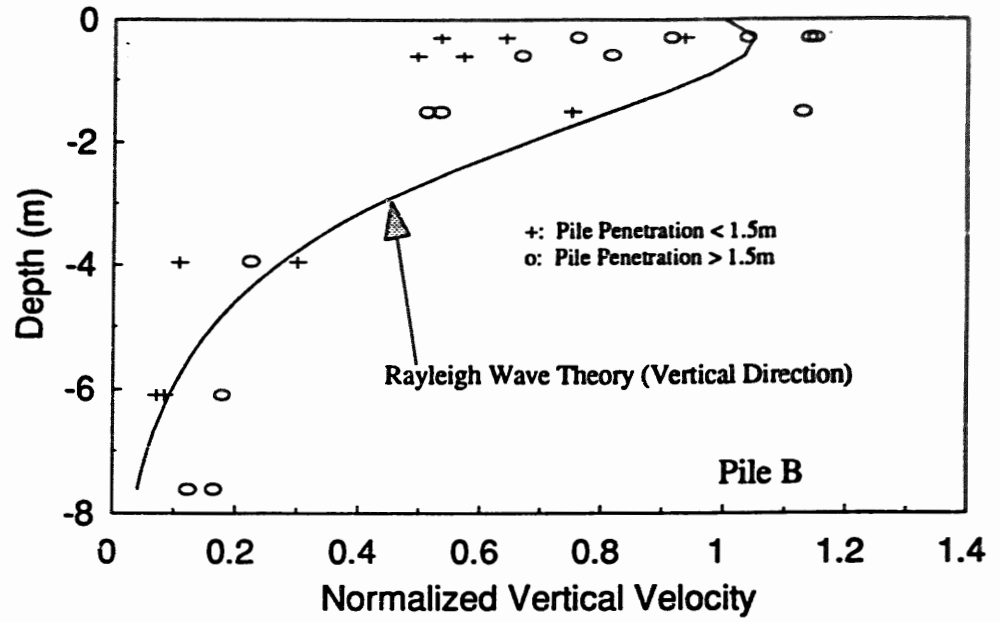


Figure 4.4 Vibration Attenuation along with Depth for Pile B

wave theory, which assumes that the Rayleigh wave is well developed in a linear elastic half space and the Poissons's ratio equals 0.25.

The test results for the vertical component agree well with that predicted by the Rayleigh wave theory. When the penetration depth was less than 1.5 m (5 ft), the vibration impact of the pile appears to be reasonably considered as a surface source that satisfies the Rayleigh wave theory assumption. As the pile penetrates deeper into the profile, the vibration source is not a surface source. For simplicity, the data generated when the pile tip elevation were deeper than 1.5 m are shown as open circles. The vibration amplitude recorded below 6 m is seem to be higher than that predicted by the Rayleigh wave theory. At this depth, the confining pressure is higher than that near the ground surface, and the vertical vibration amplitude is around 20 to 30% of that on the ground surface. Therefore, the settlement at this depth is very small compared with that near the ground surface. For most practical purpose, this deviation can be neglected when the Rayleigh wave theory is employed to calculate the dynamic settlement in a soil profile.

The shown as the horizontal component is calculated from the vector sum of the vibration velocities in the X and Y direction at each time step. The peak horizontal particle velocity is obtained from this vector sum time history. As shown in Fig 4.3 and Fig 4.4, the field tests results are much higher than that horizontal component calculated from Rayleigh wave theory. There are three reasons for this disagreement. First, the pile driving vibration not only generates Rayleigh waves, but also generates P-waves and S-waves. Although the P-wave and S-wave component attenuate faster than a Rayleigh wave, their amplitudes are relatively high in the area near the pile. Secondly, the distance

between the geophone hole and the pile is less than the Rayleigh wave length, thus, the Rayleigh wave is not well developed. Finally, when the pile penetrates into the ground, it pushes soil around the pile tip both vertically and horizontally. Therefore, the vibration source has both vertical and horizontal components. The Rayleigh wave theory only considers the vertical vibration source, so that its value is considerably less than that obtained from field tests.

From Fig. 4.3 and Fig 4.4, the normalized horizontal velocity of the field tests agrees well with the value of the vertical component calculated by Rayleigh theory. This suggests that the attenuation of the vertical component along with depth obtained by Rayleigh wave theory can be used to calculate both the vertical and horizontal vibrations in the soil profile. This method is conservative because the Rayleigh wave contains two thirds of the generated vibration energy, and its horizontal component attenuates much faster than does the vertical component.

#### 4.2.3 Characteristics of Rayleigh wave

The dominant frequency is calculated from vibration time histories by the Fast Fourier Transform (FFT) method. The FFT method establishes the relationship between a signal and its representation in the frequency domain. The definition of the Fourier transform,  $V(f)$ , of a velocity time history  $v(t)$  is:

$$V(f) = F\{v\{t\}\} = \int_{-\infty}^{+\infty} v(t)e^{-j2\pi ft} dt \quad (4.1)$$

The frequency resolution,  $\Delta f$ , can be calculated as:

$$\Delta f = \frac{f_s}{n} \quad (4.2)$$

where  $f_s$  is the sampling frequency, which is 1024 Hz in all the field tests, and  $n$  is the number of data points in both time and frequency domain. To perform FFT, it is required that the number of data points,  $n$ , is a valid power of two. An analytical program, SASW.VI, was developed in the LabView environment to perform FFT in a quick and memory efficient manner (Fig. 4.5). The dominate frequency was calculated for each vibration time history from Channel 2, which was connected to the vertical component of the surface geophone S3. The average dominate frequency is 29.6 Hz for Pile A, and 30.5 Hz for Pile B.

There are two methods to calculate the Rayleigh wave speed. The easiest method is to find the time difference of a wave peak traveling from one geophone to another as shown in Fig. 2.2. The Rayleigh wave speed is the ratio of the distance between two geophones and the wave travel time. This method is inaccurate because the wave peak sometimes is hard to recognize when Rayleigh wave travels in distance, and the time difference is hard to measure accurately, especially when the sampling rate is low. Another method to calculate Rayleigh wave speed is to perform cross power spectrum analysis. This method is more precise than the first method because all the data points of the wave form are used to calculate the wave traveling time. The wave forms from geophone WV and the vertical component of geophone S3 were recorded by channel 1 and channel 2 of the data acquisition system, respectively. The time for the Rayleigh wave

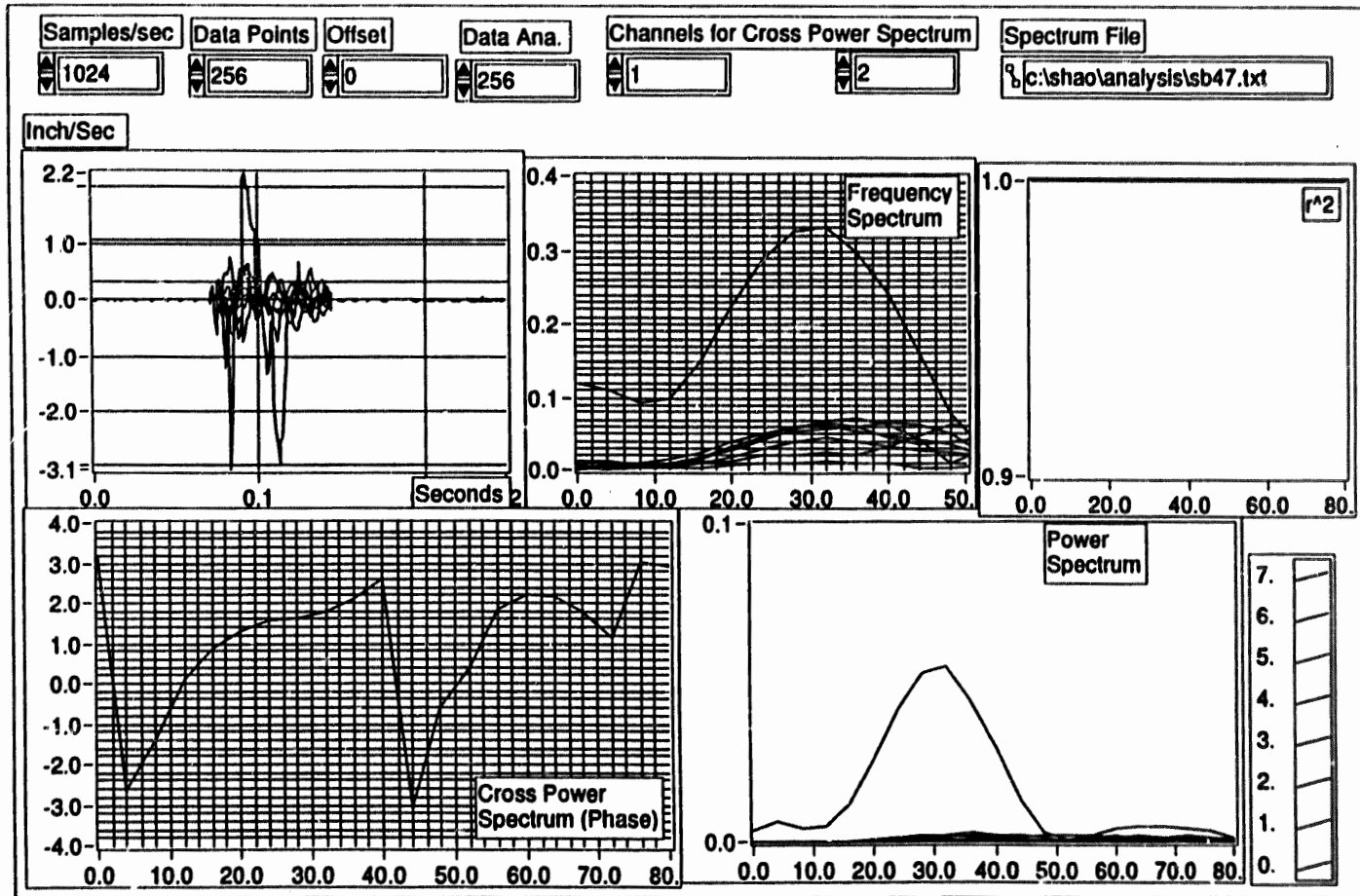


Figure 4.5 The Front Panel of wave Analysis Software, SASW.VI



to propagate from S3 to WV can be detected by the phase difference between two input signals which can be calculated by cross power spectrum as:

$$S_{xy} = \frac{1}{n^2} F^* \{X\} F\{Y\} \quad (4.3)$$

where  $S_{xy}$  represents the complex output sequence in the frequency domain,  $F^* \{X\}$  and  $F\{Y\}$  are the Fourier transformation of two input signals, and  $n$  is the number of data points. When  $n$  equals a valid power of two, the program can perform the cross power spectrum analysis very efficiently in both execution time and memory. From the complex sequence,  $S_{xy}$ , the phase difference,  $\Delta\phi(f)$ , can be calculated in the frequency domain. The phase difference between two input channels changes with frequency, thus, the Rayleigh wave velocity is a function of frequency. The Rayleigh wave velocity at the dominate frequency is defined as:

$$V_R = \frac{\Delta L}{\frac{\Delta\phi}{2\pi f_1}} \quad (4.4)$$

where  $\Delta L$  is the distance between geophone S3 and WV,  $\Delta\phi$  is the phase difference of the signals obtained from cross power spectrum analysis, and  $f_1$  is the primary frequency of Rayleigh wave. From Table 4.5, the average Rayleigh wave velocity is 142 m/sec (465.8 ft/sec) at dominant frequency 30.5 Hz obtained during Pile B driving. The Rayleigh wave length can be calculated as:

$$\lambda_1 = \frac{V_R}{f_1} \quad (4.5)$$

where  $\lambda_1$  is the Rayleigh wave length at the dominant frequency  $f_1$ .

Table 4.5 Frequency Analysis on the Time Histories of Pile B

Blow Number	Pile B Depth(m)	Primary Frequency (Hz)	Phase Angle (rad.)	Rayleigh Wave Velocity	
				(m/sec)	(ft/sec)
47	2.438	32	4.94	148.8	488.3
48		32			
49		28	5.04	127.6	418.7
51		32	4.74	155.1	508.8
52		31	5.04	141.3	463.6
53		30	4.94	139.5	457.7
55		30	4.94	139.5	457.7
56		30	4.94	139.5	457.7

The accuracy of the Rayleigh wave velocity depends on the distance between two geophones, the sampling rate, signal amplitude, and characteristics of the data acquisition system. At the sampling rate 1024 points/sec, the maximum inter-channel delay is 1 ms for the data acquisition board. For example, when the distance between geophone S3 and WV is 3.66 m, it takes 25.7 ms for Rayleigh wave to propagate. The influence of inter-channel delay is only 4% of wave travel time. When the distance between geophones decreases, the phase resolution of the cross power spectrum analysis reduces rapidly. From all the time histories recorded from field tests, while the geophone space is larger than 3m, a consistent phase difference can be obtained from wave analysis. In addition, in the area near the pile, the Rayleigh wave is not well developed. The geophone output from MV, 0.9 m from the pile, can not be used in the cross power spectrum analysis. To calculate the Rayleigh wave speed, we only performed cross power spectrum analysis on

the time histories from geophone S3 and WV where the geophone space was larger than 3m.

**CHAPTER 5**  
**RESULTS OF LABORATORY TESTS**

**5.1 Resonant Column Tests**

Resonant column tests were performed on Shelby tube samples obtained from field test Site 1 (Selma, NC). Because the samples were obtained from shallow depths (less than 2 m), resonant column tests were performed with confining pressures in the range of 12.5 kPa to 50kPa. The shear strain amplitude in the tests was always below 0.001%, and the soil specimens behaved in a linear elastic manner. The acceleration amplitude was recorded by an accelerometer on top of the specimen at the resonant frequency. From these data presented in table 5.1, the shear wave velocity, shear modulus, and shear strain amplitude can be calculated. Detailed test procedure and analysis methods are discussed by Borden, Shao and Gupta (1994).

From Table 5.1, it can be seen that the shear modulus of specimens increases with confining pressures. This trend was also observed in the resonant column tests performed in the previous two years. An analytical model of shear modulus as a function of confining pressure will be presented in Chapter 6. We believe that the shear modulus of specimen 6ST#2 was higher than the other two specimens because of the presence of some quartz fragments. Detailed resonant column tests results are included in Appendix 1.1.

Table 5.1 Shear Wave Velocity and Shear Modulus from Resonant Column Tests.

Specimen	Depth (m)	Confining Pressure (kPa)	Accel. Amp. (mV)	Resonant Freq. (Hz)	Specimen		Shear Wave Velocity (m/sec)	Shear Modulus (MPa)	Shear Str. Amp. (%)
					Length (mm)	Diam. (mm)			
6ST#2A	0.6-0.9	12.5	71	82	147.1	73.3	152.3	43.72	0.00058
		25.0	57	84	146.8	73.2	156.0	46.07	0.00045
6ST#2	0.9-1.2	12.5	54	90	147.7	72.9	165.9	54.12	0.00036
		25.0	56	106.6	147.4	72.7	196.5	76.36	0.00027
		50.0	58	117.37	147.2	72.7	216.3	92.85	0.00023
6ST#4	1.5-1.9	25.0	65	70	146.2	73.6	125.3	31.36	0.00074
		50.0	61	82	145.9	73.4	146.8	43.26	0.00051

## 5.2 Torsional Shear Tests for Dynamic Densification

After resonant column testing, torsional shear tests were performed on each of the three specimens described in Table 5.1. The dynamic volumetric change was measured as a function of confining pressure, shear strain amplitude, and number of cycles. A summary of parameters investigated is listed in Table 5.2. Detailed test procedure and analysis are discussed by Borden, Shao and Gupta (1994).

During testing, the confining pressures were incremented as shown in Table 5.2. At each confining pressure, the specimen was torsionally sheared at shear strain levels ranging from 0.005% to as high as 0.1%. Because the Stokoe's device is stress controlled, the shear strain amplitude in the table represented those nominal values which were the test objective. The real shear strain amplitude was calculated from the actual specimen deformation and it is the value that is listed in the following section for each test. At each shear strain amplitude, 1000 cycles were applied to the specimen. The cyclic

frequency was 10 Hz for all the torsional shear tests. For specimen 6ST#4, only 0.005% shear strain step was tested under 50 kPa confining pressure, because the screws on the driving plate became loose and the test was terminated.

Table 5.2 Parameters Investigated in Torsional Shear Tests for Specimens Obtained from Site 1 (Selma, NC)

Specimen No.	Confining Pressure(kPa)	Estimated Shear Strain Amplitude(%)	Number of Cycles	Cyclic Frequency(Hz)
6ST#2	12.5	0.005, 0.01, 0.025, 0.05, 0.1	1000	10
	25	0.005, 0.01, 0.025, 0.05, 0.1	1000	10
	50	0.005, 0.01, 0.025, 0.05	1000	10
6ST#2A	12.5	0.005, 0.01, 0.025, 0.05, 0.1	1000	10
	25	0.005, 0.01, 0.025, 0.05, 0.1	1000	10
6ST#4	25	0.005, 0.01, 0.025, 0.05	1000	10

The torsional shear tests were controlled and monitored by the computerized data acquisition system (Borden, Shao and Gupta, 1994). The torque moment, twist angle, height and diameter of the specimen were recorded at a sampling frequency 200 Hz. These records were processed and the relationship between the dynamic volume changes of the specimens and number of cycles, shear strain amplitude, and confining pressure are presented in Appendix 1.2.

Fig 5.1, Fig 5.2, and Fig. 5.3 show that the volumetric strain changes with respect to number of cycles and shear strain amplitude at each confining pressure for

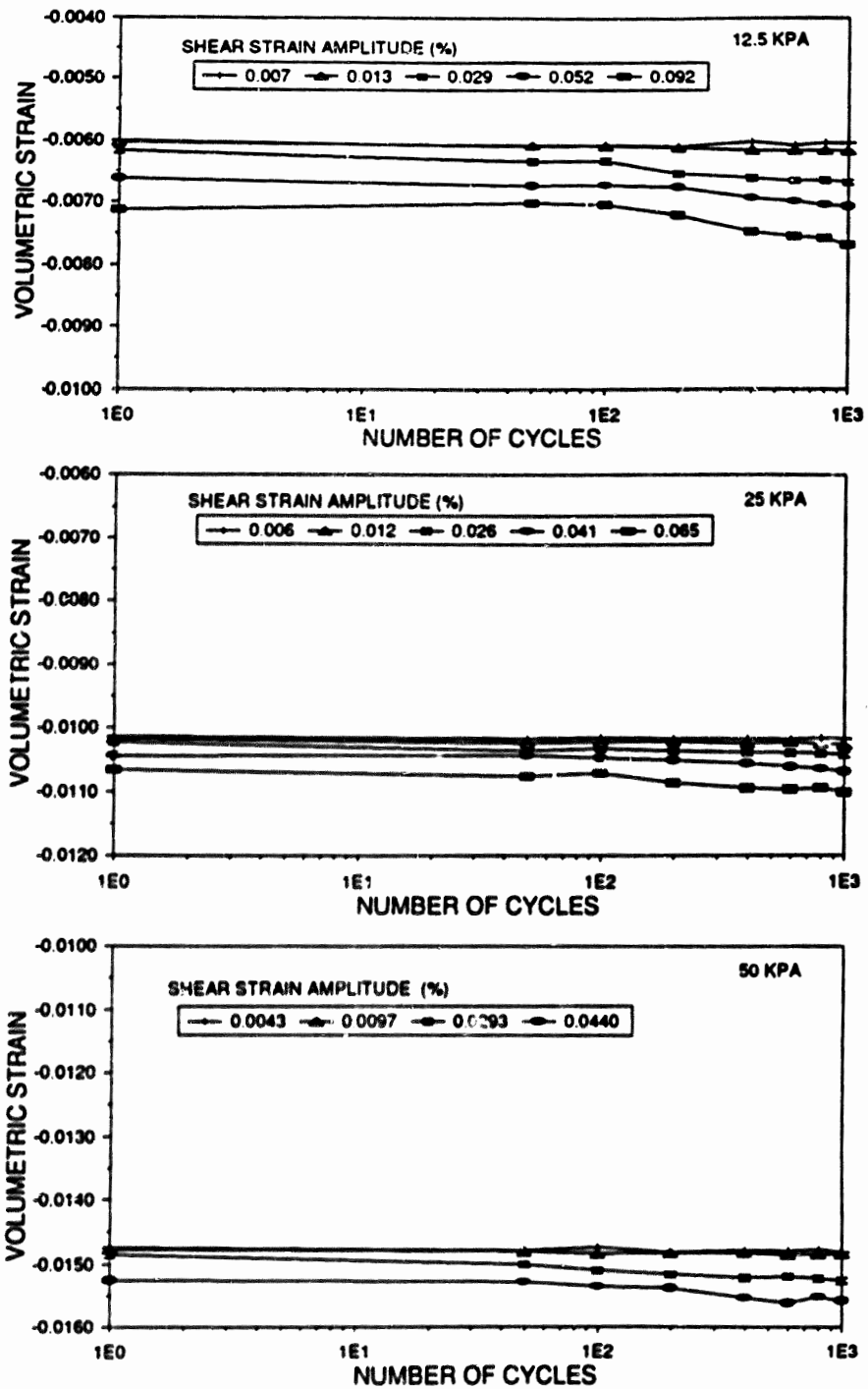


Figure 5.1 The Volumetric Strain Changes with Cyclic Number and Shear Strain Amplitude at Each Confining Pressure for Specimen 6ST#2

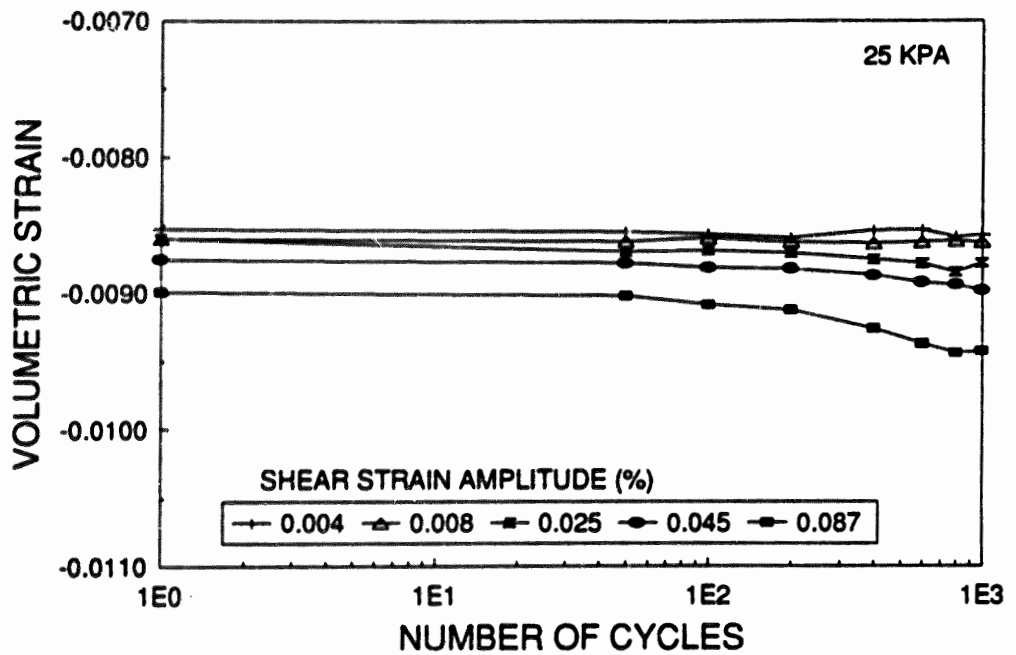
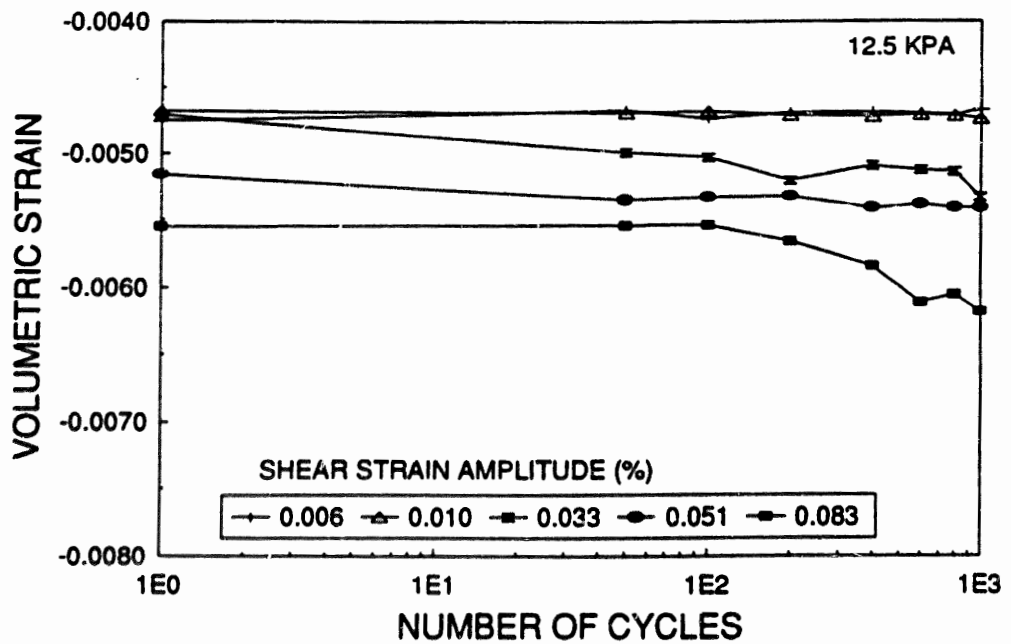


Figure 5.2 The Volumetric Strain Changes with Cyclic Number and Shear Strain Amplitude at Each Confining Pressure for Specimen 6ST#2A



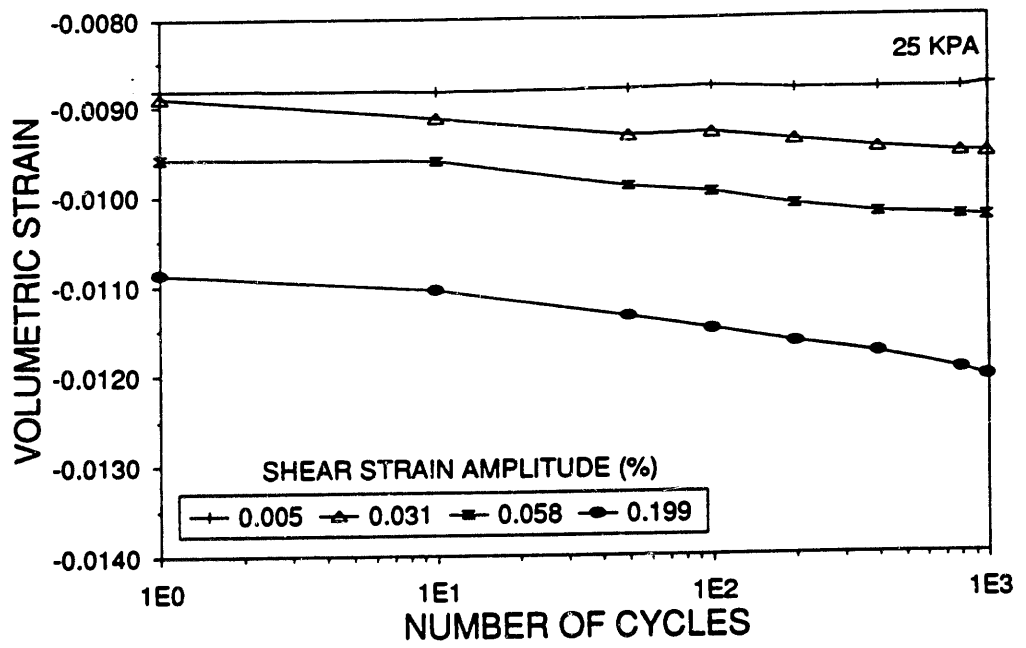


Figure 5.3 The Volumetric Strain Changes with Cyclic Number and Shear Strain Amplitude at Each Confining Pressure for Specimen 6ST#4

specimen 6ST#2, 6ST#2A and 6ST#4, respectively. The initial volume was measured at atmospheric pressure before the torsional shear test. Then, the specimen was fully consolidated under the specified confining pressure over night. This static volumetric strain at each confining pressure is shown in these figures as the first cycle of the first shear strain step (lowest shear strain amplitude). In the torsional shear test, the height and diameter of specimen changed due to the cyclic shear. Each line in these figures represents the volumetric strain over 1000 cycles for each shear strain amplitude. The real shear strain amplitude was calculated from twist angles on the top of the specimen recorded by the data acquisition system. It was observed by Borden, Shao and Gupta (1994) that the dynamic volumetric change followed a same trend for up to one million cycles. For tests on these three specimens, 1000 cycles were applied.

The influence of confining pressure on the dynamic volumetric strain was investigated by tests at different confining pressures. The relation between the dynamic volumetric strain at 1000 cycles and shear strain amplitude will be plotted and analyzed in Chapter 6. It can be observed that the dynamic volumetric strain reduces when the confining pressure increases. This trend was also reported in our previous research. Because depths from which the samples were obtained were shallow and the confining pressures were low, the disturbance during Shelby tube sampling could be expected to be relatively substantial.

### 5.3 Shear Modulus Changes with Shear Strain Amplitude and Confining Pressure

The residual soil behaves as an elastic material at low shear strain amplitude, and behaves as a nonlinear material at high shear strain. The shear modulus obtained from resonant column tests at small shear strain amplitude,  $G_{max}$  is considered as an elastic modulus. The shear modulus decreases as the shear strain amplitude increases, as shown in Table 5.3. The ratio between the shear modulus at different shear strain amplitudes obtained from torsional shear tests and  $G_{max}$  is called normalized shear modulus. The normalized shear modulus versus shear strain amplitude is plotted in Fig. 5.4. Besides torsional shear tests in a range of 0.005% to 0.1% shear strain, triaxial tests were also performed at even higher shear strain amplitude. The specimens for triaxial tests came from the same Shelby tube samples from which the torsional shear tests specimens were trimmed.

The modeling of the dynamic volumetric change and shear modulus will be discussed in the next chapter.

Table 5.3 Relationship between Shear Modulus and Shear Strain Amplitude

Specimen	Pressure (kPa)	Estimate Strain %	Twist Angle (rad)	Shear Strain(%)	G(MPa)	C/Gmax
6ST#2	12.5	Gmax from RC test			54.14	1.000
		0.005	3.509E-04	0.007	33.87	0.626
		0.010	6.635E-04	0.013	27.11	0.501
		0.025	1.468E-03	0.029	19.09	0.353
		0.050	2.659E-03	0.052	14.97	0.277
		0.100	4.672E-03	0.092	10.85	0.200
	25.0	Gmax from RC test			76.38	1.000
		0.005	3.079E-04	0.006	53.53	0.701
		0.010	6.248E-04	0.012	38.33	0.502
		0.025	1.316E-03	0.026	30.32	0.397
		0.050	2.074E-03	0.041	25.20	0.330
		0.100	3.308E-03	0.065	20.47	0.268
	50.0	Gmax from RC test			92.87	1.000
		0.005	2.161E-04	0.004	74.84	0.806
		0.010	4.913E-04	0.010	61.56	0.663
		0.025	1.487E-03	0.029	40.52	0.436
		0.050	2.233E-03	0.044	34.85	0.375
	6ST#2A	12.5	Gmax from RC test			43.72
0.005			2.875E-04	0.006	33.85	0.774
0.010			5.082E-04	0.010	28.63	0.655
0.025			1.669E-03	0.033	17.46	0.399
0.050			2.558E-03	0.051	15.06	0.344
0.100			4.189E-03	0.083	11.47	0.262
25.0		Gmax from RC test			46.08	1.000
		0.005	1.865E-04	0.004	51.95	1.127
		0.010	3.916E-04	0.008	44.19	0.959
		0.025	1.248E-03	0.025	28.29	0.614
		0.050	2.242E-03	0.045	22.04	0.478
		0.100	4.348E-03	0.087	16.41	0.356
6ST#4	25.0	Gmax from RC test			31.37	1.000
		0.010	2.411E-04	0.005	47.66	1.519
		0.025	1.547E-03	0.031	24.70	0.787
		0.050	2.879E-03	0.058	19.92	0.635

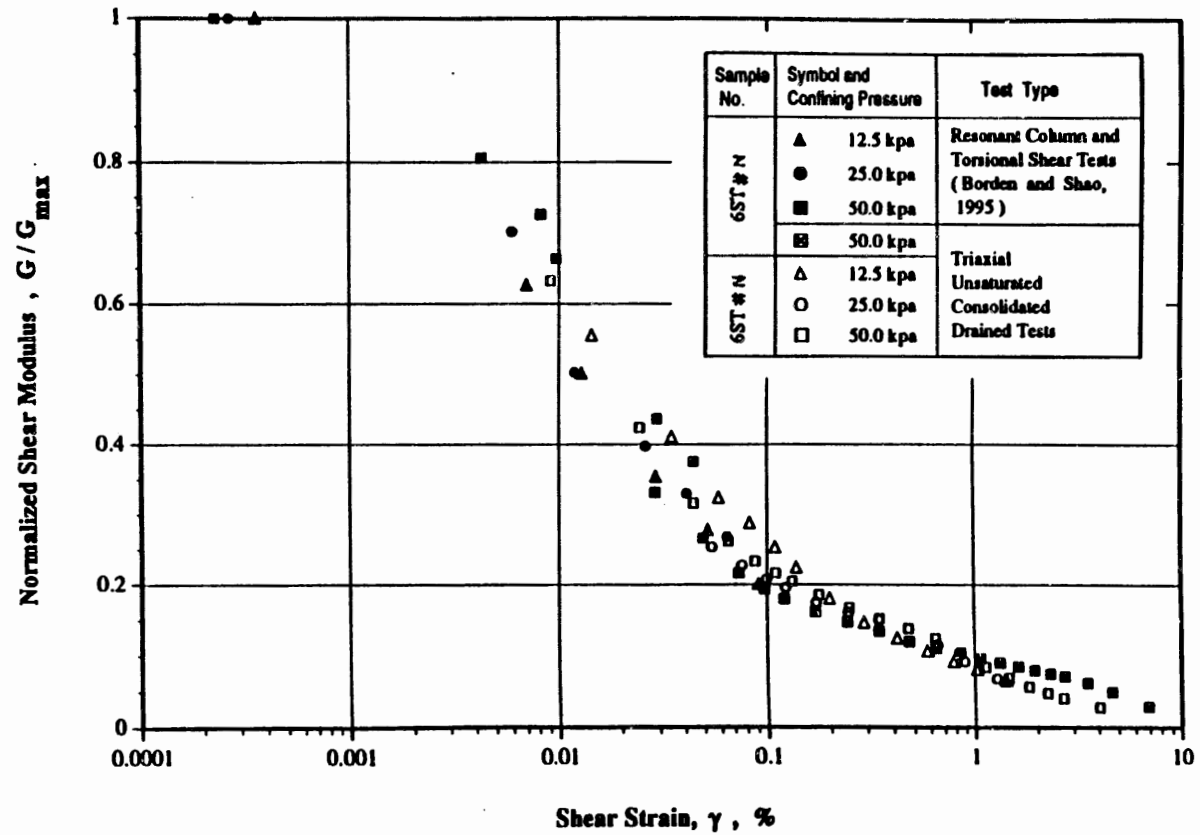


Figure 5.4 Normalized Shear Modulus as a Function of Shear Strain for Samples Obtained from Selma, NC

## CHAPTER 6

### MODELING

#### 6.1 Attenuation of Construction Induced Vibrations in Soil Profile

Vibration amplitude attenuates with distance from the source and there is a theoretical solution for a vertical impact on the ground surface. As shown in Fig. 2.8, the body waves (P-waves and S-waves) travel through the soil profile with hemispherical wave fronts, while Rayleigh waves propagate radially outwards along a cylindrical wave front. When body waves spread out along a hemispherical wave front, the energy is distributed over an area that increases with the square of the radius:

$$E' \propto \frac{1}{r^2} \quad (6.1)$$

where  $E'$  is the energy per unit area and  $r$  is the radius. The vibration amplitude is proportional to the square root of the energy per area and therefore the amplitude of body waves are proportional to  $1/r$ .

$$\text{Body Wave Amplitude} \propto \frac{1}{r} \quad (6.2)$$

Similarly, the amplitude of Rayleigh waves, which spread out in a cylindrical wave front, are proportional to  $\frac{1}{\sqrt{r}}$ . Thus the attenuation of the amplitude of Rayleigh waves is much slower than that for the body waves.

The loss of the vibration amplitude of waves due to spreading is called geometrical damping. In addition, there is another type of loss, termed material damping, that from

absorption of energy in soil. Thus, accounting for both types of damping, the attenuation of Rayleigh waves can be given by the relation:

$$A = A_1 \left( \frac{r_1}{r} \right)^{1/2} \exp[-\alpha(r - r_1)] \quad (6.3)$$

where  $A$  is the amplitude of particle velocity at a distance  $r$  from the source,  $A_1$  is the amplitude of particle velocity at a reference point a distance  $r_1$  from the source, and  $\alpha$  denotes the coefficient of material damping. The coefficient of material damping,  $\alpha$ , can be obtained from field measurements or can be calculated by :

$$\alpha = \frac{2\pi f \eta}{V_R} \quad (6.4)$$

where  $f$  is the vibration frequency,  $V_R$  is the Rayleigh wave velocity and  $\eta$  is the material damping ratio, which can be obtained from resonant column/torsional shear tests.

Because Rayleigh waves carry 67% of the total vibration energy and attenuate much slower than body waves, Equation 6.3 is widely used in engineering practice to calculate wave propagation along the ground surface. Figure 6.1 compares the vibration attenuation of pile driving from our field tests with that published in the literature. As discussed in Chapter 4, the pile driving energy for each blowing varies, so that the vibration amplitudes recorded on the ground surface for individual impacts are not the same. Some typical blows are plotted in Fig. 6.1 to show the trend of the wave attenuation. Tests results from Wahls (1981) and Woods (1980) are presented in the figure by using Eq. 6.3. From Fig. 6.1, it can be observed that the wave attenuation of our field tests is faster than that from the literature. If Eq. 6.3 was used to fit the tests point as

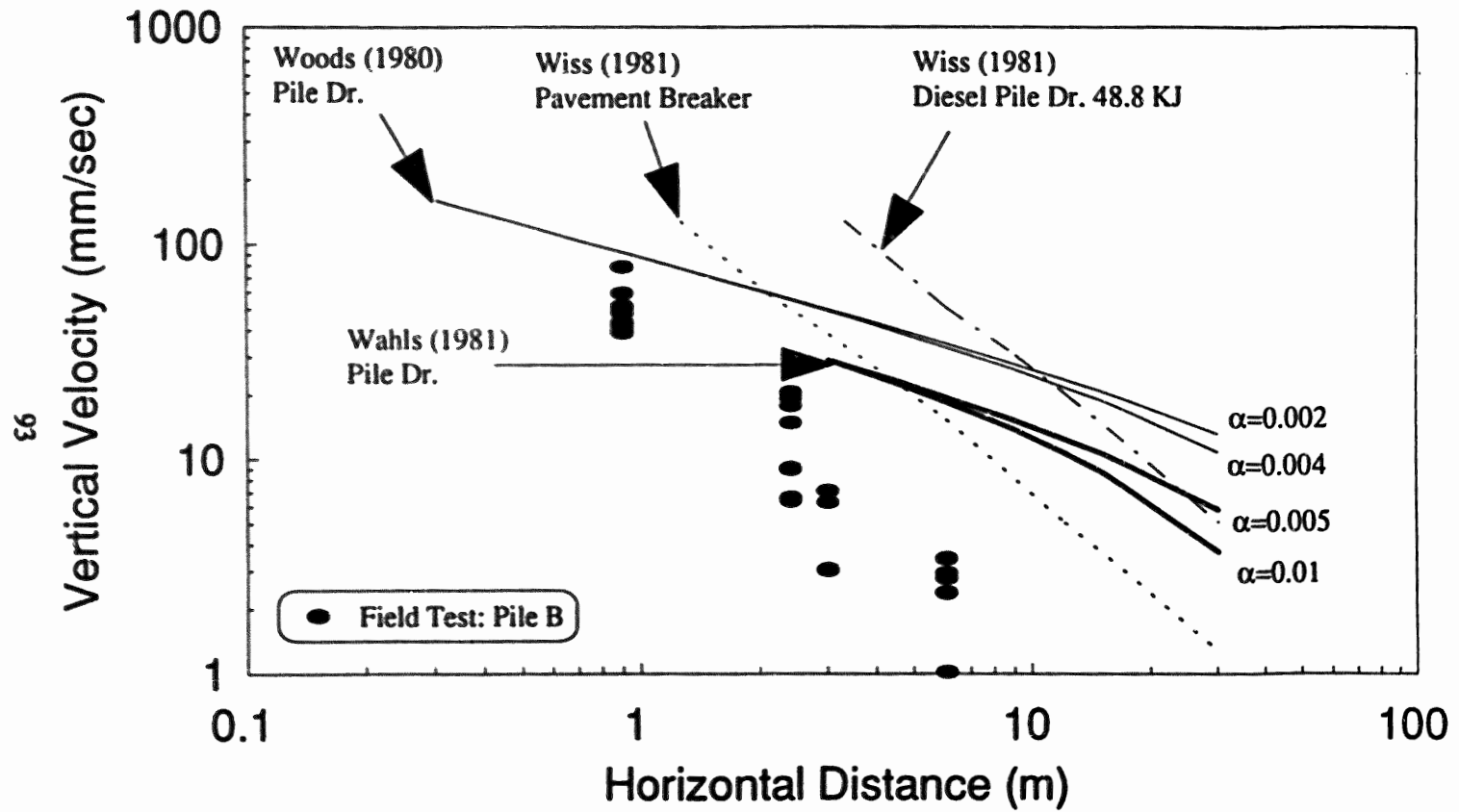


Figure 6.1 Comparison of Vibration Attenuation on the Ground Surface between Field Tests and Literature Reports



shown in Fig. 4.2, the calculated coefficient of material damping,  $\alpha$ , would be 0.15. This is because the geophones were placed near the pile (0.9 m to 6.0 m) and the measured Rayleigh wave length was 4.7 m. Within this distance, the body wave components were still relatively large and the Rayleigh wave was not well developed. The field verification tests suggest that Eq. 6.3 is conservative for the piedmont residual soils. Therefore, we recommend that it be used in calculating the vibration attenuation on the ground surface.

For finite line sources, such as bulldozers, pans and trucks, one might use Eq. 6.5 proposed by Wahls (1981):

$$A = A_1 \sqrt{\frac{\frac{L}{\pi} + r_1}{\frac{L}{\pi} + r}} \exp[-\alpha (r - r_1)] \quad (6.5)$$

where  $L$  is the length of the source.

Attenuation of the vertical component with depth in the soil profile is given by Rayleigh wave theory as:

$$\frac{A_z}{A_{z=0}} = 1.366 \left( -e^{-1.695 \pi \frac{z}{\lambda}} + 1.732 e^{-0.786 \pi \frac{z}{\lambda}} \right) \quad (6.6)$$

where  $A_z$  is the vertical amplitude at depth  $z$ ,  $\lambda$  is the wave length of the Rayleigh wave, and Poisson's ratio is assumed to be 0.25.

The field verification data agrees very well with that predicted by Eq. 6.6. In Fig 4.3 and Fig 4.4, the normalized velocities from the field tests are compared with Rayleigh wave theory. The test data points are marked for the different pile penetration depth. In the vertical direction, when the penetration depth was less than 1.5 m, the data points

agree well with theory. The pile is considered as a surface vibration source, which coincides with Rayleigh wave theory assumption. When the pile penetrated deeper than 1.5 m, the vibration amplitude on the ground surface diminished. Thus, the data points of normalized velocity locate on the right side of the theoretical curve. If the reference velocity on the ground surface was selected when the pile penetration depth less than 1.5 m, these data points would agree well with the curve.

However, the normalized horizontal velocity points are far away from those calculated by Rayleigh wave theory on horizontal direction. The reason is discussed in Chapter 4. It was found that the normalized horizontal velocity points agreed well with the curve obtain by Rayleigh wave theory for the vertical direction. This suggested that both the horizontal and vertical velocities can be estimated by Eq. 6.6 within the soil profile.

## 6.2 Modification of the Shear Modulus Model

From July 1, 1992 to June 30, 1993, a data base was built up based on resonant column and torsional shear test results of 33 specimens. Borden, Shao and Gupta (1994) presented a bi-linear model to describe the relation between normalized shear modulus and shear strain amplitude. In this additional phase of research, the shear modulus model for residual soils has been modified as an unified model. This model considers the influence of soil type, confining pressure, and shear strain amplitude.

### 6.2.1 Modeling of maximum shear modulus

The low shear strain amplitude or maximum shear modulus, ( $G_{max}$ ), is listed in Table 6.1 on the basis of soil type. These values were obtained by resonant column test at shear strains less than 0.001%. For each soil type in Table 6.1, the results are presented in the order of increasing percent sand content. The average of all the  $G_{max}$  data at each confining pressure was determined for each soil type. The average curve shown in Fig. 6.2 (solid line) is the best fit curve for these average  $G_{max}$  at each confining pressure. The object function of these average curves relating maximum shear modulus,  $G_{max}$  (MPa) to effective confining pressure ( $\bar{\sigma}_c$ ) is :

$$G_{max} = p(\bar{\sigma}_c)^q \quad (6.7)$$

where  $p$  and  $q$  are constants presented in Table 6.2 for each soil type. Figure 6.3 shows these average curves (as per the above model) for piedmont residual soils on the basis of soil type.

It can be observed that confining pressure has a significant influence on the maximum shear modulus and that  $G_{max}$  increases with confining pressure (Fig. 6.2). However, for most of the specimens,  $G_{max}$  varied with confining pressure to a power less than 0.5, usually 0.35 to 0.4, with higher values being associated with the more coarse grained soils. Specimens 4ST#1 and 4ST#4 were obtained from depths below the ground water table and exhibited much lower shear moduli (Fig. 6.2D). This suggests that degree of saturation has a significant influence on shear modulus of these soils. It was also

Table 6.1 Maximum Shear Modulus and Minimum Damping on the Basis of Soil Types

Soil Type (USCS)	Sp. No.	Depth (m)	w/c (%)	e (ini)	G <sub>s</sub>	S (%)	LL	PL	PI	Sand (%)	Silt (%)	Clay (%)	Con. Pr. (kPa)	G <sub>max</sub> (MPa)	D <sub>min</sub> (%)
MH	3ST#11A	1.8 - 2.4	50.3	1.78	2.74	77.6	78	56	22	5.8	84.2	10	25	29.55	0.98
	3ST#11B	1.8 - 2.4	36.6	1.48	2.74	67.7	78	56	22	5.8	84.2	10	25	29.27	0.87
			50	34.03	1.20										
			100	40.48	1.30										
	SST#2	3.4 - 4.0	50.9	1.48	2.86	98.7	59	45	14	8.9	86.1	5	50	20.11	1.51
	RC-3	0.9 - 1.5	39.2	1.25	2.81	88	57	43	14	10.3	61.7	28	25	15.13	4.50
			50	21.04	5.60										
			100	25.36	4.90										
	RC-4	0.9 - 1.5	40.7	1.31	2.81	87	57	43	14	10.3	61.7	28	25	13.69	5.40
			50	21.50	4.70										
			100	27.51	4.70										
	RC-5	0.9 - 1.5	41.9	1.35	2.81	87	57	43	14	10.3	61.7	28	25	15.94	4.50
			50	20.33	4.10										
			100	30.49	4.00										
	3ST#10L	1.0 - 1.6	34.8	1.42	2.76	67.5	52	46	6	15.7	75.3	9	25	36.17	3.29
2ST#2	0.9 - 1.5	33.1	1.43	2.85	65.9	75	48	27	16.4	53.6	30	100	53.23	1.49	
3ST#12	1.2 - 1.8	35.6	1.43	2.72	67.7	56	43	13	19.5	72.5	8	25	35.35	1.35	
		50	42.72	1.20											
		100	52.17	1.30											
2ST#1	0.9 - 1.5	33.5	1.41	2.79	66.0	75	46	29	22.6	47.4	30	50	70.53	2.41	
		50	44.03	1.16											
		100	62.51	2.03											
2ST#3	0.9 - 1.5	38.9	1.64	2.79	66.2	92	61	31	27.7	44.3	28	25	32.47	3.72	
		50	46.76	2.38											
		100	62.51	2.03											

Soil Type (USCS)	Sp. No.	Depth (m)	w/c (%)	e (ini)	G <sub>s</sub>	S (%)	LL	PL	PI	Sand (%)	Silt (%)	Clay (%)	Con. Pr. (kPa)	G <sub>max</sub> (MPa)	D <sub>min</sub> (%)
ML	3ST#9	0.9 - 1.5	15.3	0.86	2.74	48.8	35	30	5	22.3	69.7	8	50	59.18	1.40
			100	73.07	1.66										
			50	46.47	2.06										
	3ST#6	1.8 - 2.4	19.5	0.93	2.75	57.5	33	-	NP	29.1	69.9	1	50	46.47	2.06
			100	60.29	2.08										
			50	45.61	1.77										
	3ST#3	2.3 - 2.7	26.8	1.14	2.67	63.0	34	-	NP	30.2	67.8	2	50	45.61	1.77
			100	61.51	1.77										
			25	29.46	1.88										
	3ST#4	1.5 - 2.1	23.6	1.17	2.66	53.6	35	-	NP	32.9	65.1	2	25	29.46	1.88
			50	39.25	1.82										
			100	50.72	1.96										
	3ST#8	1.2 - 1.8	22.8	1.24	2.72	50.2	36	-	NP	35	61.9	3.1	25	30.10	1.85
50			39.79	1.77											
100			54.54	2.26											
3ST#5L	1.2 - 1.8	18.4	1.16	2.69	42.7	37	-	NP	36.2	62.8	1	25	35.29	1.64	
TS-1	2.7 - 3.4	37.8	1.50	2.69	68	44	34	10	42	44	14	25	38.21	2.10	
		50	47.35	1.50											
		100	61.27	1.60											
TS-2	2.7 - 3.4	36.8	1.42	2.69	70	44	34	10	42	44	14	25	30.19	2.22	
		50	38.37	1.90											
		100	46.37	1.36											
TS-3	2.7 - 3.4	29.6	1.18	2.69	67	44	34	10	42	44	14	100	43.79	1.20	

Table 6.1 Continued

Soil Type (USCS)	Sp. No.	Depth (m)	w/c (%)	e (ini)	G <sub>s</sub>	S (%)	LL	PL	PI	Sand (%)	Silt (%)	Clay (%)	Con. Pr. (kPa)	G <sub>max</sub> (MPa)	D <sub>min</sub> (%)
SM-ML	2ST#9	0.9 - 1.5	26.2	1.01	2.69	69.8	-	-	NP	35.6	40.4	24	25 50 100 25	63.71 76.36 88.85 65.55	1.27 1.91 2.75 2.67
	2ST#11	0.9 - 1.5	29.6	1.14	2.71	70.6	-	-	NP	36	44	20	50	68.31	2.26
	2ST#10	0.9 - 1.5	29.6	1.12	2.75	72.9	-	-	NP	43.6	41.4	15	100	97.62	2.50
	3ST#2	1.2 - 1.8	23.9	1.32	2.75	49.7	29	-	NP	46.8	48.2	5	25 50 100	33.38 42.76 57.17	1.96 2.12 1.97
	3ST#2L	1.2 - 1.8	22.9	1.24	2.75	50.6	29	-	NP	46.8	48.2	5	25	34.52	1.62
	RC-1	0.8 - 1.3	24.6	0.89	2.74	75	48	40	8	52	25	23	25 50 100	43.42 67.15 89.41	3.90 3.40 4.00
	RC-2	0.8 - 1.3	30.5	1.00	2.74	84	48	40	8	52	25	23	25 50 100	43.01 66.69 85.85	4.50 3.70 3.40

Soil Type (USCS)	Sp. No.	Depth (m)	w/c (%)	e (ini)	G <sub>s</sub>	S (%)	LL	PL	PI	Sand (%)	Silt (%)	Clay (%)	Con. Pr. (kPa)	G <sub>max</sub> (MPa)	D <sub>min</sub> (%)
SM	2ST#5	1.5 - 2.1	14.8	0.79	2.60	48.4	-	-	NP	69.6	19.4	11	50 100	99.35 127.90	1.68 1.59
	2ST#7	1.5 - 2.1	12.6	0.84	2.60	39.1	-	-	NP	74.3	19.7	6	25 50 100	63.95 82.78 105.87	1.80 1.77 1.74
	2ST#8	2.1 - 2.7	15.0	0.87	2.60	45.0	-	-	NP	70.6	18.4	11	100 50	98.05 83.57	1.74 1.44
	4ST#1	4.0 - 4.6	16.6	0.49	2.81	96.1	-	-	NP	80.4	18.1	1.5	50 100	33.73 51.91	2.96 3.22
	4ST#4	4.7 - 5.3	24.7	0.72	2.79	96.6	-	-	NP	84.7	9.8	0.2	50 100	36.23 55.86	2.33 2.32

NP = Nonplastic

RC = Resonant frequency (Resonant column test)

Sand = Sand size particles, 0.074 - 4.75 mm (#4 - #200)

Silt = Silt size particles, 0.074 - 0.002 mm

Clay = Clay size particles, < 0.002 mm

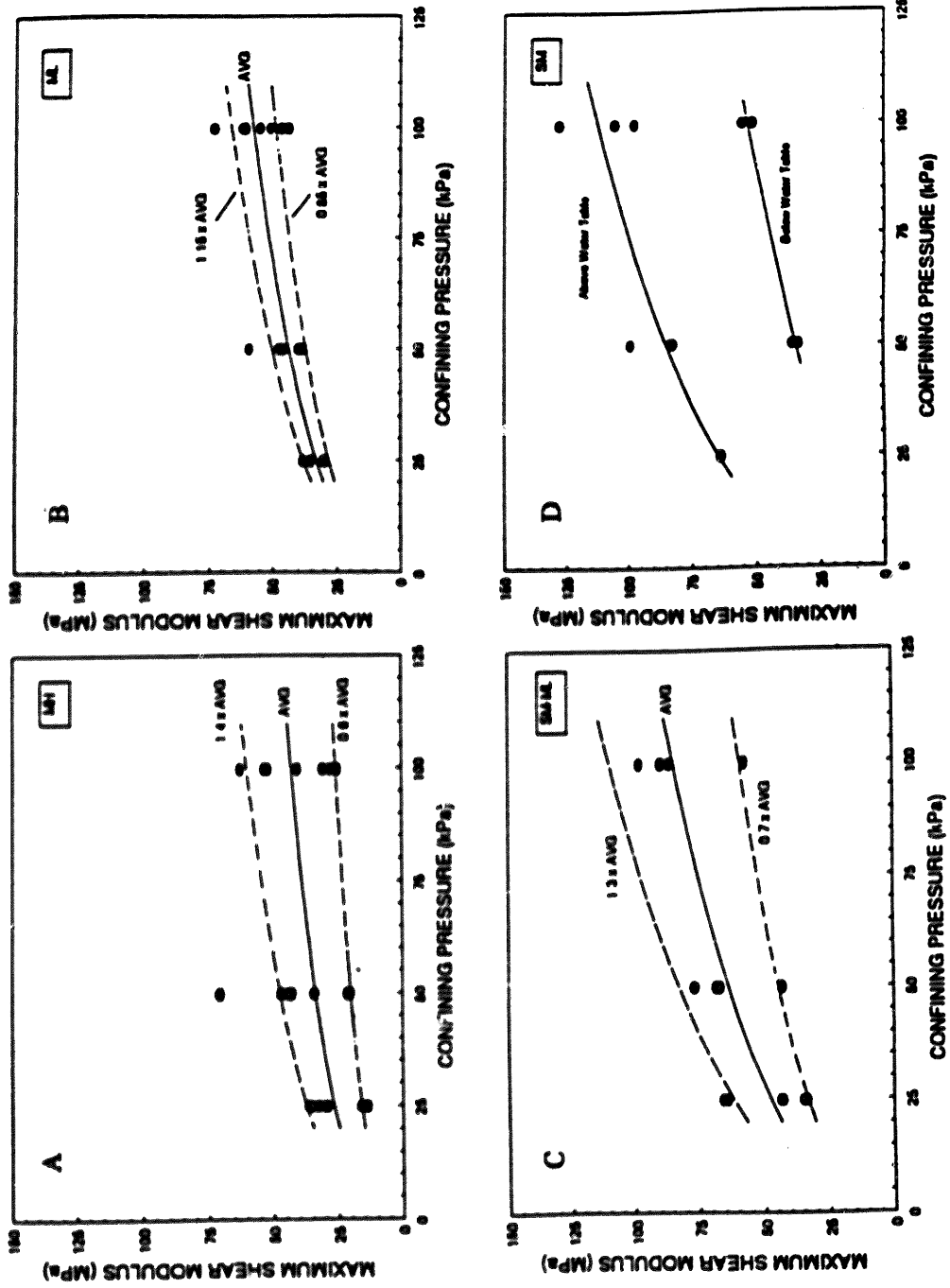


Figure 6.2 Modeling of  $G_{max}$  as a Function of Confining Pressure for Four Types of Residual Soil

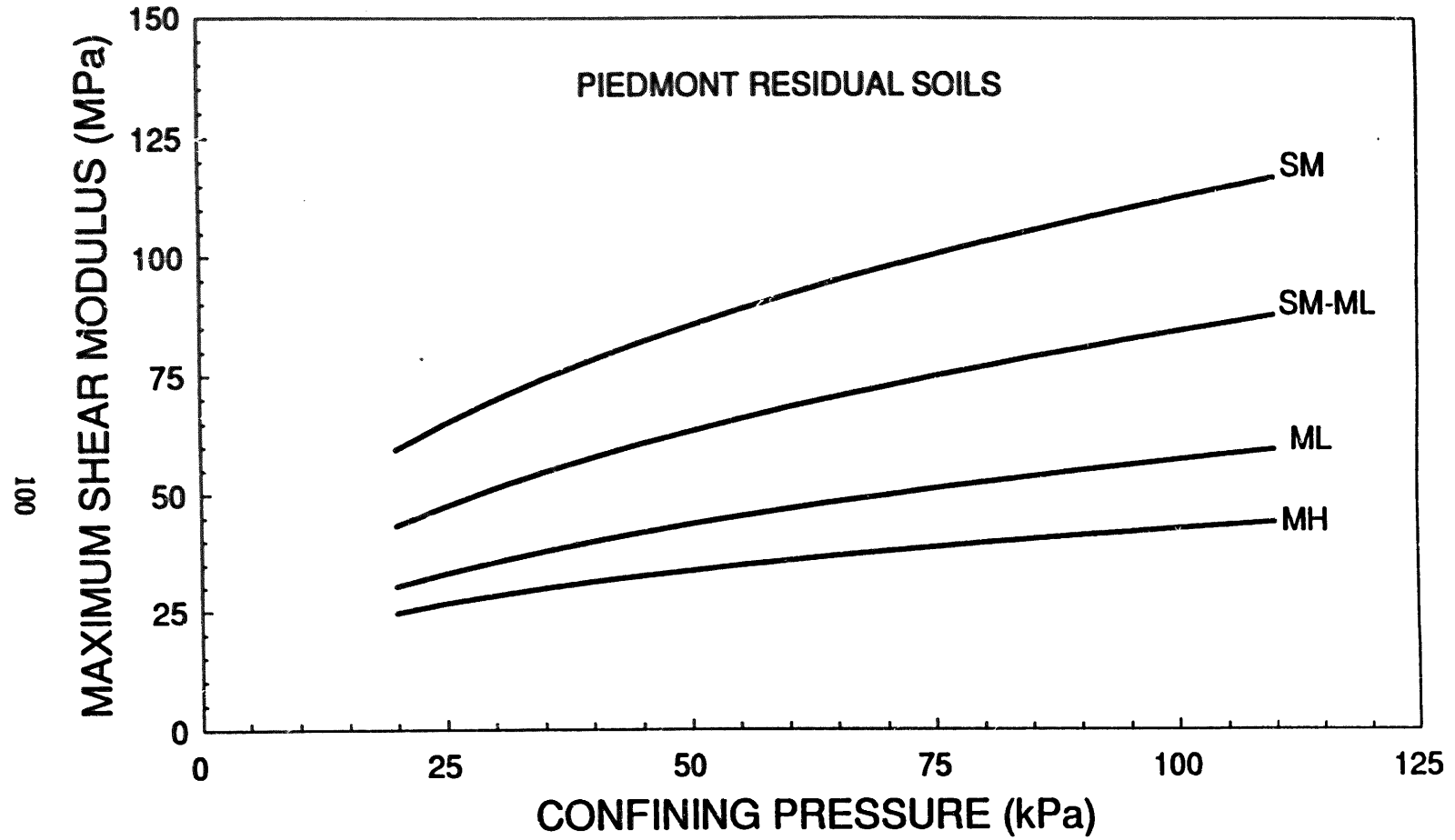


Figure 6.3 Summary of  $G_{max}$  Model on the Basis of Soil Type

observed that upon unloading,  $G_{max}$  was slightly higher at the same confining pressure (specimens 3ST#12 and 2ST#9).

Table 6.2 Values of the Constants and Square of Coefficient of Regression for the Model of  $G_{max}$ .

Soil Type	$p$	$q$	$R^2$ (%)
MH	8.87	0.342	96.2
ML	9.31	0.395	98.9
SM-ML	12.60	0.413	99.8
SM	18.23	0.395	98.8

### 6.2.2 Shear modulus as a function of confining pressure, shear strain, and soil type

For all specimens tested, shear moduli at various shear strain amplitudes were obtained. The value of shear modulus obtained by torsional shear tests is reported as the average for all the cycles of applied. Shear moduli at higher shear strain amplitudes were normalized with respect to  $G_{max}$  (measured at  $\gamma < 0.001\%$ ) for respective specimens. Figure 6.4 shows the decrease in this normalized shear modulus with increasing shear strain amplitude at the three confining pressures on the basis of soil type. All the values of normalized shear modulus fall into a narrow band. Thus, if  $G_{max}$  is estimated or measured in the field, the shear modulus at any higher shear strain amplitude can be reasonably estimated. The threshold strain (shear strain below which  $G$  is almost equal to  $G_{max}$ ) for



these residual soils was observed to be in the range of 0.001 to 0.002%. It was also observed that at same shear strain amplitude, normalized shear modulus for SM is lower than that for MH. This suggests that the normalized shear modulus of coarse grained soils decays at a faster rate with increase in the shear strain amplitude.

The data presented in Fig. 6.4 were modeled using best fit curve by least square method at the three confining pressures for each soil type. The curves represent normalized shear modulus (on a linear scale) plotted against shear strain amplitude (in percent) on a logarithmic scale. The object function for the best fit curves is :

$$\frac{G}{G_{\max}} = \frac{1}{\{1 + \beta_1(\gamma)^{\beta_2}\}^{\beta_3}} \quad (6.8)$$

where  $\gamma$  = shear strain amplitude in percent. The values of the constants  $\beta_1$ ,  $\beta_2$ ,  $\beta_3$ , and square of coefficient of regression ( $R^2$ ) are presented in Table 6.3.

From Fig. 6.4, it can be observed that these models represents the data reasonably well. Further, in general, the normalized shear modulus curves shift to the right as confining pressure increases with the shape of these curves remaining almost the same. Similar results have been reported by Stokoe et al. (1980) for offshore soils (clayey silts and silty clays).

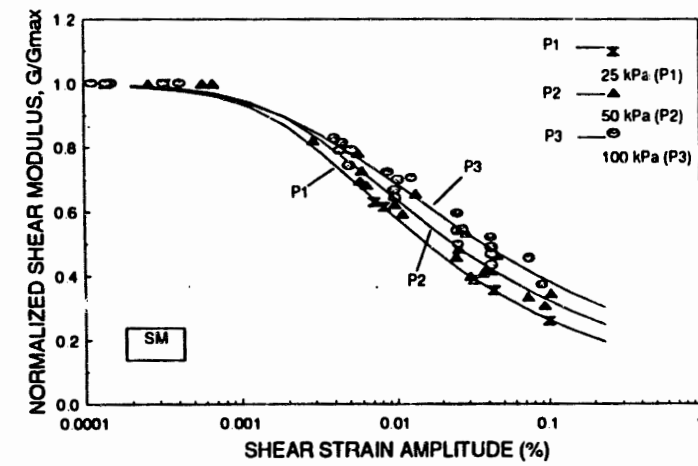
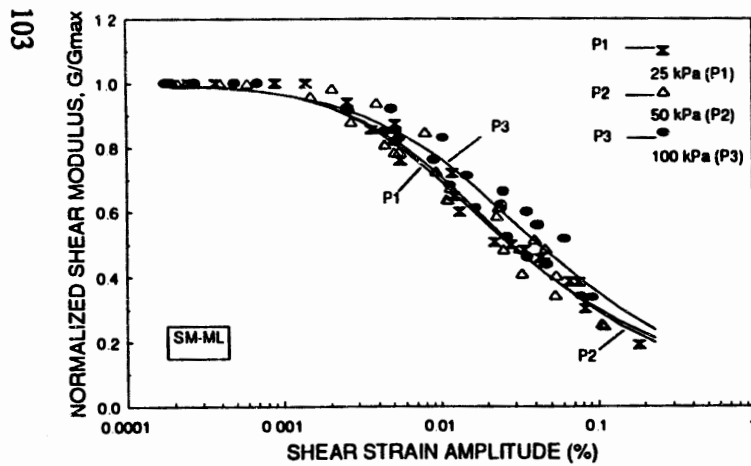
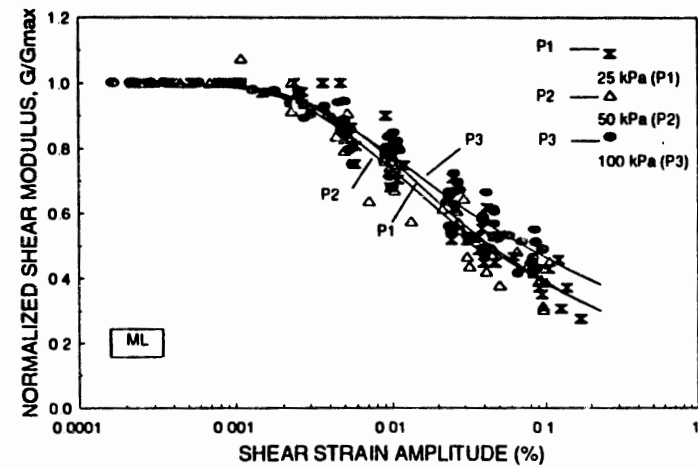
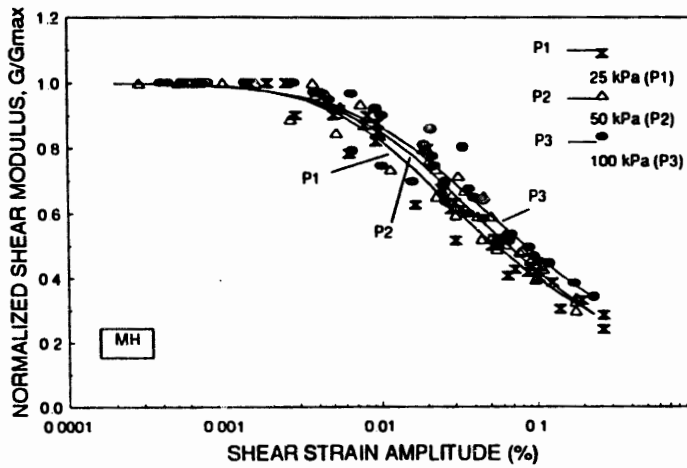


Figure 6.4 Modeling of Normalized Shear Modulus as a Function of Shear Strain Amplitude at the Three Confining Pressures

**Table 6.3 Values of the Constants and Square of Coefficient of Regression for the Normalized Shear Strain Modulus Model (Eq. 6.8)**

Soil Type	Confining Pressure (kPa)	$\beta_1$	$\beta_2$	$\beta_3$	$R^2$ (%)
MH	25	733	1.43	0.28	97.1
	50	120	1.19	0.40	97.0
	100	101	1.17	0.37	94.5
ML	25	1.13e+4	1.76	0.18	94.6
	50	1.47e+4	1.73	0.17	95.4
	100	9.50e+3	1.65	0.14	94.0
SM-ML	25	530	1.23	0.35	97.8
	50	235	1.14	0.42	96.4
	100	54	0.97	0.54	95.2
SM	25	7.63e+3	1.47	0.24	99.9
	50	5.01e+3	1.43	0.22	97.8
	100	617	1.12	0.25	98.0

### 6.2.3 Comparison with other studies

The results of all tests performed in this study are plotted in Fig. 6.5. For comparison purposes, results from Seed and Idriss (1970), Stokoe and Lodde (1978), Isenhower (1979), and Stokoe et al. (1980) have also been included. Seed and Idriss presented results for sands and saturated clays, Stokoe and Lodde and Isenhower conducted tests on San Francisco Bay Mud, and Stokoe et al. reported these median curves for tests conducted on offshore marine soils (clayey silts to silty clays). It can be

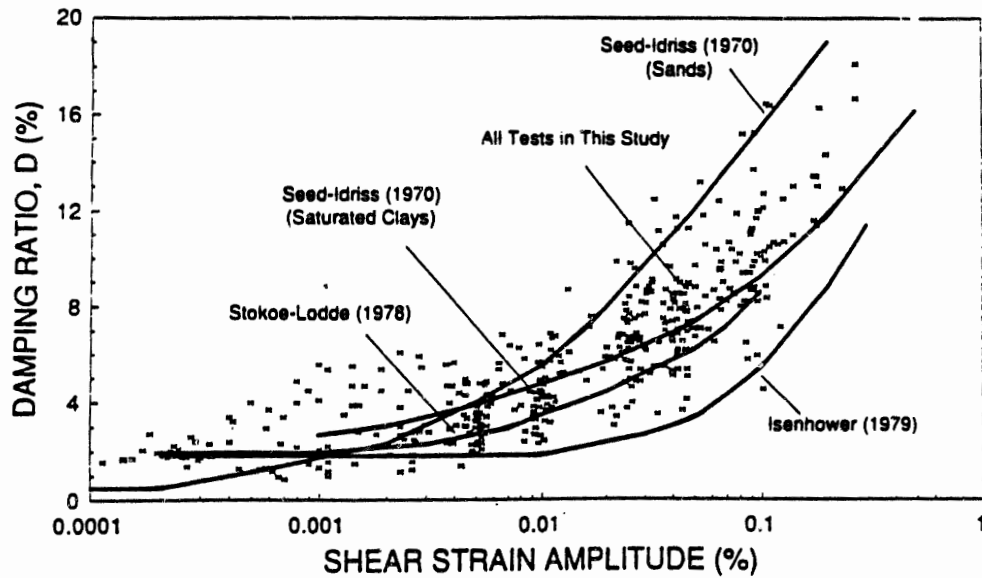
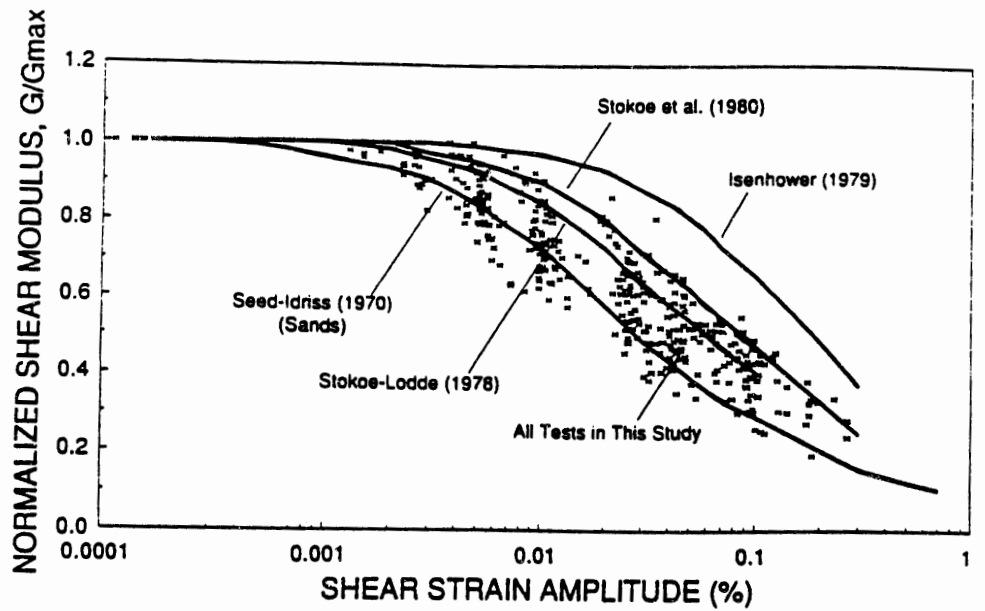


Figure 6.5 Comparison of All the Test Results in this Study with Other Studies in the Literature

observed that the normalized shear modulus and damping of piedmont residual soils are in the same range as reported by other authors.

#### **6.2.4 Modeling of material damping**

The minimum damping ratio values for all the specimens tested in this study are presented in Table 6.1. These damping ratio values were obtained by resonant column tests at shear strain amplitudes less than 0.001%. It was observed that the influence of confining pressure is less pronounced on damping ratio than on shear modulus.

Figure 6.6 shows the damping values obtained at various shear strain amplitudes for all the specimens tested on the basis of soil type. Hysteretic damping ratios ( obtained by torsional shear tests) reported here are those obtained for the first few cycles of loading. The damping values increased with increase in shear strain amplitude. The influence of shear strain amplitude is more pronounced on damping ratio than it is on shear modulus. The threshold shear strain for these residual soils was observed to be around 0.0005 to 0.001%. For all the test data in Fig. 6.6, the dashed lines show the approximate upper bound and lower bound whereas the solid line represents the average relationship. This average relationship should provide damping ratio values for piedmont residual soils with sufficient accuracy for many practical purposes.

The normalized shear modulus and damping ratio versus shear strain amplitude plots are shown in Fig. 6.4 and Fig. 6.6, respectively. Comparing these two figures, the damping ratio data are seen to be more scattered than that of normalized shear modulus. A very interesting relationship between the normalized shear modulus and the damping

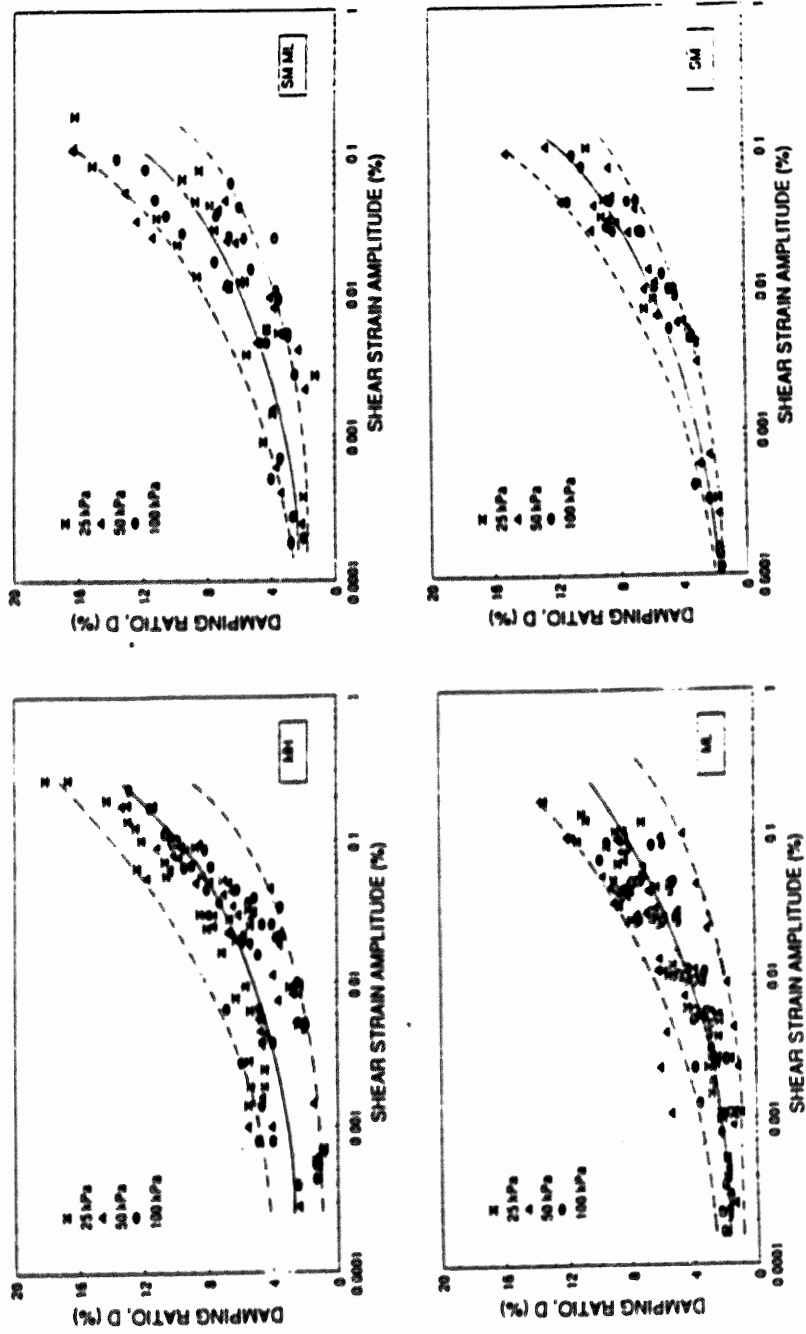


Figure 6.6 Damping Values Obtained at Various Shear Strain Amplitudes for on the Basis of Soil Type

ratio can be presented by plotting these two values in one figure. All the data point fall in a relatively narrow band as shown in Fig. 6.7, and the best fit curve, obtained by the least square method, can be expressed as:

$$D(\%) = 20.4 \left( \frac{G}{G_{\max}} - 1 \right)^2 + 3.1 \quad (6.9)$$

It was observed that the confining pressure does not have an affect on the damping ratio and normalized shear modulus relationship. Also, the four types of residual soil tested, MH, ML, SM-ML, and SM have almost the same best fit curves. Therefore, Equation (4) can be used to estimate the damping ratio from the normalized shear modulus at any given shear strain amplitude. The relationship between the normalized shear modulus and shear strain amplitude are well defined by Seed (1970), Hardin and Drnevich(1972) for sands and clay, and residual soils in this research. It is usually difficult to establish a model to express the relationship between the damping ratio and shear strain amplitude directly, because the data points are very scattered. It appears that the relationship between normalized shear modulus and damping ratio can be conveniently used as a bridge to calculate damping from the model of normalized shear modulus.

Figure 6.8 shows the relationship between normalized shear modulus and damping ratio obtained from our research and that reported in the literature. In general, these results suggest that the dynamic behavior of these residual soils is intermediate of that exhibited by sands and clays -- the normalized shear modulus decreases and damping ratio increases at a rate faster than that for clays but slower than that exhibited by sands.

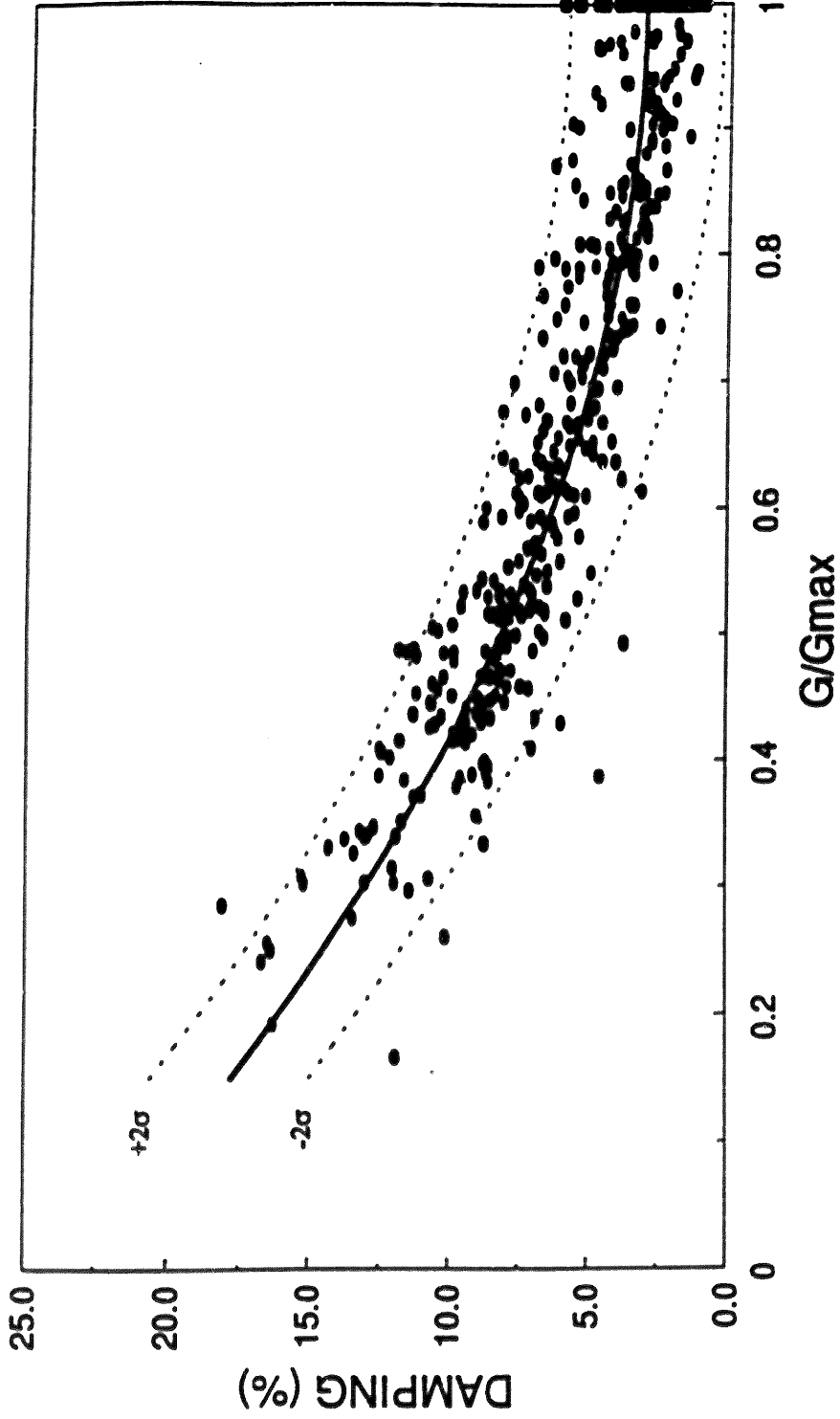


Figure 6.7 Modeling of the Relationship between Damping Ratio and Normalized Shear Modulus



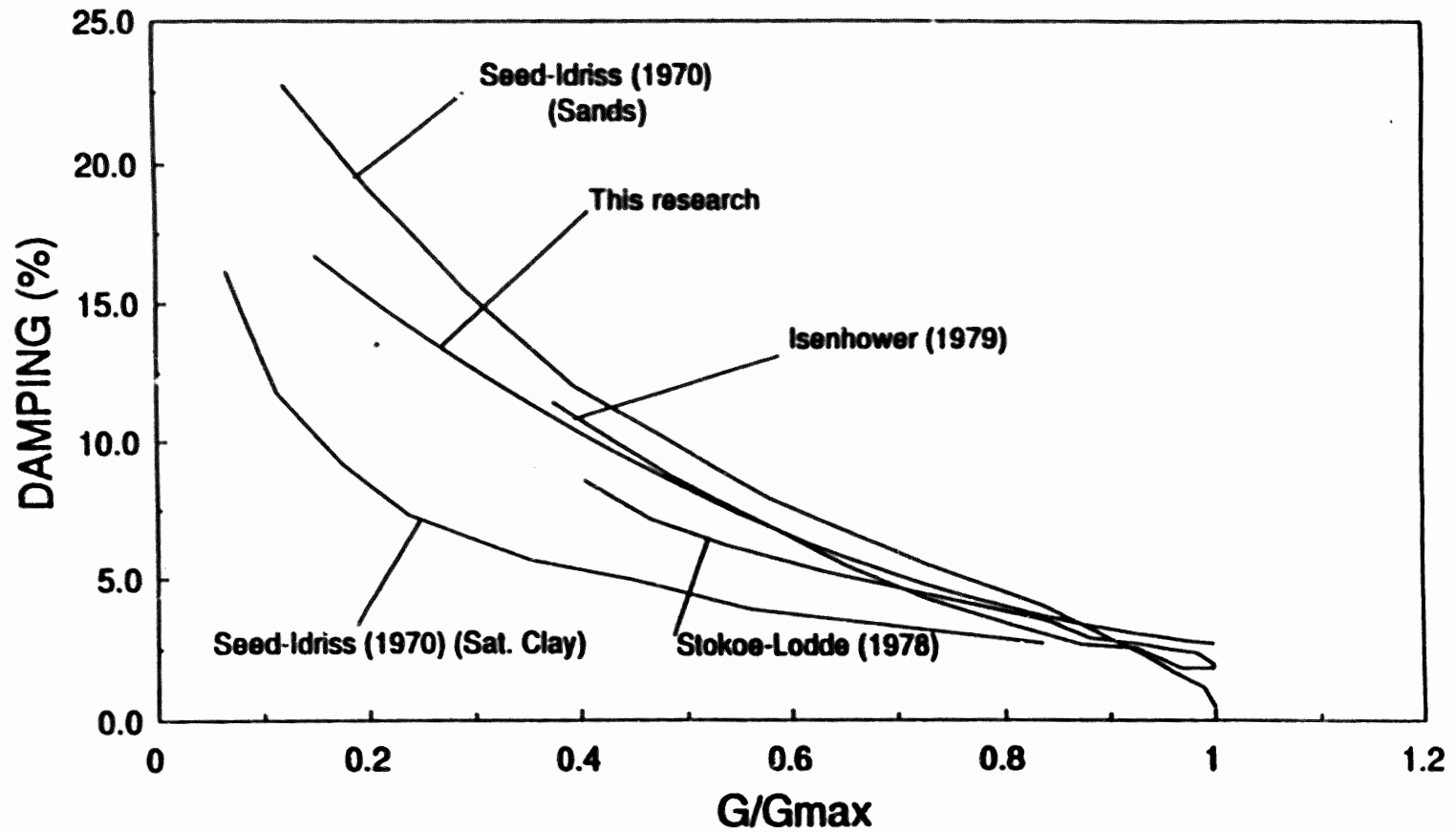


Figure 6.8 The Relationship between Normalized Shear Modulus and Damping Obtained from this Study and that Reported in the Literature

### 6.3 Verification of Dynamic Settlement Model

From the torsional shear test results, the volume change caused by static isotropic consolidation and that resulting from dynamic torsional shear are considered separately. The dynamic volumetric strain can be expressed as a function of confining pressure, shear strain amplitude and number of cycles for different soil types. This relation can be modeled by regression method as :

$$\Delta \epsilon_{vol} = a(\gamma - \gamma_c)(\log N)^b \quad (6.10)$$

where  $\Delta \epsilon_{vol}$  is the dynamic volumetric strain under  $N$  cycles of torsional shear, factors  $a$  and  $b$  are functions of soil type and confining pressure,  $\gamma_c$  is the threshold shear strain amplitude (in %) of the specimen at each confining pressure and  $\gamma$  is the current shear strain amplitude (in %). If the shear strain amplitude is below  $\gamma_c$ , dynamic settlement is unlikely to happen.

A comparison between measured and modeled test results for specimens 6ST#2, 6ST#2A and 6ST#4 are plotted in Fig. 6.9, Fig. 6.10, and Fig. 6.11, respectively. Factors used in modeling the dynamic settlement are listed in Table 6.4.

Figure 6.12 shows the dynamic volumetric strain versus shear strain amplitude at 1000 cycles. For the same number of cycles, the dynamic volumetric strain increases linearly with shear strain amplitude. The data are plotted in conjunction with best-fit linear functions. In addition, dynamic densification is seen to decrease with increasing of the confining pressure.

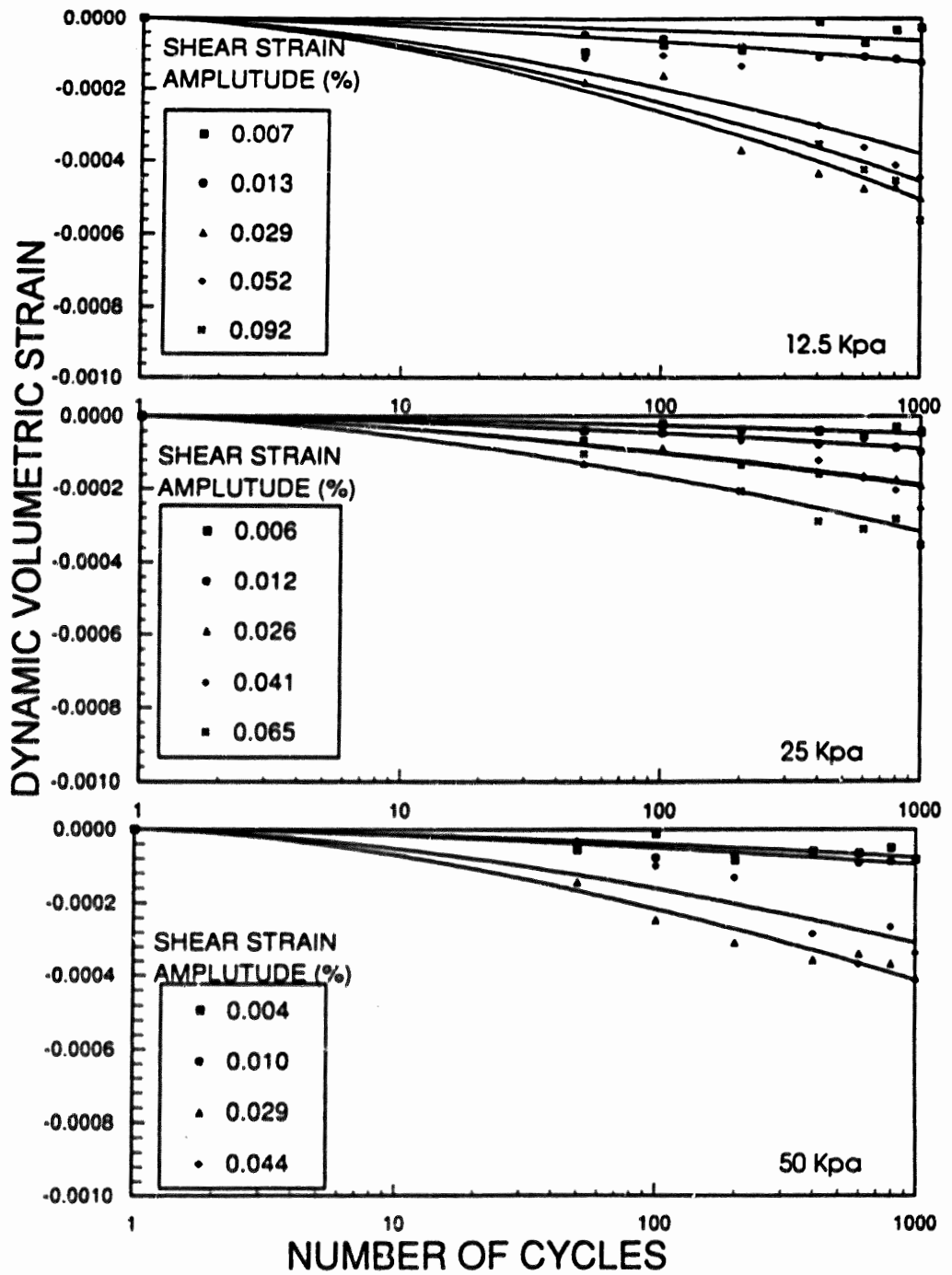


Figure 6.9 Modeling of Dynamic Volumetric Strain as a Function of Shear Strain Amplitude and Number of Cycles for Specimen 6ST#2

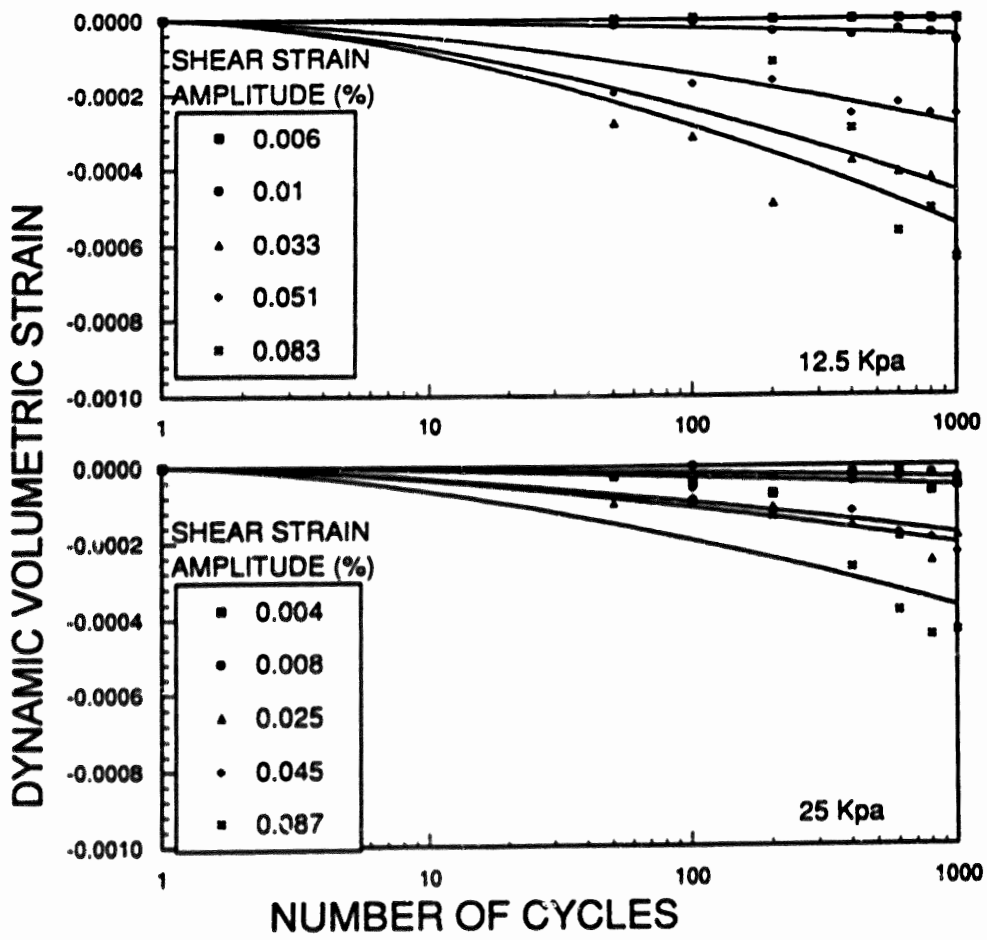


Figure 6.10 Modeling of Dynamic Volumetric Strain as a Function of Shear Strain Amplitude and Number of Cycles for Specimen 6ST#2A

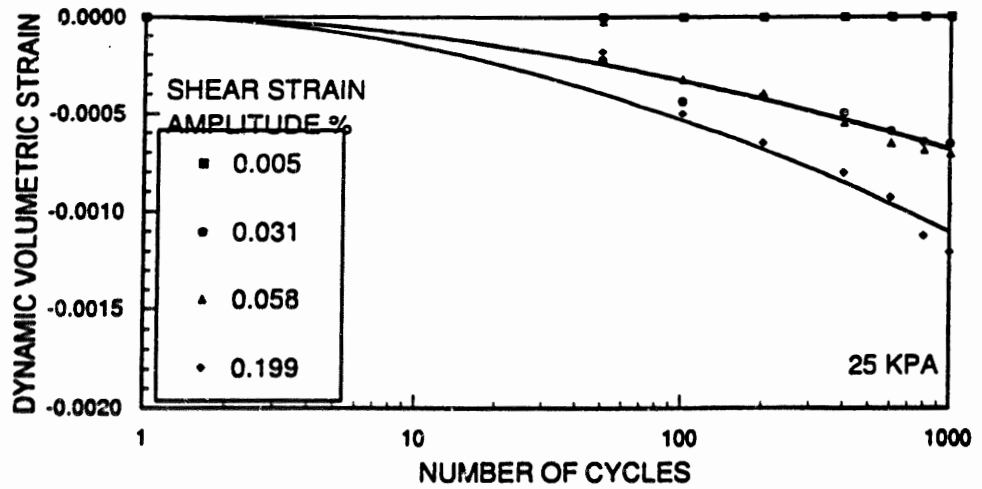


Figure 6.11 Modeling of Dynamic Volumetric Strain as a Function of Shear Strain Amplitude and Number of Cycles for Specimen 6ST#4

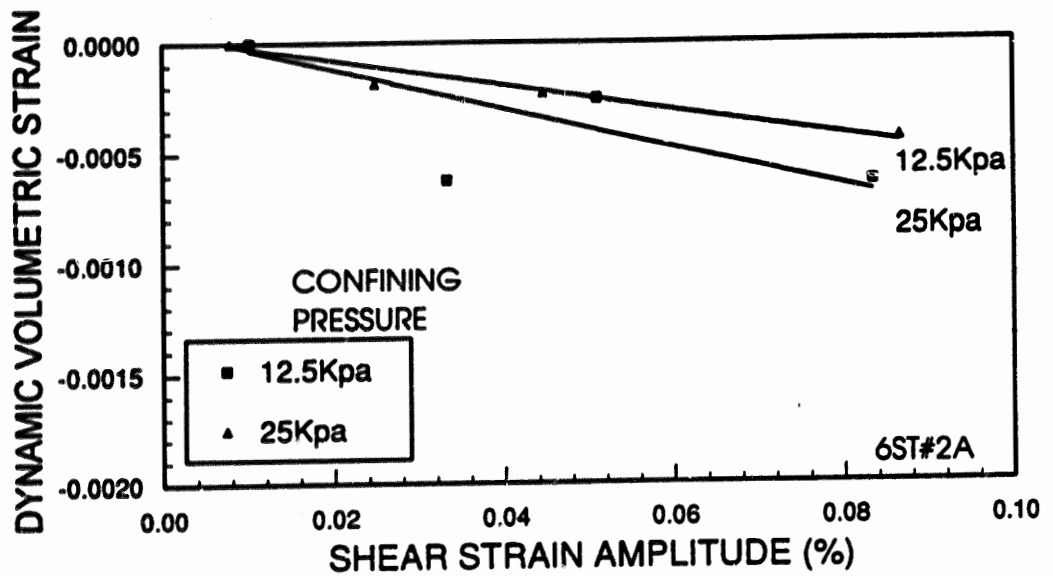


Figure 6.12 Dynamic Volumetric Strain Versus Shear Strain Amplitude at 1000 Cycles for Specimen 6ST#2A

Table 6.4 Modeling of Dynamic Settlement for Samples Obtain from Site 1 (Selma, NC)

Specimen	6ST#2 A			6ST#2			6ST#4		
Factors	a	b	$\gamma_c$ (%)	a	b	$\gamma_c$ (%)	a	b	$\gamma_c$ (%)
Confining Pressure									
12.5 (kPa)	0.00152	1.6	6.29e-3	0.00122	1.6	1.92e-3			
25.0 (kPa)	0.00097	1.6	5.85e-3	0.00122	1.6	1.00e-3	0.00256	1.6	2.97e-3
50.0 (kPa)				0.00210	1.6	8.83e-3			

#### 6.4 Comparison between Experimental Results and Model Predictions

The dynamic settlement in the field tests was monitored using the extensometer system described in Chapter 4. The dynamic volumetric strain of specimens was measured in laboratory torsional shear tests and modeled according to Eq. 6.10. The analytical model presented in Section 6.3 can be used to calculate the foundation settlement under construction induced vibration based on soil properties resulting from laboratory test.

For the field verification test at Selma, NC, the peak particle velocities recorded by surface 3-D geophone are listed in table 4.4. These vibration records obtained at the same distance from the source as was the extensometer. The average peak particle velocity (vector sum of velocities in three directions) induced by Pile B driving was 18.2 mm/sec with a standard deviation of 7.6 mm/sec. At 95% confidence level, the peak particle velocity would therefore be 33.4 mm/sec. In the following analysis, both the average velocity and velocity for 95% confidence level are considered.

To prepare the input data for the analytical program, CVIS, the dominant vibration frequency was selected to be 30.5 Hz, as measured in the field. As presented in Chapter 4, the Rayleigh wave velocity was determined in the field to be 142 m/sec. Thus, the shear wave velocity can be calculated as  $V_s = \frac{V_R}{0.919} = 154.6 \text{ (m/sec)}$ . It was assumed that the vibration amplitudes are the same for each pile strike and that the total number of blows was 400. The soil profile was divided into three layers of thickness 2 m, 2.5m and 3m, in which the dynamic soil properties were represented by specimens as listed in Table 6.5.

Table 6.5 Calculation of Dynamic Settlement on Site 1 (Selma, NC)

		Layer 1	Layer 2	Layer 3
Depth (m)		0.0-2.0	2.0-4.5	4.5-7.5
Specimen Number		6ST#2A	6ST#2	6ST#2
Average Amplitude 18.2 (mm/sec)	Shear Strain Amplitude (%)	0.012	0.0056	0.0012
	Settlement (mm)	0.06	0	0
95% Amplitude 33.4 (mm/sec)	Shear Strain Amplitude (%)	0.023	0.011	0.002
	Settlement (mm)	0.26	0.03	0

The shear strain amplitude and dynamic settlement were calculated by using the program, CVIS, with the values provided in Table 6.5. Under the pile driving induced vibration, the cumulative ground surface settlement is 0.06 mm and 0.29 mm for the average and 95% confidence ground vibration, respectively.

The ground surface settlement and the settlement with depth within the soil profile were monitored by the extensometer. No significant settlement on the ground surface or within the soil profile was measured. The resolution of the extensometer is 2 mm. Detailed records of measurement can be found in Section 4.1.

The pile driving induced settlement in the field verification test was very small. The previous analysis shows that the model prediction based on laboratory tests and field measured settlement was in good agreement. The very small magnitude of both measured and predicted settlement are the result of several factors: (1) the soil at the test site has a relatively high shear modulus. Thus, the soil deformation (i.e. the shear strain amplitude) was correspondingly small and (2) the average peak particle velocity recorded was only 18.2 mm/sec at the distance of 2.4 m from the pile; of cause large energy level and increased number of hammer blows would be expected to produce increased settlement.

Compared with the settlement prediction in Chapter 3 before the field test, the post-test settlement predictions presented in Table 6.5 based on actual resonant column / torsional shear test data on site specific specimens are smaller. This is because the soil in the test site was found more stiff than that initially anticipated. The shear modulus of specimen 6ST#2 is 50% higher than that of 3ST#8, upon which the pre-test prediction in Chapter 3 was based. Further more, the vibration amplitude and number of pile driving blows were smaller in the field test than that estimated prior to the test. The settlement measured in the field agreed well with that calculated by our proposed analytical model.



## CHAPTER 7

### CONCLUSIONS AND RECOMMENDATIONS

The objective of this research described in the report was to provide field verification of an analytical model developed to predict ground surface settlement due to construction induced vibrations. This work was performed as a second phase to a previous project entitled "Construction Induced Vibrations" conducted during 1992 and 1994.

Three test sites with residual soil profile were investigated. At one of the sites, in Selma, North Carolina, settlement of the residual soil profile was measured during pile driving. In addition, the characteristics of the vibration source, as well as the wave propagation behavior were monitored. Laboratory resonant column and torsional shear tests were performed on samples obtained from the site. Predicted settlement based on an laboratory densification behavior compared well with that measured in the field.

The vibration attenuation and dynamic densification within the residual soil profile were investigated for the first time. The following specific conclusions can be derived from the research work:

- Vibration attenuation with distance on the ground surface can be conservatively estimated by Rayleigh wave theory.

- Attenuation of both vertical and horizontal vibration components as a function of depth in the soil profile agrees well with Eq. 6. 6.
- By using the proposed analytical model and existing data base, the predicted vibration induced settlement on the ground surface before the field test coincided with that measured.
- Laboratory resonant column and torsional shear tests were performed on specimens obtained from the test site. The post-test settlement prediction based on these laboratory data also agreed well with the field observation. The analytical model was shown to provide a conservative estimate of ground surface settlement.
- The dominant vibration frequency monitored during pile driving was around 30 Hz.
- The Rayleigh wave velocity measured during the test agreed well with that obtained from resonant column test results. This suggests that the propagation of Rayleigh wave can be predicted based on laboratory test results.

## CHAPTER 8

### IMPLEMENTATION AND TECHNOLOGY TRANSFER

The research documented in this report and report FHWA/NC/94-007 has resulted in the development of a procedure for predicting the ground surface settlement induced by construction vibrations. This procedure is outlined below:

1. The source characteristics of construction induced vibrations can be determined from field measurement or literature, such as plotted in Fig. 8.1 or Fig 8.2 (Fig. 2.1 and Fig. 6.1). These characteristics include vibration amplitude, number of events (i.e., number of pile driving blows, number of truck passes, etc.), and dominant frequency.
2. The peak particle velocity on the ground surface at the site of the building foundation can be obtained by field measurement, or Rayleigh wave attenuation theory (Eq. 8.1 [Eq. 6.3 *bis*] or Eq. 8.4 [Eq. 6.5 *bis*]). For a point source, like pile driving near the ground surface, the surface vibration amplitude can be expressed as :

$$A = A_1 \left( \frac{r_1}{r} \right)^{1/2} \exp[-\alpha(r - r_1)] \quad (8.1)(6.3 \text{ bis})$$

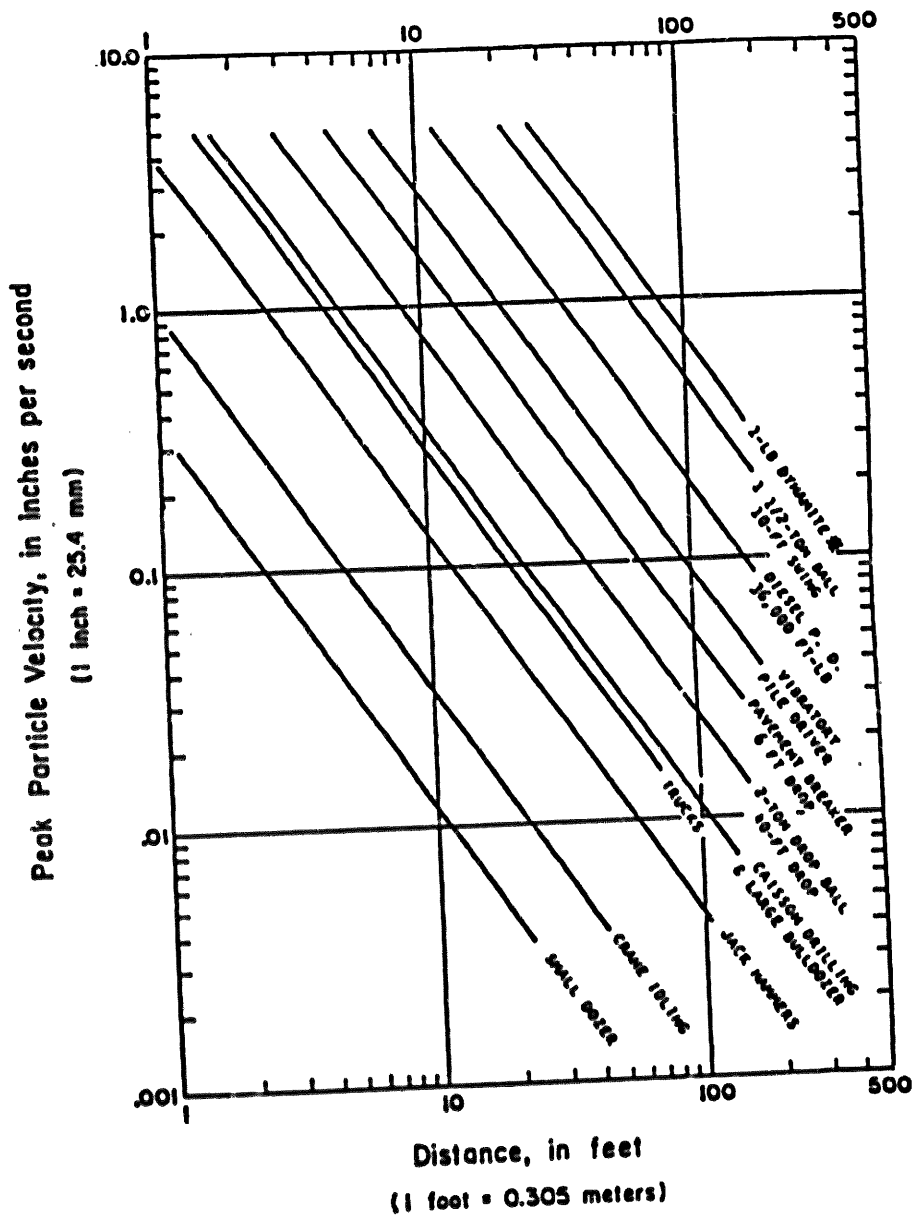


Figure 8.1 Relative Intensities of Construction Vibrations (Wiss, 1981)  
(Reprint of Figure 2.1)

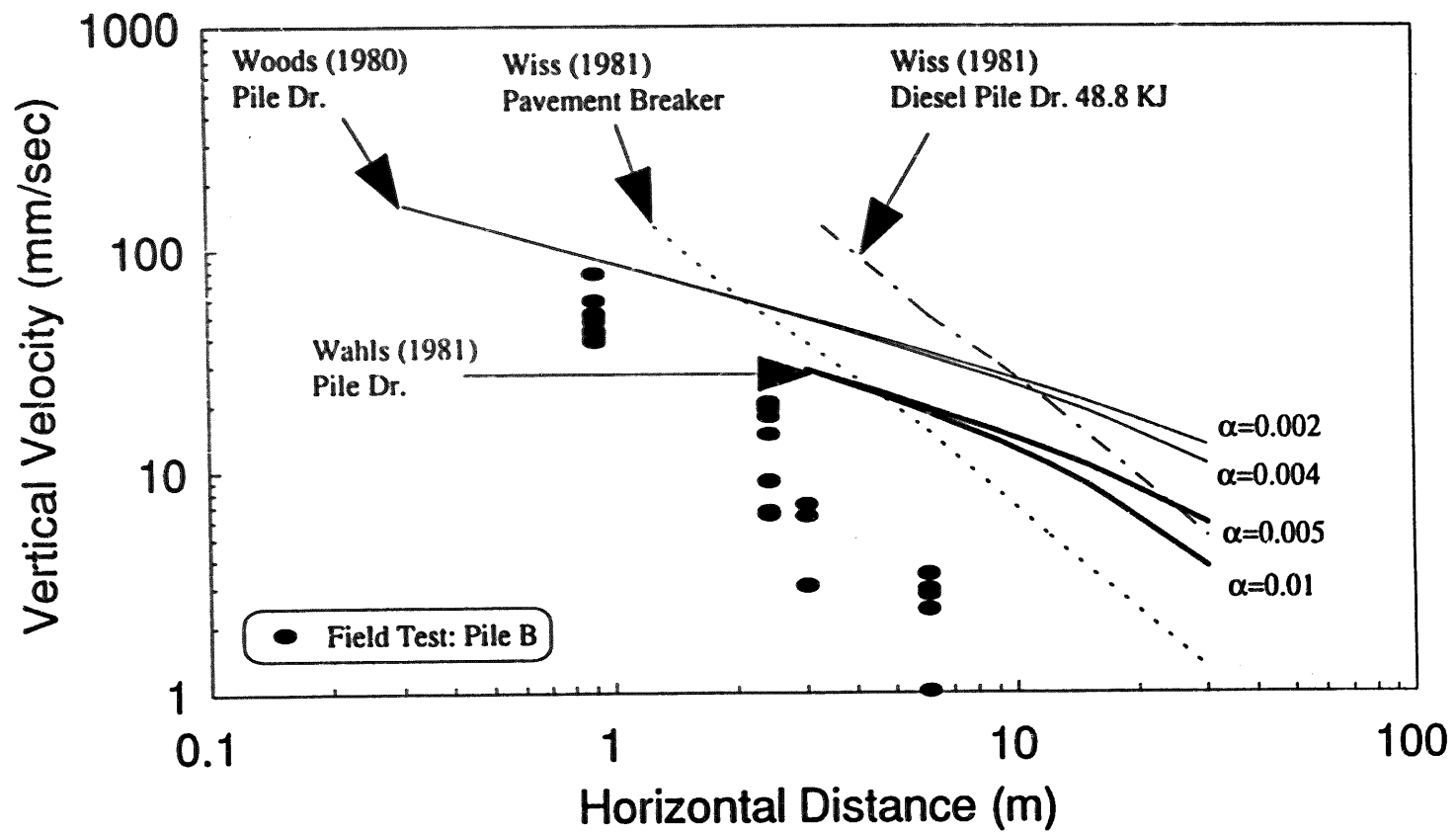


Figure 8.2 Comparison of Vibration Attenuation on the Ground Surface between Field Tests and Literature Reports (Reprint of Figure 6.1)

where  $A$  is the amplitude of particle velocity at a distance  $r$  from the source,  $A_1$  is the amplitude of particle velocity at a reference point, at a distance  $r_1$ , from the source, and  $\alpha$  denotes the coefficient of material damping. The coefficient of material damping,  $\alpha$ , can be obtained from field measurements or can be calculated by :

$$\alpha = \frac{2\pi f D}{V_R} \quad (8.2)(6.4 \text{ bis})$$

where  $f$  is the vibration frequency,  $V_R$  is the Rayleigh wave velocity and  $D$  is the material damping ratio, which can be obtained from Eq 8.3 (6.9 bis).

$$D(\%) = 20.4 \left( \frac{G}{G_{\max}} - 1 \right)^2 + 3.1 \quad (8.3)(6.9 \text{ bis})$$

For a finite line source (i.e., bulldozer, pan and truck) , the surface vibration amplitude at a distance  $r$  from the source can be expressed as :

$$A = A_1 \sqrt{\frac{\frac{L}{\pi} + r_1}{\frac{L}{\pi} + r}} \exp[-\alpha (r - r_1)] \quad (8.4)(6.5 \text{ bis})$$

where  $L$  is the length of the source.

3. The equivalent number of cycles of each event can be estimated by field time history records or by the simplified method proposed in the research report FHWA/MC/94-007; Two computer programs, TRUCKPAS and BULLD, can calculate the equivalent number of cycles for trucks and bulldozers passing by,

respectively. It is necessary to emphasize that construction induced vibrations are very complicated and depend on type of equipment, road condition, operating condition of equipment, and soil profile. The best way to estimate the equivalent number of cycles is from field measurement and the simplified method only provides a preliminary estimate when field records are not available.

4. The particle velocity amplitude at different depths (for example, 1.5 m, 3.0 m and 6.0 m) can be calculated by the Rayleigh wave attenuation theory as:

$$\frac{A_z}{A_{z=0}} = 1.366 \left( -e^{-1.695 \frac{\pi z}{\lambda}} + 1.732 e^{-0.786 \frac{\pi z}{\lambda}} \right) \quad (8.5)(6.6 \text{ bis})$$

where  $A_z$  is the vibration amplitude at depth  $z$ , and  $\lambda$  is the wave length of the Rayleigh wave. The peak particle velocity decreases rapidly with depth. When the depth equals one Rayleigh wave length, the particle velocity amplitude is only 10% ~20% of the ground surface amplitude. Below this depth, the magnitude of vibration induced settlement is unlikely to be significant. The Rayleigh wave length of residual soil profiles is around 5m ~ 8m for the frequency ranging from 15 Hz to 30 Hz.

5. The shear strain amplitude at different depths can be found by;

$$\gamma = \frac{A_z}{V_R} \quad (8.6)(2.5 \text{ bis})$$

The Rayleigh wave velocity,  $V_R$ , can be calculated as a function of shear wave velocity and Poisson's ratio as shown in Fig. 2.10. By using an iteration procedure to obtain convergence of the relationship between  $\gamma \sim V_R \sim V_s \sim G \sim \gamma$  as shown in Fig. 8.3 (Fig 2.11 *bis*), the correct shear strain amplitude is obtained.

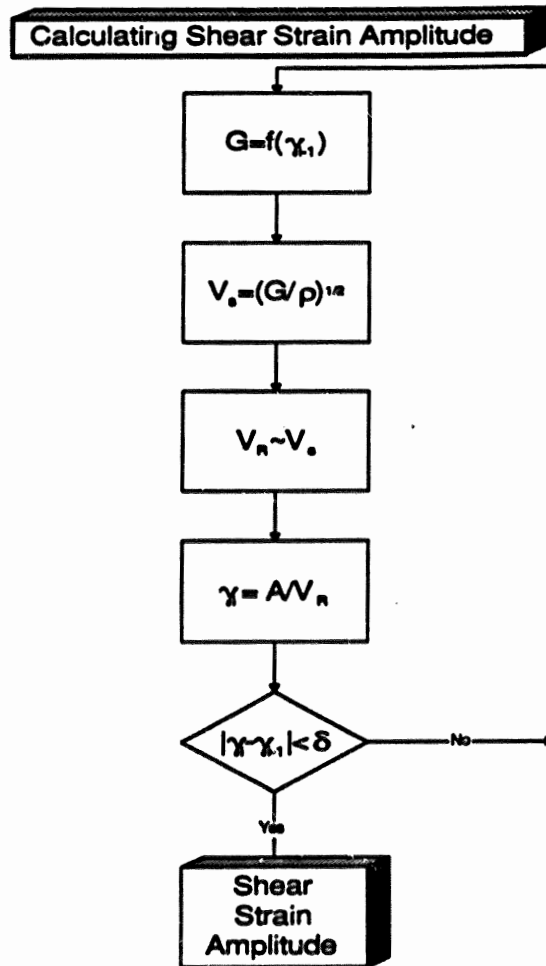


Fig. 8.3 The Flow Chart of Calculating the Shear Strain Amplitude. (Reprint of Fig. 2.11)



The shear modulus of residual soils is a function of shear strain amplitude, which can be expressed as:

$$\frac{G}{G_{\max}} = \frac{1}{\{1 + \beta_1(\gamma)^{\beta_2}\}^{\beta_3}} \quad (8.7)(6.8 \text{ bis})$$

where  $\gamma$  = shear strain amplitude in percent. The values of the constants  $\beta_1$ ,  $\beta_2$ ,  $\beta_3$ , and square of coefficient of regression ( $R^2$ ) are presented in Table 8.1 (Table 6.3 bis).

**Table 8.1 Values of the Constants and Square of Coefficient of Regression for the Normalized Shear Strain Modulus Model (Reprint of Table 6.3)**

Soil Type	Confining Pressure (kPa)	$\beta_1$	$\beta_2$	$\beta_3$	$R^2$ (%)
MH	25	733	1.43	0.28	97.1
	50	120	1.19	0.40	97.0
	100	101	1.17	0.37	94.5
ML	25	1.13e+4	1.76	0.18	94.6
	50	1.47e+4	1.73	0.17	95.4
	100	9.50e+3	1.65	0.14	94.0
SM-ML	25	530	1.23	0.35	97.8
	50	235	1.14	0.42	96.4
	100	54	0.97	0.54	95.2
SM	25	7.63e+3	1.47	0.24	99.9
	50	5.01e+3	1.43	0.22	97.8
	100	617	1.12	0.25	98.0

The low shear strain amplitude or maximum shear modulus, ( $G_{max}$ ), is listed in Table 6.1 on the basis of soil type. The average maximum shear modulus,  $G_{max}$  (MPa), is a function of the effective confining pressure ( $\bar{\sigma}_c$ ) for each type of residual soils, which is expressed as :

$$G_{max} = p(\bar{\sigma}_c)^q \quad (8.8)(6.7 \text{ bis})$$

where p and q are constants presented in Table 8.2 (Table 6.2 bis) for each soil type.

Table 8.2 Values of the Constants and Square of Coefficient of Regression for the Model of  $G_{max}$  (Reprint of Table 6.2).

Soil Type	p	q	R <sup>2</sup> (%)
MH	8.87	0.342	96.2
ML	9.31	0.395	98.9
SM-ML	12.60	0.413	99.8
SM	18.23	0.395	98.8

6. In each layer, the dynamic settlement can be obtained as a function of the equivalent number of cycles at the appropriate shear strain amplitude from the following expression.

$$\Delta \varepsilon_{vol} = a(\gamma - \gamma_c)(\log N)^b \quad (8.9)(2.8 \text{ bis})$$

where  $\Delta\varepsilon_{vol}$  is the dynamic volumetric strain under  $N$  cycles of torsional shear,  $a$  and  $b$  are constants which depends only on the confining pressure and type of soil,  $\gamma_c$  is the threshold shear strain amplitude (in %) of the specimen at each confining pressure and  $\gamma$  is the current shear strain amplitude (in %). If the shear strain amplitude is below  $\gamma_c$ , dynamic settlement is unlikely. By using the model (Eq. 8.9 [Eq. 2.8 bis]), one can predict the settlement caused by cyclic shear strain.

For the same kind of dynamic load (shear strain amplitude and number of cycles), the dynamic settlement is a function of the soil properties and confining pressure. The finer the particle size, the smaller is the observed settlement. Table 8.3 (Table 2.5 bis) lists factors  $a$ ,  $b$ , and  $\gamma_c$  for different classifications of residual soil under confining pressures of 25 kPa, 50 kPa, and 100 kPa. When site-specific data is not available, one can match the soil at different depths to Table 8.3 (Table 2.5 bis) by the nearest soil classification and grain size distribution, and then select values for factors  $a$ ,  $b$ , and  $\gamma_c$ .

7. Obtain the total vibration induced settlement by adding the settlement from each layer.

A computer program, CVIS, was developed to perform the analysis of the construction vibration induced settlement from step 4 through step 7. The user needs to follow steps 1, 2, 3, and provides the input data including the vibration amplitude on the

Table 8.3 Factors for the Dynamic Soil Densification Modeling (Reprint of Table 2.5)

Type of Soil	SM			ML			ML		
Specimen Number	4ST#4			3ST#3			3ST#8		
Factors	a	b	rc (%)	a	b	rc (%)	a	b	rc (%)
Confining Pressure (Kpa)									
25							0.002812	1	0.00683
50	0.00344	1.3	0.0052	0.00597	1.75	0.00725	0.00113	1.5	0.00375
100	0.00333	1.7	0.0023	0.00242	2.5	0.003			

Type of Soil	ML			MH			MH		
Specimen Number	2ST#3			3ST#11B			5ST#2		
Factors	a	b	rc (%)	a	b	rc (%)	a	b	rc (%)
Confining Pressure (Kpa)									
25	0.00534	1.5	0.0071	0.00144	1.6	0.00705			
50	0.00232	1.8	0.003	0.00111	1.6	0.00449	9.9E-05	3.5	0.01692
100	0.00112	3	0.0121	0.0012	2	0.0109			

Type of Soil	SM-ML		ML	
Specimen Number	RC-1,2		RC-3,4,5	
Factors	G1	rg (%)	G1	rg (%)
Confining Pressure (Kpa)				
25	0.382	0.00136	0.416	0.00412
50	0.400	0.00134	0.400	0.00405
100	0.409	0.00192	0.384	0.00448

ground surface, equivalent number of cycles, dominant frequency, as well as soil dynamic properties. Some example problems are included in Appendix 2.1 of Report FHWA/NC/94-007 with this program for different kinds of construction vibrations and different types of residual soils.

The popularly used recommendations on allowable differential settlement of structures are provided in Table 8.4 (Table 2.6 *bis*) following the recommendations proposed by Skempton and MacDonald (1956) and Burland et al. (1977). It needs to be emphasized that the tolerable foundation settlement in this table is total settlement, i.e., settlement during and after construction. The construction vibration induced settlement is just one mechanism potentially responsible for post-construction settlement and therefore, the design criteria for determining tolerable levels for this component must be based on engineering judgment.

Table 8.4 Guidelines for Tolerable Foundation Settlement (Reprint of Table 2.6)

	Sands	Clayey Soils
<b>Isolated Foundation:</b>		
Total Settlement	40 mm	65 mm
Differential Settlement	25 mm	40 mm
Relative Rotation	1/500	1/500
Tilt	Determined in Design	Determined in Design
<b>Raft Foundation:</b>		
Total Settlement	40 - 65 mm	65 mm - 100 mm

The field verification conducted as part of the work reported herein confirmed at one residual soil site that the predicted settlement due to pile driving was quite small and on the order of that predicted by the procedure outlined above. Increased confidence in the proposed approach will be enhanced by the evaluation of observed settlements at future sites.

## REFERENCES

- Barneich, John A. (1985), "Vehicle Induced Ground Motion", Proceedings of Conference on Vibration Problems in Geotechnical Engineering, Detroit, MI.
- Borden, Roy H., Shao, Lisheng, and Gupta, Ayushman (1994), "Construction Induced Vibration", Research Report to North Carolina Department of Transportation.
- Borden, Roy H., Shao, Lisheng, and Gupta, Ayushman (1995), "Dynamic Properties of Piedmont Residual Soil", Journal of the Geotechnical Engineering Division, ASCE, in press.
- Das, Braja M. (1983), "Fundamentals of Soil Dynamics", Elsevier Science Publishing Co., Inc.
- DeAlba, P., Seed, H. B. and Chan, C. K. (1976), "Sand Liquefaction in Large-Scale Simple Shear Tests," Journal of the Geotechnical Engineering Division, ASCE, Vol. 102, No. GT9, Proc. Paper 12403, Sept., pp. 909-927.
- Dowding, C. H. (1991), "Permanent Displacement and Pile Driving Vibrations", Proceedings of 16th Annual Members Conference of the Deep Foundations Institute, V. F. Parola, Ed., Soarta, NJ.
- Dowding, C. H. (1991), "Vibration Effects of Pile Driving", Proceedings of 39th Annual Geotechnical Engineering Conference, Continuing Education and Extension, University of Minnesota, Minneapolis, MN.
- Dowding, C. H. (1992), "Frequency Based Control of Urban Blasting", Excavation and Support for the Urban Infrastructure: Design and Construction Considerations, T.

D. O'Rourke & Hobelman, Eds, Special Geotechnical Publication, ASCE, New York, NY

Finn, W. D. L. (1972), "Soil Dynamics - Liquefaction of Sands," Proceedings of the International Conference on Microzonation, Seattle, Oct. 30 - Nov. 3, Vol. 1, pp. 87-112.

Hardin, B. O. and Black, W. L. (1968), "Vibration Modulus of Normally Consolidated Clay," Journal of the Soil Mechanics and Foundations Division, ASCE, Vol. 94, No. SM2, Proc. Paper 5833, March, pp. 353-368.

Heartz, William T. and Lambe, Philip C. (1986), "Properties of Piedmont Residual Soil", Final Report for Project Supported by the National Science foundation, Grant No. CEE-8307208, Dept. of Civil Engineering, North Carolina State University at Raleigh.

Isenhower, William M. (1979), "Torsional Simple Shear/Resonant Column Properties of San Francisco Bay Mud", Geotechnical Engineering Thesis GT80-1, Geotechnical Engineering Center, Dept. of Civil Engineering, University of Texas at Austin.

Lacy, H. S. and Gould, J. P. (1985), "Settlement from Pile Driving in Sands", Proceedings of Conference on Vibration Problems in Geotechnical Engineering, Detroit, MI.

Lambe, P.C. and Whitman, R. V. (1985), "Dynamic Centrifugal Modeling of a Horizontal Dry Sand Layer", Journal of the Geotechnical Engineering Division, ASCE, Vol. 101, No. GT5, pp. 423-438.



- Martin, G. R., Finn, W. D., Liam, and Seed, H. B. (1975), "Liquefaction Under Cyclic Loading", Journal of the Geotechnical Division, ASCE, Vol. 101, No. GT5, May, pp. 423-438.
- NCDOT, (1982), "Measurement of Ground Motion Induced by Moving Vehicle at the Coring Glass Plant in Wilmington, NC", Prepared by The Geotechnical Unit of NCDOT, Division of Highways.
- Prevost, J. H. and Hoeg, K. (1976), "Reanalysis of Simple Shear Soil Testing," Canadian Geotechnical Journal, Vol. 13, No. 4, Nov., pp. 418-429.
- Pyke, R., Seed, H. B., and Clarence, K. Chan (1975), "Settlement of Sand Under Multidirectional Shaking", Journal of the Geotechnical Engineering Division, ASCE, Vol. 101, No. GT4, pp. 379-398.
- Richart, F. E., Hall, J. R., Jr. and Woods, R. D. (1970), "Vibrations of Soils and Foundations", Prentice-Hall, Inc., Englewood Cliffs, NJ.
- Seed, H. B. (1976), "Evaluation of Soil Liquefaction Effects on Level Ground During Earthquakes," State-of-the-Art Paper, Liquefaction Problems in Geotechnical Engineering, Meeting Preprint 2752, ASCE Annual Convention, Sept. 27 - Oct. 1, Philadelphia, Pa., pp. 1-104.
- Seed, H. B. (1979), "Soil Liquefaction and Cyclic Mobility Evaluation for Level Ground During Earthquakes", Journal of the Geotechnical Engineering Division, ASCE(GT2), pp. 201-255.
- Seed, H. B. and Idriss, I. M. (1970), "Soil Moduli and Damping Factors for Dynamic Response Analyses," Report No. EERC 70-10, University of California, Berkeley.

- Seed, H. B., Idriss, I. M., Makdisi, F. and Banerjee, N. (1975), "Representation of Irregular Stress - Time Histories by Equivalent Uniform Stress Series in Liquefaction Analysis", Report No. EERC 75-29, Earthquake Engineering Research Center, University of California, Berkeley, CA.
- Seed, H. B. and Lee, K. L. (1966), "Liquefaction of Sands During Cyclic Loading", Journal of the Soil Mechanics and Foundations Division, ASCE, Vol. 92, No. SM6, Nov., pp. 105-134.
- Seed, H. B., Mori, K. and Chan, C. K. (1977), "Influence of Seismic History of Liquefaction of Sands," Journal of the Geotechnical Engineering Division, ASCE, Vol. 103, No. GT4, Proc. Paper 12841, April, pp. 257-270.
- Seed, H. B. and Peacock, W. H. (1971), "Test Procedure for Measuring Soil Liquefaction Characteristics", Journal of the Soil Mechanics and Foundations Division, ASCE, Vol. 97, No. SM8, Aug., pp. 1099-1119.
- Seed, H. B., and Silver, M. (1972), "Settlement of Dry Sands During Earthquakes", Journal of Soil Mechanics and Foundation Division, ASCE, Vol. 98 No. SM4, pp. 381-397.
- Silver, M. and Seed, H. B. (1971), "Deformation Characteristics of Sand Under Cyclic Loading", Journal of Soil Mechanics and Foundation Division, ASCE Vol. 97 No. SM8, pp. 1081-1098.
- Silver, M. and Seed, H. B. (1971), "Volume Change in Sands During Cyclic Loading", Journal of Soil Mechanics and Foundation Division, ASCE Vol. 97 No. SM9, pp. 1171-1182.

- Skempton, A. W. and Mac Donald, D. H. (1956), "Allowable Settlement of Buildings,"  
Proc. Institution of Civil Engineers, Part III, pp. 727-768.
- Stokoe, K. H. II, Isenhower, W. M. and Hsu, J. R. (1980), "Dynamic Properties of  
Offshore Silty Samples," OTC 3771, Offshore Technology Conference, 1980.
- Stokoe, K. H. II and Lodde, P. F. (1978), "Dynamic Response of San Francisco Bay  
Mud," Proceedings of the Earthquake Engineering and Soil Dynamics Conference,  
ASCE, Vol. II, pp. 940-959.
- Taniguchi, Ehchi and Sawada, Kenkichi (1979), "Attenuation with Distance of Traffic-  
Induced Vibrations", Soils and Foundations, Vol. 19, No. 2, Japanese Society of  
Soil Mechanics and Foundation Engineering.
- Wahls, H. E. (1981), "Memorandum to NCDOT for Ground Motion Attenuation at  
Corning Plant Site, Wilmington, NC".
- Wahls, H. E. (1994), "Tolerable Deformations", Will be published in the Conference on  
Settlement, ASCE.
- Wiss, John F. (1981), "Construction Vibrations: State-of -the-Art", Journal of the  
Geotechnical Engineering Division, Feb. 1981.
- Woods, R. D. (1968), "Screening of Surface Waves in Soils," Journal of the Soil  
Mechanics and Foundations Divisions, ASCE, July, pp. 951-979.
- Woods, R. D. (1978), "Measurement of Dynamic Soil Properties," Proceedings of the  
Earthquake Engineering and Soil Dynamics Conference, ASCE, Pasadena, CA,  
June 19-21, Vol. I, pp. 91-178.

Woods, Richard D. and Jedele, Larry P. (1985), "Energy - Attenuation Relationships from Construction Vibrations", Proceedings of Conference on Vibration Problems in Geotechnical Engineering, Detroit, MI.

Youd, T. L. (1972)," Compaction of Sands by Repeated Shear Straining", Journal of Soil Mechanics and Foundation Division, ASCE Vol. 98 No. SM7, pp. 709-725.

**Appendix A 1**

**LABORATORY EXPERIMENT RESULTS**

**A1.1 Data Summary of Resonant Column Tests Results**

**SAMPLE # 6ST#2**

**Initial Data**

Diam. (in) 5.822    Weight (lb) 2.671    w/c 0.224    Sp Grav 2.714    Vol. (ft<sup>3</sup>) 0.021842    Unit Wt (pcf) 122.2882    Dry Wt. (lb) 2.18219    Dry Den. (pcf) 99.90868    Voids (ft<sup>3</sup>) 0.012865    Void Ratio 0.655084    Saturation 0.874823    Initial LVDT 10.434    I<sub>o</sub> Dr. Plane 0.002141

Date	Confining Pressure (kPa)	Accel a (mV)	Resonant Freq (Hz)	Period p (mSec)	LVDT Reading	Specimen Length (in)	Diam (in)	Vol (ft <sup>3</sup> )	Weight (lb)	Void Ratio	I (ft-lbs <sup>2</sup> )	I/I <sub>o</sub>	BETA	Shear Vel Velocity (ft/sec)	Shear Modulus (ksi)	Shear Modulus (MPa)	Shear Str. Amp. (%)
4/13/95	12.5	54	90	11.11111	10250	5.81495	2.889521	0.021783	2.671	0.688833	0.000583	0.277248	0.50341	544.33	1130426	54.12479	0.000364
4/17/95	25	56	106.6	9.380963	10052	5.8034	2.883821	0.021633	2.671	0.678889	0.000581	0.278147	0.5025	644.62	1594801	76.35907	0.000269
4/18/95	50	58	117.37	8.520065	9836	5.7971	2.860713	0.021563	2.671	0.673428	0.00059	0.275548	0.502	709.68	1939290	92.85319	0.00023





**SAMPLE # 6ST#4**

Initial Data

Diam (in)	Length (in)	Weight (lb)	w/c	Sp Grav.	Vol (ft <sup>3</sup> )	Unit Wt (pcf)	Dry Wt. (lb)	Dry Den. (pcf)	Voids (ft <sup>3</sup> )	Void Ratio	Saturation	Initial LVDT	Dr.F. rate
2.8683	5.761	2.734	0.2484	2.776	0.021965	124.2662	2.190003	99.56677	0.012843	0.739761	0.932137	8790	0.002141

Date	Confining Pressure (kPa)	Accel a (mV)	Resonant Freq (Hz)	Period p (mSec)	LVDT Reading	Specimen Length (in)	Diam (in)	Vol (ft <sup>3</sup> )	Weight (lb)	Void Ratio	BETA	Shear Wa Velocity (ft/sec)	Shear Modulus (MPa)	Shear Modulus (psi)	Shear Str. Amp. (%)
3/30/95	25	65	70	14.28571	8694	5.7562	2.895885	0.02194	2.734	0.735416	0.51304	411.23	655035.6	31.36311	0.000739
3/31/95	50	61	82	12.18512	8483	5.74585	2.890578	0.02182	2.734	0.725892	0.51219	481.64	903511.3	43.26012	0.000505

**A1.2 Data Summary of Torsional Shear Tests Results**

SAMPLE: 6ST#2

INITIAL LENGTH 5.822 INCH  
INITIAL DIAMETER 2.873 INCH

e0= 0.70  
V0= 37.74 INCH<sup>3</sup> Vs= 22.27 INCH<sup>3</sup>

12.5Kpa SHEAR STRAIN AMPLITUDE (%)																
0.0069																
CYCLES	LVDT	#1	#2	#3	SETTLEMENT	VERT. STRAIN	HORI STRAIN	Evol	0.0131							
									LVDT	#1	#2	#3	SETTLEMENT	VERT. STRAIN	HORI STRAIN	Evol
1	-6.842	0.459	0.443	0.417	0.00713	-0.00122	-0.00239	-0.00600	-6.839	0.464	0.440	0.416	0.00741	-0.00127	-0.00238	-0.00603
50	-6.840	0.463	0.441	0.417	0.00728	-0.00125	-0.00242	-0.00610	-6.837	0.464	0.439	0.416	0.00758	-0.00130	-0.00239	-0.00608
100	-6.840	0.463	0.441	0.417	0.00734	-0.00126	-0.00241	-0.00608	-6.835	0.464	0.439	0.416	0.00768	-0.00132	-0.00239	-0.00609
200	-6.839	0.463	0.440	0.418	0.00739	-0.00127	-0.00241	-0.00609	-6.834	0.464	0.439	0.417	0.00776	-0.00133	-0.00239	-0.00611
400	-6.839	0.462	0.440	0.417	0.00740	-0.00127	-0.00237	-0.00601	-6.832	0.464	0.439	0.417	0.00790	-0.00136	-0.00239	-0.00614
600	-6.839	0.464	0.439	0.417	0.00741	-0.00127	-0.00240	-0.00607	-6.831	0.464	0.439	0.416	0.00799	-0.00137	-0.00239	-0.00614
800	-6.838	0.463	0.439	0.417	0.00744	-0.00128	-0.00238	-0.00603	-6.831	0.464	0.439	0.417	0.00799	-0.00137	-0.00239	-0.00615
1000	-6.838	0.463	0.439	0.417	0.00747	-0.00128	-0.00237	-0.00603	-6.831	0.464	0.439	0.417	0.00801	-0.00138	-0.00239	-0.00616

12.5Kpa SHEAR STRAIN AMPLITUDE (%)																
0.0289																
CYCLES	LVDT	#1	#2	#3	SETTLEMENT	VERT. STRAIN	HORI STRAIN	Evol	0.0524							
									LVDT	#1	#2	#3	SETTLEMENT	VERT. STRAIN	HORI STRAIN	Evol
1	-6.830	0.464	0.439	0.417	0.00807	-0.00139	-0.00239	-0.00617	-6.808	0.474	0.435	0.416	0.00973	-0.00167	-0.00248	-0.00662
50	-6.821	0.469	0.437	0.416	0.00875	-0.00150	-0.00242	-0.00635	-6.800	0.479	0.430	0.416	0.01037	-0.00178	-0.00248	-0.00674
100	-6.818	0.469	0.435	0.416	0.00899	-0.00154	-0.00239	-0.00633	-6.793	0.483	0.425	0.415	0.01089	-0.00187	-0.00243	-0.00673
200	-6.814	0.473	0.435	0.416	0.00927	-0.00159	-0.00247	-0.00653	-6.786	0.487	0.420	0.415	0.01144	-0.00196	-0.00240	-0.00676
400	-6.811	0.474	0.435	0.416	0.00952	-0.00163	-0.00248	-0.00660	-6.779	0.489	0.420	0.416	0.01193	-0.00205	-0.00244	-0.00692
600	-6.809	0.474	0.435	0.417	0.00966	-0.00166	-0.00249	-0.00664	-6.777	0.490	0.420	0.415	0.01213	-0.00208	-0.00245	-0.00698
800	-6.808	0.474	0.435	0.416	0.00972	-0.00167	-0.00248	-0.00663	-6.775	0.492	0.420	0.415	0.01228	-0.00211	-0.00246	-0.00703
1000	-6.807	0.474	0.435	0.416	0.00981	-0.00169	-0.00249	-0.00667	-6.774	0.492	0.419	0.415	0.01236	-0.00212	-0.00247	-0.00707

12.5Kpa																
0.0922																
CYCLES	LVDT	#1	#2	#3	SETTLEMENT	VERT. STRAIN	HORI STRAIN	Evol								
									LVDT	#1	#2	#3	SETTLEMENT	VERT. STRAIN	HORI STRAIN	Evol
1	-6.773	0.493	0.420	0.415	0.01242	-0.00213	-0.00250	-0.00713								
50	-6.770	0.494	0.417	0.414	0.01261	-0.00217	-0.00242	-0.00701								
100	-6.763	0.499	0.412	0.413	0.01315	-0.00226	-0.00239	-0.00705								
200	-6.749	0.505	0.405	0.413	0.01427	-0.00245	-0.00238	-0.00721								
400	-6.736	0.510	0.403	0.413	0.01520	-0.00261	-0.00243	-0.00748								
600	-6.731	0.512	0.401	0.413	0.01564	-0.00269	-0.00243	-0.00755								
800	-6.728	0.513	0.401	0.412	0.01588	-0.00273	-0.00243	-0.00758								
1000	-6.725	0.515	0.401	0.413	0.01607	-0.00276	-0.00248	-0.00769								

A-7

SAMPLE: 6ST#2

25Kpa		SHEAR STRAIN AMPLITUDE (%)															
		0.0061								0.0123							
CYCLES	LVDT	#1	#2	#3	SETTLEMENT	VERT. STRAIN	HORI STRAIN	Evol	LVDT	#1	#2	#3	SETTLEMEN	VERT. STRAIN	HORI STRAIN	Evol	
1	-6.690	0.537	0.409	0.430	0.01871	-0.00321	-0.00346	-0.01013	-6.688	0.538	0.410	0.430	0.01890	-0.00325	-0.00346	-0.01017	
50	-6.689	0.537	0.410	0.430	0.01884	-0.00324	-0.00347	-0.01017	-6.685	0.538	0.410	0.430	0.01908	-0.00328	-0.00348	-0.01023	
100	-6.688	0.537	0.410	0.430	0.01888	-0.00324	-0.00345	-0.01015	-6.686	0.538	0.410	0.430	0.01906	-0.00327	-0.00347	-0.01021	
200	-6.688	0.537	0.410	0.430	0.01887	-0.00324	-0.00346	-0.01017	-6.685	0.538	0.410	0.430	0.01909	-0.00328	-0.00347	-0.01021	
400	-6.688	0.537	0.409	0.430	0.01889	-0.00324	-0.00346	-0.01017	-6.686	0.539	0.409	0.430	0.01905	-0.00327	-0.00349	-0.01024	
600	-6.688	0.538	0.410	0.430	0.01889	-0.00325	-0.00347	-0.01018	-6.685	0.538	0.410	0.430	0.01910	-0.00328	-0.00347	-0.01023	
800	-6.688	0.537	0.409	0.430	0.01889	-0.00324	-0.00346	-0.01016	-6.685	0.539	0.409	0.430	0.01914	-0.00329	-0.00348	-0.01025	
1000	-6.688	0.537	0.410	0.430	0.01886	-0.00324	-0.00347	-0.01017	-6.685	0.539	0.410	0.430	0.01911	-0.00328	-0.00349	-0.01027	

25Kpa		SHEAR STRAIN AMPLITUDE (%)															
		0.0260								0.0409							
CYCLES	LVDT	#1	#2	#3	SETTLEMENT	VERT. STRAIN	HORI STRAIN	Evol	LVDT	#1	#2	#3	SETTLEMEN	VERT. STRAIN	HORI STRAIN	Evol	
1	-6.686	0.538	0.410	0.430	0.01902	-0.00327	-0.00348	-0.01023	-6.680	0.543	0.408	0.430	0.01951	-0.00335	-0.00354	-0.01043	
50	-6.683	0.541	0.410	0.429	0.01924	-0.00330	-0.00352	-0.01035	-6.678	0.544	0.407	0.430	0.01963	-0.00337	-0.00353	-0.01042	
100	-6.682	0.541	0.409	0.429	0.01932	-0.00332	-0.00350	-0.01031	-6.676	0.545	0.407	0.429	0.01977	-0.00340	-0.00353	-0.01046	
200	-6.681	0.542	0.409	0.429	0.01938	-0.00333	-0.00351	-0.01036	-6.674	0.546	0.406	0.429	0.01993	-0.00342	-0.00354	-0.01050	
400	-6.681	0.542	0.409	0.429	0.01945	-0.00334	-0.00352	-0.01038	-6.673	0.547	0.405	0.430	0.02006	-0.00345	-0.00355	-0.01055	
600	-6.679	0.542	0.408	0.430	0.01955	-0.00336	-0.00352	-0.01039	-6.671	0.548	0.405	0.430	0.02022	-0.00347	-0.00356	-0.01060	
800	-6.679	0.542	0.409	0.429	0.01958	-0.00336	-0.00352	-0.01040	-6.669	0.548	0.405	0.430	0.02033	-0.00349	-0.00357	-0.01064	
1000	-6.679	0.543	0.408	0.430	0.01957	-0.00336	-0.00353	-0.01042	-6.668	0.548	0.405	0.431	0.02038	-0.00350	-0.00359	-0.01069	

25Kpa		SHEAR STRAIN AMPLITUDE (%)									
		0.0653									
CYCLES	LVDT	#1	#2	#3	SETTLEMENT	VERT. STRAIN	HORI STRAIN	Evol			
1	-6.669	0.548	0.405	0.431	0.02034	-0.00349	-0.00358	-0.01065			
50	-6.666	0.550	0.404	0.430	0.02060	-0.00354	-0.00361	-0.01075			
100	-6.662	0.552	0.400	0.430	0.02083	-0.00358	-0.00356	-0.01069			
200	-6.658	0.556	0.399	0.431	0.02119	-0.00364	-0.00361	-0.01086			
400	-6.653	0.560	0.396	0.430	0.02155	-0.00370	-0.00362	-0.01094			
600	-6.650	0.561	0.394	0.431	0.02176	-0.00374	-0.00361	-0.01096			
800	-6.648	0.562	0.392	0.431	0.02193	-0.00377	-0.00358	-0.01093			
1000	-6.647	0.564	0.391	0.431	0.02201	-0.00378	-0.00361	-0.01100			

8-V

SAMPLE: 6ST#2

50Kpa	SHEAR STRAIN AMPLITUDE (%)															
	0.0043								0.0097							
	CYCLES	LVDT	#1	#2	#3	SETTLEMENT	VERT. STRAIN	HORI STRAIN	Evol	LVDT	#1	#2	#3	SETTLEMEN	VERT. STRAIN	HORI STRAIN
1	-6.607	0.595	0.410	0.459	0.02504	-0.00430	-0.00522	-0.01474	-6.606	0.594	0.410	0.459	0.02516	-0.00432	-0.00522	-0.01477
50	-6.605	0.595	0.410	0.459	0.02523	-0.00433	-0.00523	-0.01480	-6.603	0.595	0.411	0.459	0.02537	-0.00436	-0.00523	-0.01481
100	-6.605	0.594	0.411	0.459	0.02522	-0.00433	-0.00521	-0.01475	-6.602	0.595	0.410	0.459	0.02541	-0.00436	-0.00524	-0.01485
200	-6.605	0.596	0.411	0.459	0.02523	-0.00433	-0.00525	-0.01482	-6.603	0.596	0.410	0.459	0.02537	-0.00436	-0.00524	-0.01484
400	-6.604	0.595	0.410	0.459	0.02526	-0.00434	-0.00523	-0.01480	-6.602	0.596	0.410	0.459	0.02545	-0.00437	-0.00523	-0.01483
600	-6.605	0.595	0.410	0.459	0.02523	-0.00433	-0.00524	-0.01481	-6.602	0.596	0.410	0.459	0.02544	-0.00437	-0.00524	-0.01486
800	-6.604	0.595	0.410	0.459	0.02526	-0.00434	-0.00523	-0.01479	-6.602	0.596	0.410	0.459	0.02546	-0.00437	-0.00524	-0.01486
1000	-6.604	0.595	0.411	0.459	0.02527	-0.00434	-0.00524	-0.01482	-6.602	0.596	0.410	0.459	0.02544	-0.00437	-0.00524	-0.01485

50Kpa	SHEAR STRAIN AMPLITUDE (%)															
	0.0293								0.0440							
	CYCLES	LVDT	#1	#2	#3	SETTLEMENT	VERT. STRAIN	HORI STRAIN	Evol	LVDT	#1	#2	#3	SETTLEMEN	VERT. STRAIN	HORI STRAIN
1	-6.603	0.596	0.410	0.459	0.02536	-0.00436	-0.00525	-0.01486	-6.585	0.604	0.407	0.459	0.02673	-0.00459	-0.00533	-0.01525
50	-6.595	0.599	0.410	0.458	0.02593	-0.00445	-0.00527	-0.01500	-6.581	0.604	0.406	0.460	0.02702	-0.00464	-0.00532	-0.01523
100	-6.593	0.600	0.410	0.458	0.02612	-0.00449	-0.00531	-0.01510	-6.580	0.605	0.406	0.460	0.02712	-0.00466	-0.00535	-0.01535
200	-6.591	0.601	0.410	0.459	0.02631	-0.00452	-0.00532	-0.01517	-6.577	0.605	0.405	0.460	0.02732	-0.00469	-0.00535	-0.01538
400	-6.588	0.601	0.410	0.459	0.02652	-0.00455	-0.00533	-0.01521	-6.573	0.607	0.404	0.461	0.02765	-0.00475	-0.00539	-0.01554
600	-6.586	0.601	0.408	0.459	0.02665	-0.00458	-0.00531	-0.01520	-6.571	0.610	0.404	0.461	0.02781	-0.00478	-0.00542	-0.01562
800	-6.585	0.602	0.408	0.459	0.02673	-0.00459	-0.00532	-0.01522	-6.569	0.609	0.401	0.461	0.02794	-0.00480	-0.00536	-0.01552
1000	-6.584	0.603	0.407	0.460	0.02677	-0.00460	-0.00533	-0.01526	-6.567	0.610	0.401	0.462	0.02808	-0.00482	-0.00538	-0.01559

A-9

SAMPLE: 6ST#2A

INITIAL LENGTH- 5.795 INCH  
INITIAL DIAMETE 2.887 INCH

e0= 0.75  
V0= 37.93 INCH<sup>3</sup> Vs= 21.64 INCH<sup>3</sup>

CYCLES	12.5Kpa SHEAR STRAIN AMPLITUDE (%)															
	0.0058								0.0102							
	LVDT	#1	#2	#3	SETTLEMENT	VERT. STRAIN	HORI STRAIN	Evol	LVDT	#1	#2	#3	SETTLEMENT	VERT. STRAIN	HORI STRAIN	Evol
1	-6.553	0.415	0.410	0.464	0.00503	-0.00087	-0.00194	-0.00476	-6.550	0.415	0.407	0.464	0.00529	-0.00091	-0.00188	-0.00468
50	-6.551	0.415	0.407	0.464	0.00521	-0.00090	-0.00189	-0.00468	-6.548	0.415	0.407	0.464	0.00542	-0.00093	-0.00188	-0.00470
100	-6.550	0.415	0.408	0.464	0.00523	-0.00090	-0.00192	-0.00474	-6.548	0.415	0.406	0.464	0.00542	-0.00094	-0.00188	-0.00469
200	-6.550	0.415	0.407	0.464	0.00524	-0.00090	-0.00189	-0.00469	-6.547	0.415	0.406	0.465	0.00546	-0.00094	-0.00189	-0.00471
400	-6.550	0.415	0.407	0.464	0.00527	-0.00091	-0.00189	-0.00469	-6.546	0.415	0.406	0.465	0.00555	-0.00096	-0.00188	-0.00472
600	-6.549	0.415	0.407	0.464	0.00531	-0.00092	-0.00189	-0.00470	-6.546	0.415	0.406	0.465	0.00556	-0.00096	-0.00188	-0.00471
800	-6.549	0.415	0.408	0.464	0.00534	-0.00092	-0.00190	-0.00472	-6.546	0.415	0.406	0.465	0.00560	-0.00097	-0.00188	-0.00472
1000	-6.550	0.415	0.407	0.464	0.00528	-0.00091	-0.00188	-0.00467	-6.545	0.415	0.406	0.465	0.00562	-0.00097	-0.00189	-0.00474

A-10

CYCLES	12.5Kpa															
	0.0335								0.0513							
	LVDT	#1	#2	#3	SETTLEMENT	VERT. STRAIN	HORI STRAIN	Evol	LVDT	#1	#2	#3	SETTLEMENT	VERT. STRAIN	HORI STRAIN	Evol
1	-6.546	0.415	0.406	0.465	0.00553	-0.00095	-0.00188	-0.00471	-6.525	0.415	0.405	0.469	0.00716	-0.00124	-0.00196	-0.00516
50	-6.531	0.415	0.405	0.467	0.00671	-0.00116	-0.00192	-0.00499	-6.509	0.417	0.402	0.470	0.00835	-0.00144	-0.00196	-0.00536
100	-6.528	0.416	0.404	0.467	0.00696	-0.00120	-0.00191	-0.00503	-6.511	0.419	0.400	0.470	0.00823	-0.00142	-0.00196	-0.00533
200	-6.515	0.415	0.404	0.468	0.00792	-0.00137	-0.00192	-0.00521	-6.513	0.420	0.399	0.470	0.00808	-0.00139	-0.00196	-0.00532
400	-6.527	0.416	0.404	0.468	0.00701	-0.00121	-0.00194	-0.00509	-6.508	0.421	0.399	0.471	0.00844	-0.00146	-0.00198	-0.00541
600	-6.526	0.415	0.405	0.469	0.00708	-0.00122	-0.00195	-0.00512	-6.511	0.421	0.398	0.471	0.00825	-0.00142	-0.00198	-0.00538
800	-6.523	0.415	0.404	0.469	0.00730	-0.00126	-0.00194	-0.00514	-6.509	0.421	0.398	0.471	0.00835	-0.00144	-0.00199	-0.00541
1000	-6.510	0.415	0.404	0.469	0.00829	-0.00143	-0.00195	-0.00533	-6.509	0.421	0.398	0.471	0.00839	-0.00145	-0.00198	-0.00542

CYCLES	12.5Kpa											
	0.0840											
	LVDT	#1	#2	#3	SETTLEMENT	VERT. STRAIN	HORI STRAIN	Evol				
1	-6.510	0.420	0.400	0.474	0.00830	-0.00143	-0.00206	-0.00555				
50	-6.502	0.423	0.397	0.471	0.00894	-0.00154	-0.00200	-0.00555				
100	-6.502	0.424	0.396	0.471	0.00888	-0.00153	-0.00201	-0.00554				
200	-6.493	0.425	0.396	0.471	0.00963	-0.00166	-0.00200	-0.00566				
400	-6.485	0.426	0.395	0.472	0.01018	-0.00176	-0.00204	-0.00584				
600	-6.469	0.426	0.397	0.473	0.01143	-0.00197	-0.00207	-0.00612				
800	-6.473	0.426	0.396	0.473	0.01109	-0.00191	-0.00207	-0.00606				
1000	-6.468	0.426	0.397	0.474	0.01146	-0.00198	-0.00210	-0.00619				

SAMPLE: 6ST#2A

25Kpa																
SHEAR STRAIN AMPLITUDE (%)																
0.0037																
0.0078																
CYCLES	LVDT	#1	#2	#3	SETTLEMENT	VERT. STRAIN	HORI STRAIN	Evol	LVDT	#1	#2	#3	SETTLEMENT	VERT. STRAIN	HORI STRAIN	Evol
1	-6.441	0.415	0.429	0.497	0.01353	-0.00234	-0.00309	-0.00852	-6.441	0.415	0.430	0.498	0.01356	-0.00234	-0.00313	-0.00859
50	-6.440	0.415	0.429	0.497	0.01362	-0.00235	-0.00310	-0.00855	-6.439	0.415	0.430	0.498	0.01367	-0.00236	-0.00313	-0.00862
100	-6.440	0.415	0.430	0.497	0.01363	-0.00235	-0.00311	-0.00857	-6.439	0.415	0.430	0.497	0.01372	-0.00237	-0.00311	-0.00859
200	-6.440	0.415	0.430	0.498	0.01363	-0.00235	-0.00312	-0.00859	-6.439	0.415	0.430	0.498	0.01372	-0.00237	-0.00313	-0.00862
400	-6.440	0.415	0.429	0.497	0.01364	-0.00235	-0.00309	-0.00854	-6.439	0.415	0.430	0.498	0.01373	-0.00237	-0.00313	-0.00863
600	-6.440	0.415	0.429	0.497	0.01365	-0.00236	-0.00309	-0.00854	-6.438	0.415	0.430	0.497	0.01375	-0.00237	-0.00313	-0.00862
800	-6.440	0.415	0.430	0.497	0.01367	-0.00236	-0.00311	-0.00859	-6.438	0.415	0.430	0.497	0.01379	-0.00238	-0.00312	-0.00862
1000	-6.440	0.415	0.429	0.497	0.01364	-0.00235	-0.00311	-0.00857	-6.439	0.415	0.430	0.498	0.01373	-0.00237	-0.00313	-0.00863

25Kpa																
SHEAR STRAIN AMPLITUDE (%)																
0.0247																
0.0445																
CYCLES	LVDT	#1	#2	#3	SETTLEMENT	VERT. STRAIN	HORI STRAIN	Evol	LVDT	#1	#2	#3	SETTLEMENT	VERT. STRAIN	HORI STRAIN	Evol
1	-6.440	0.415	0.430	0.498	0.01365	-0.00236	-0.00312	-0.00859	-6.435	0.415	0.430	0.499	0.01400	-0.00242	-0.00317	-0.00875
50	-6.436	0.415	0.430	0.498	0.01395	-0.00241	-0.00314	-0.00869	-6.435	0.416	0.428	0.500	0.01401	-0.00242	-0.00318	-0.00877
100	-6.436	0.415	0.430	0.498	0.01397	-0.00241	-0.00313	-0.00868	-6.434	0.416	0.429	0.500	0.01408	-0.00243	-0.00319	-0.00881
200	-6.434	0.415	0.430	0.498	0.01406	-0.00243	-0.00314	-0.00870	-6.433	0.415	0.429	0.501	0.01414	-0.00244	-0.00319	-0.00882
400	-6.434	0.415	0.430	0.499	0.01407	-0.00243	-0.00316	-0.00875	-6.432	0.415	0.430	0.501	0.01425	-0.00246	-0.00320	-0.00887
600	-6.434	0.415	0.430	0.500	0.01408	-0.00243	-0.00317	-0.00878	-6.432	0.415	0.430	0.502	0.01424	-0.00246	-0.00323	-0.00892
800	-6.429	0.416	0.428	0.500	0.01450	-0.00250	-0.00317	-0.00884	-6.431	0.415	0.430	0.502	0.01434	-0.00247	-0.00323	-0.00894
1000	-6.434	0.415	0.430	0.500	0.01407	-0.00243	-0.00317	-0.00878	-6.430	0.415	0.430	0.503	0.01440	-0.00249	-0.00325	-0.00898

25Kpa									
SHEAR STRAIN AMPLITUDE (%)									
0.0862									
CYCLES	LVDT	#1	#2	#3	SETTLEMENT	VERT. STRAIN	HORI STRAIN	Evol	
1	-6.430	0.415	0.430	0.503	0.01436	-0.00248	-0.00326	-0.00899	
50	-6.428	0.418	0.426	0.505	0.01454	-0.00251	-0.00325	-0.00902	
100	-6.423	0.421	0.423	0.505	0.01492	-0.00258	-0.00325	-0.00908	
200	-6.422	0.423	0.419	0.507	0.01500	-0.00259	-0.00327	-0.00912	
400	-6.416	0.423	0.418	0.509	0.01546	-0.00267	-0.00330	-0.00926	
600	-6.412	0.423	0.418	0.510	0.01576	-0.00272	-0.00333	-0.00937	
800	-6.410	0.423	0.418	0.511	0.01591	-0.00275	-0.00335	-0.00944	
1000	-6.407	0.423	0.417	0.511	0.01617	-0.00279	-0.00332	-0.00943	

A-11

SAMPLE: 6ST#4

INITIAL LENGTH= 5.761 INCH  
INITIAL DIAMETER= 2.898 INCH

e0= 0.74  
V0= 38.01 inch^3 Vs= 21.84 inch^3

CYCLES	25Kpa SHEAR STRAIN AMPLITUDE (%)															
	0.0050								0.0310							
	LVDT	#1	#2	#3	SETTLEMENT	VERT. STRAIN	HORI STRAIN	Evol	LVDT	#1	#2	#3	SETTLEMENT	VERT. STRAIN	HORI STRAIN	Evol
1	-5.782	0.420	0.473	0.444	0.00486	-0.00084	-0.00398	-0.00881	-5.779	0.420	0.474	0.444	0.00512	-0.00089	-0.00400	-0.00889
10	-5.780	0.420	0.473	0.444	0.00500	-0.00087	-0.00398	-0.00883	-5.771	0.415	0.479	0.447	0.00573	-0.00099	-0.00406	-0.00912
50	-5.780	0.419	0.474	0.443	0.00505	-0.00088	-0.00397	-0.00881	-5.763	0.411	0.483	0.448	0.00629	-0.00109	-0.00412	-0.00933
100	-5.779	0.419	0.474	0.443	0.00511	-0.00089	-0.00395	-0.00878	-5.762	0.410	0.483	0.448	0.00643	-0.00112	-0.00409	-0.00931
200	-5.779	0.419	0.474	0.443	0.00511	-0.00089	-0.00397	-0.00882	-5.760	0.410	0.484	0.449	0.00655	-0.00114	-0.00413	-0.00939
400	-5.779	0.418	0.474	0.444	0.00513	-0.00089	-0.00396	-0.00882	-5.759	0.409	0.486	0.449	0.00665	-0.00115	-0.00416	-0.00948
800	-5.778	0.418	0.474	0.443	0.00519	-0.00090	-0.00396	-0.00882	-5.758	0.408	0.487	0.449	0.00671	-0.00116	-0.00419	-0.00954
1000	-5.778	0.417	0.474	0.444	0.00517	-0.00090	-0.00395	-0.00879	-5.757	0.408	0.488	0.450	0.00675	-0.00117	-0.00419	-0.00955

A-12

CYCLES	25Kpa															
	0.0580								0.1990							
	LVDT	#1	#2	#3	SETTLEMENT	VERT. STRAIN	HORI STRAIN	Evol	LVDT	#1	#2	#3	SETTLEMENT	VERT. STRAIN	HORI STRAIN	Evol
1	-5.759	0.409	0.488	0.449	0.00665	-0.00115	-0.00421	-0.00957	-5.723	0.391	0.508	0.464	0.00937	-0.00163	-0.00462	-0.01086
10	-5.755	0.407	0.488	0.450	0.00691	-0.00120	-0.00420	-0.00960	-5.713	0.388	0.509	0.467	0.01014	-0.00176	-0.00464	-0.01105
50	-5.745	0.403	0.493	0.452	0.00766	-0.00133	-0.00428	-0.00990	-5.699	0.383	0.508	0.475	0.01119	-0.00194	-0.00471	-0.01136
100	-5.742	0.401	0.495	0.453	0.00791	-0.00137	-0.00430	-0.00997	-5.692	0.379	0.508	0.479	0.01170	-0.00203	-0.00474	-0.01151
200	-5.739	0.400	0.497	0.455	0.00813	-0.00141	-0.00435	-0.01012	-5.684	0.377	0.506	0.484	0.01232	-0.00214	-0.00476	-0.01167
400	-5.737	0.399	0.498	0.456	0.00830	-0.00144	-0.00439	-0.01022	-5.675	0.375	0.502	0.489	0.01304	-0.00226	-0.00476	-0.01179
800	-5.735	0.398	0.498	0.457	0.00846	-0.00147	-0.00439	-0.01026	-5.667	0.372	0.500	0.495	0.01366	-0.00237	-0.00481	-0.01198
1000	-5.734	0.399	0.498	0.457	0.00850	-0.00148	-0.00440	-0.01028	-5.660	0.372	0.498	0.496	0.01417	-0.00246	-0.00480	-0.01207



---

**APPENDIX A2**

**ORIGINAL PROJECT AUTHORIZATION WORK PLAN**

NORTH CAROLINA STATE UNIVERSITY  
OFFICE OF SPONSORED PROGRAMS  
NOTICE OF SPONSORED PROJECT AWARD

DATE: 07/20/1994  
TO: Borden, R. H.  
FROM: Interim Vice Chancellor for Research, Outreach and Extension

North Carolina State University has entered into an agreement as herein described. Initiation of the expenditure of funds is authorized in accordance with the terms and conditions set forth in the attached sponsor's award document and/or policy statement. Please provide the Office of Contracts and Grants a detailed budget and request for trust fund initiation for the amount shown below under "Amount of this Action". Expenditures in excess of the total funded project amount will be the responsibility of the Department and College.

Proposal No.: 43-0007  
College/Unit: COLLEGE OF ENGINEERING  
Department: Civil Engineering  
Project Title: Construction Related Vibrations: Field Vibration Induced Settlement Model  
Sponsor: Institute for Transportation Research and Education  
Agency Reference No.: 23241-95-5 FAS No.: 531222  
Amount of this Action: \$40,191  
Current Budget Period: 07/01/1994 to 06/30/1995  
Total Funding to Date: \$40,191  
Total Project Period: 07/01/1994 to 06/30/1995  
Program Type: Research Program Status: Internal  
Tech. Report Freq.: First Report Due:  
Specific Conditions:

\_\_\_ Requires NCSU to issue Subcontract

Copies to: Director, Contracts & Grants  
Information Services  
College Administrative Office

NCSU Engineering Research Programs	
Copies To:	
_____	<i>Borden</i>
_____	<i>Khosla</i>
_____	<i>Judy</i>
_____	<i>Britt</i>
Initials of Sender: <i>SC</i>	
Date: <i>7-29-94</i>	

0109 75-0001

PROJECT AUTHORIZATION NO.: 23241-95-5

under

**MASTER AGREEMENT FOR RESEARCH AND TRAINING SERVICES  
BETWEEN THE DIVISION OF HIGHWAYS, NORTH CAROLINA  
DEPARTMENT OF TRANSPORTATION: THE UNC INSTITUTE FOR  
TRANSPORTATION RESEARCH AND EDUCATION (ITRE); AND THE  
CENTER FOR TRANSPORTATION ENGINEERING STUDIES AT  
NORTH CAROLINA STATE UNIVERSITY (CTES)**

Project Title: Construction Related Vibrations: Field Verification of Vibration Induced Settlement Model

Date of Project Authorization: July 1, 1994

Project Authorization Number: 23241-95-5

Formal Statement of Work: See attachment

Period of Performance: 7/1/94 - 6/30/95

Budget Authorization: See attachment

Property to be Furnished by the Department: None

Key Personnel: Dr. Roy H. Borden

Additional Terms and Conditions: None

IN WITNESS WHEREOF, the parties hereto have executed this Project Authorization as

of July 1, 1994.

UNC INSTITUTE FOR TRANSPORTATION  
RESEARCH AND EDUCATION

CENTER FOR TRANSPORTATION  
ENGINEERING STUDIES, NCSU

By: Robert S. Foyce  
Director, ITRE

By: J. M. Fuchsler  
Director, CTES

NORTH CAROLINA DEPARTMENT  
OF TRANSPORTATION

By: Jay R. Bonds  
State Highway Administrator



Research Proposal  
on

**CONSTRUCTION RELATED VIBRATIONS:  
FIELD VERIFICATION OF  
VIBRATION INDUCED SETTLEMENT MODEL**

Submitted by

Dr. Roy H. Borden  
and  
Lisheng Shao

Department of Civil Engineering  
North Carolina State University

March 7, 1994

## I. IDENTIFICATION

a. Amount Requested:

July 1, 1994 - June 30 1995

\$40,191

b. Title of Study:

Construction Related Vibrations: Field Verification of Vibration Induced Settlement Model

c. Purpose of Proposal:

New Proposal

Change

Extension

d. Name and Address of Proposer:

North Carolina State University

e. Major Subdivision Conducting Work:

Center for Transportation Engineering Studies  
Department of Civil Engineering

f. Name, Title, and Address of Principal Investigator:

Dr. Roy H. Borden  
Associate Professor  
Department of Civil Engineering  
North Carolina State University  
Raleigh, NC 27695-7908  
Telephone: (919) 515-7630  
FAX: (919) 515-7908

## TABLE OF CONTENTS

	Page
I RESEARCH OBJECTIVE	1
II. BACKGROUND	1
III. STATUS OF CURRENT WORK	2
A. Data Base of Laboratory Resonant Column and Torsional Shear Tests	2
B. Development of Vibration Induced Settlement Model	3
1. Sources of Construction Vibrations	3
2. Attenuation	4
3. Analytical Procedure	6
IV. NEED FOR FIELD VERIFICATION	6
V. PROPOSED FIELD VERIFICATION OF VIBRATION INDUCED SETTLEMENT MODEL	7
VI. EXPECTED RESULTS	8
VII. SCHEDULE AND BUDGET	9
VIII. REFERENCES	10

## **CONSTRUCTION RELATED VIBRATIONS: FIELD VERIFICATION OF VIBRATION INDUCED SETTLEMENT MODEL**

### **I. RESEARCH OBJECTIVE**

The objective of the proposed research is to provide field verification of an analytical model for predicting ground surface settlement due to construction induced vibrations. In order to accomplish this verification, it is proposed that investigations will be performed at three sites representing a range of relevant soil conditions. Utilizing the database of resonant column/torsional shear data developed in the current project and a knowledge of the intended vibration sources, site geometry and test-footing loading conditions, pre-test predictions of settlement versus number of vibration source events (i.e. pile strikes, truck passes, etc.) will be made. Based on a comparison of predicted and measured particle velocity and settlement as a function of depth below the loaded footings, modifications to the existing model will be suggested as appropriate.

### **II. BACKGROUND**

In response to the need for a quantitative basis for evaluating the potential settlement of structures as the result of soil densification due to construction vibrations, a two-year investigation, Highway Research Project 93-7, was initiated on July 1, 1992. The objective of the on-going 2-year project on "Construction Related Vibrations" is to develop a procedure for evaluating soil response to both impulse and steady state construction induced vibrations. Resonant column and torsional shear tests on a wide range of soils including silty and clayey sands have been performed to develop an experimental data base. The settlement potential of these soils is being evaluated based on both frequency and amplitude response. Analytical modeling techniques are being developed to predict ground-surface settlement as a function of soil type and vibration source characteristics and location.

On January 24, 1994, the project technical advisory committee met to review the progress to date and discuss the anticipated outcome of this research. As a result of this discussion and further discussions with the Division of Highways geotechnical engineering

staff and soils and foundations staff, and between Mr. Pat Strong, State Highway Research Engineer and Federal Highway Administration Division Office staff, it has generally been agreed that an additional phase of research needs be undertaken to provide verification of the analytical methods developed on actual construction projects. Accordingly, this work plan for an additional one-year investigation was developed. The following section provides a brief description on the accomplishments of the current project.

### III. STATUS OF CURRENT WORK

#### A. Data Base of Laboratory Resonant Column and Torsional Shear Tests

To date, samples from sites along NC55 in Rockingham county, Centennial Parkway in Raleigh, and US64 in Wake county have been obtained and tested. Sample characterization has included water content, specific gravity, grain size distribution and plasticity characteristics. The vibration induced settlement tests have concentrated on the influence of:

- 1) number of cycles (for a given normal stress and amplitude of shear strain);
- 2) amplitude of shear strain ( for a given value of normal stress and number of cycles);
- 3) normal pressure ( for a given amplitude of shear strain and number of cycles);
- 4) soil samples with different grain size distribution and densities recovered from different sites and at different depth; and,
- 5) degree of soil saturation.

Over 25 resonant column tests and torsional shear tests have been performed on specimens obtained from Shelby tube samples at depths ranging from 1 to 5 meters. The tests performed and the basic soil properties obtained are included in Table 3, and Fig. 1.

In these tests, the threshold shear strain amplitude for dynamic settlement has been found to be on the order of 0.005% ~ 0.01% for these materials, with slightly larger values for the highest confining pressures, as shown in Fig. 2 and Fig. 3. Compared with the literature, this threshold shear strain is between the reported values for sand and clay.



Some typical results of vertical strain versus number of cycles under different cyclic torsional shear strain are plotted in Fig. 4 and 5. Fig. 6 presents the result of a long-term test performed on sample 3ST#2L carried to nearly 200,000 cycles under a 25Kpa confining pressure.

## B. Development of Vibration Induced Settlement Model

The modeling of vibration induced settlement includes three major steps. The vibration energy and number of cycles are determined by the characteristics of the sources. The peak particle velocity, and therefore, shear strain amplitude in the soil profile is influenced by the attenuation of vibration waves. And, finally, the resulting soil densification is a function of the initial state of the material, the shear strain amplitude and number of cycles.

### 1. Sources of Construction Vibrations

Construction vibrations are of three different types: (1) transient or impact vibration; (2) steady-state or continuous; and (3) pseudo-steady-state vibrations. Examples of transient construction vibrations are those that occur from blasting with explosives, impact pile driving, demolition, and wrecking balls. Steady-state vibrations may be generated by vibratory pile drivers, large pumps used in jacking underground pipes, and compressors. Pseudo-steady-state vibrations are so called because they are of a random nature or a series of impact vibrations that are at short enough intervals to approach essentially a steady-state condition. Examples of these are jackhammers, pavement breakers, trucks, and scrapers. The relative intensities of construction vibration are shown in Fig. 7. (Wiss, 1981)

Some typical vibration data characteristics of vehicular induced ground motion were given by Barneich (1985) and Taniguchi (1979). The vibration amplitude and frequency are dependent on wheel base, speed of vehicle and road roughness. Frequencies are generally in the 3 to 30 Hz range with most data in the range of 10 to 30 Hz. The time history and Fourier spectra of a truck induced vibration are shown in Fig. 8 and Fig. 9 respectively. Horizontal vibration amplitude is one-half to two-thirds of vertical amplitude in the same frequency range.

Dowding (1991) gave a comprehensive evaluation of pile driving vibrations. The dominant frequency of impact motion is dependent upon driving conditions and the pile and hammer properties, but will range between 10 and 50 Hz for typical hammers. Vibratory hammers produce ground motions at the hammer frequency, which typically is in the range between 15 to 30 Hz.

The above data are needed in the field verification phase to enable proper selection of vibration monitoring instrumentation, i.e. geophones and data acquisition system characteristics.

## 2. Attenuation

Vibrations lose energy during wave propagation through ground. The decay of amplitude of vibrations with distance can be attributed to geometrical damping and material damping. From an evaluation of wave propagation theory and field tests reported in the literature, it has been concluded that for surface impacts such as trucks, heavy equipment and dynamic compaction, Rayleigh waves dominate the vibration transfer in the ground. For a point source, like pile driving near the ground surface, the surface vibration amplitude can be expressed as:

$$A = A_1 \left( \frac{r_1}{r} \right)^{\frac{1}{2}} \exp[-\alpha(r - r_1)] \quad (1)$$

where  $A$  is the amplitude of particle velocity at a distance  $r$  from the source,  $A_1$  is the amplitude of particle velocity at referent point, at a distance  $r_1$  from the source, and  $\alpha$  denotes the coefficient of material damping. The coefficient of material damping,  $\alpha$ , can be obtained from field measurement or calculated by:

$$\alpha = \frac{2\pi f\eta}{V_R} \quad (2)$$

where  $f$  is the vibration frequency,  $V_R$  is the Rayleigh wave velocity, and  $\eta$  is the material damping ratio which can be obtained from resonant column/torsional shear test. Frequency of traffic-induced vibrations is mainly determined by ground soil conditions. Published results suggest that vibrations produced by large trucks (mass about 20 Mg or 22 tons) have almost the same frequency as those produced by small trucks (mass about

10Mg). The damping ratio,  $\eta$ , depends on the shear strain amplitude and soil type, as shown in Fig. 10B for tests performed during the current project.

Equation (1) is the wave attenuation expression for point source. However, bulldozers, pans and trucks are finite line sources for which the point source equation is not strictly valid. For this case, no exact solutions are available. Dr. Wahls, North Carolina State University, developed the following approximate analysis method in 1981 based on geometric damping and energy conservation theory:

$$A = A_1 \sqrt{\frac{\frac{L}{\pi} + r_1}{\frac{L}{\pi} + r}} \exp[-\alpha(r - r_1)] \quad (3)$$

where  $L$  is the length of the source. This method agrees very well with data obtained from field tests performed in Wilmington, NC in 1981.

Beneath the ground surface, the peak particle velocity distribution can be calculated by Rayleigh wave propagation theory as shown in Fig. 11. The resulting shear strain amplitude decreases rapidly with depth. When the depth equals one Rayleigh wave length, the particle velocity amplitude is only 10% ~20% of the ground surface amplitude. Below this depth, the magnitude of vibration induced settlement is unlikely to be significant. For example, the ground vibration frequency caused by a loaded truck is in the range of 20 Hz to 30 Hz. The Rayleigh wave length of residual soil profile is around 5m ~ 7m in this frequency range. For this reason, cyclic torsional shear tests were performed using confining pressure less than 100 Kpa. From above analysis, it is clear that the wave attenuation depends on horizontal distance, depth, type of soil, and vibration amplitude.

After peak particle velocity profile is obtained, the shear strain amplitude can therefore be calculated as:

$$\gamma = \frac{A}{V_R} \quad (4)$$

The Rayleigh wave velocity can be calculated as a function of shear wave velocity and Poisson's ratio. The shear wave velocity,  $V_s$ , can be obtained from shear modulus by  $V_s = (G/\rho)^{1/2}$  and the shear modulus,  $G$ , can be found from our laboratory test results as a

function of shear strain amplitude and confining pressure, as shown in Fig. 10A. By using an iteration procedure, and when convergence of the relationship between  $\gamma \sim V_R \sim V_s \sim G \sim \gamma$  is achieved, the shear strain amplitude is obtained. Fig. 12 shows shear strain amplitude as a function of distance from the source at three different depths due to a loaded truck (20.0 Mg) driving over an 18-mm plank at 60 km/hour. These results are based on the measured peak particle velocities as a function of depth reported in the literature at a particular site in Japan. As this is the only data of its kind known to be in the literature, the substantiation of this function should be a significant component of the field verification.

### 3. Analytical Procedure

After the peak particle velocity as a function of horizontal distance is obtained as described above, the soil profile can be divided into several sublayers and peak particle velocity can be calculated as a function of depth. The shear strain distribution can then be obtained from the peak particle velocity profile. The resultant ground surface settlement will be calculated as the cumulative settlement of each of the layers. The relationship between densification and shear strain amplitude, number of cycles, and confining pressure have been determined from the data base of resonant column and torsional shear tests.

## IV. NEED FOR FIELD VERIFICATION

In the study of soil settlement during vibration, it becomes necessary to determine the equivalent number of significant uniform stress or strain cycles for construction vibrations that have an irregular time history. The effect of the stress or strain history on a given soil deposit should be same as the equivalent number of uniform cycles. The basic procedure included in developing the equivalent stress cycle method has been described by Seed et al (1975,1976,1979) from the point of view of soil liquefaction during earthquake. Fig. 13 is generated using the results of the soil liquefaction study by simple shear tests.

Equivalent numbers of uniform stress cycles for several earthquakes with magnitudes of 5.3 - 7.7 are shown in Fig. 14. Similar relations need to be developed to evaluate construction induced vibrations at different energy levels as explained above .

As shown in Fig. 15, vibratory ground motion during pile driving can be as high as 100 mm/sec within 1.5 m of the pile, but decreases rapidly to 25 mm/sec at 3 m. Dowding (1991) found that densification can extend approximately as far as the piling is long.

Dowding (1991) noted that densification and thus settlement results from a complex combination of vibration amplitude, number of repetitions, soil properties, and position of the water table. "The number of repetitions or pulses depends upon the number of piles, their length, and the number of blows or vibratory cycles required per unit penetration." Even though the magnitude of single or short term vibration is not enough to result in a considerable settlement, long-term accumulative vibration effects may result in settlement causing damage to adjacent buildings and therefore must be investigated in order to establish safe design guidelines. In addition, the ground motion attenuates very rapidly with distance from source. As a consequence, the differential settlement caused by differential ground motion is much more dangerous for building. It is needed to emphasize that all of the above cases concentrated on the settlement of sand. There is no published data describing the response of silty or clayey sandy, residual soils or slightly cemented soils under construction vibrations.

## **V. PROPOSED FIELD VERIFICATION OF VIBRATION INDUCED SETTLEMENT MODEL**

In order to provide field verification of the vibration induced settlement model being developed under the current project, it is proposed that field studies be undertaken at possibly three field sites. At each site it is likely that basic soil classification data, including grain size distribution, water content, specific gravity, unit weight, etc., will already be available from NCDOT exploration. Accordingly, work at each site will involve:

- (1) Performance of laboratory resonant column/torsional shear tests on specimens obtained from Shelby tubes at depths of 0.5m, 1m, 2m, 4m and 6m. These depths correspond to the proposed depths for particle velocity measurements.
- (2) Slabs of concrete, 1.2m x 1.2m by 0.3-m thick will be formed and poured in the field. Each slab will be constructed with a 150-mm diameter hole in the center and lifting lugs on the perimeter. It is intended that two or three of these slabs will be stacked to

produce a ground surface pressure of 15 to 22 Kpa, commensurate with dead-load ground contact pressures in residential and lightly loaded structures, as shown in Fig. 16.

(3) A location for the test footing (conceivably two could be used if site constraints permit) would be determined and settlement points installed at the ground surface and at depths of 1m, 2m, 4m and 6m. After placement of the first slab over the telltails, elastic settlements could be measured due to the application of subsequent loads.

(4) Adjacent to the footing location (approximately 2m away), geophones will be installed at the ground surface, and at depths of 0.5m, 1m, 2m, 4m and 6m. (Fig. 16)

(5) The introduction of construction vibrations will produce ground response. Particle velocity and settlement, as a function of depth below the loaded area, will be recorded via multi-channel data acquisition equipment as a function of time.

Determination of appropriate construction sites for the experiments described as well as construction vibration sources will require input from NCDOT personnel and the NCSU research team, prior to making final decisions.

Prior to the performance of tests on any of the proposed sites, it will be necessary to select geophones with appropriate performance characteristics and natural frequency well below the wave propagation frequency, to calibrate the geophones and data acquisition instruments, and to calibrate the settlement measuring system.

## VI. EXPECTED RESULTS

It is anticipated that the results of field tests proposed herein will produce data necessary to validate the vibration induced settlement model currently under development. In addition to providing a direct comparison between model footing settlement and that predicted by the NCSU analytical procedure, the particle velocity versus depth data and particle velocity versus ground surface position data will provide a basis upon which to evaluate the basic assumptions incorporated into the model. The laboratory resonant column/torsional shear data from undisturbed specimens obtained at each of the sites will also provide validation of the material characterization model developed on North Carolina using over 25 tests from the current work and that reported in the literature.

## VII. SCHEDULE AND BUDGET

It is anticipated that the proposed scope of work can be accomplished in the 12 month period beginning on July 1, 1994 and concluding on June 30, 1995, as shown in Table 1. The estimated budget for the project is \$39,271, as shown in Table 2.

## VIII. REFERENCE

1. Barnaich, John A. (1985), "Vehicle Induced Ground Motion" Proceedings of Conference on Vibration Problems in Geotechnical Engineering, Detroit, MI.
2. Das, Braja M. (1983), "Fundamentals of Soil Dynamics" Elsevier Science Publishing Co., Inc.
3. Dowding, C. H. (1992), "Frequency Based Control of Urban Blasting", Excavation and Support for the Urban Infrastructure: Design and Construction Considerations, T. D. O'Rourke & Hobelman, Eds, Special Geotechnical Publication, ASCE, New York, NY
4. Dowding, C. H. (1991), "Vibration Effects of Pile Driving", Proceedings of 39th Annual Geotechnical Engineering Conference, Continuing Education and Extension, University of Minnesota, Minneapolis, MN.
5. Dowding, C. H. (1991), "Permanent Displacement and Pile Driving Vibrations", Proceedings of 16th Annual Members Conference of the Deep Foundations Institute, V. F. Parola, Ed., Soarta, NJ.
6. Lam, Yoon Cheong (1989), "Laboratory Evaluation of Geophone Performance at High Frequencies", M.S. report for Department of Civil Engineering, University of Texas at Austin.
7. New, Barry M. (1992), "Construction Induced Vibration in Urban Environments", Geotechnical Special Publication No. 33, Excavation and Support for the Urban Infrastructure, New York, NY.
8. Pyke R., Seed, H.B., Clarence K. Chan (1975), "Settlement of Sand Under Mutidirectional Shaking", Journal of the Geotechnical Engineering Division, ASCE, Vol.101, No. GT4, pp 379-398.
9. Seed, H. B., and Silver, M. (1972), "Settlement of Dry Sands During Earthquakes", Journal of Soil Mechanics and Foundation Division, ASCE, Vol. 98 No. SM4, pp 381-397.



10. Silver, M., Seed, H.B. (1971), "Deformation Characteristics of Sand Under Cyclic Loading", Journal of Soil Mechanics and Foundation Division, ASCE Vol. 97 No. SM8, pp 1081-1098.
11. Silver, M., Seed, H.B. (1971), "Volume Change in Sands During Cyclic Loading", Journal of Soil Mechanics and Foundation Division, ASCE Vol. 97 No. SM9, pp 1171-1182.
12. Taniguchi, Ehchi and Sawada, Kenkichi, (1979), "Attenuation with Distance of Traffic-Induced Vibrations", Soils and Foundations, Vol. 19, No.2, Japanese Society of Soil Mechanics and Foundation Engineering.
13. Wiss, John F. (1981), "Construction Vibrations: State-of -the-Art" Journal of the Geotechnical Engineering Division. Feb 1981
14. Woods, Richard D., Jedele, Larry P. (1985), "Energy - Attenuation Relationships From Construction Vibrations" Proceedings of Conference on Vibration Problems in geotechnical Engineering, Detroit, MI.

Table 1 Proposed Project Schedule \*

Months	1	2	3	4	5	6	7	8	9	10	11	12
1. Identification of Test Sites	X											
2. Calibration of Field Instrumentation	X											
3. Laboratory Resonant Column/ Torsional Shear Tests		X			X			X				
4. Perform Pre-test Prediction		X			X			X				
5. Installation of Instrumentation and Construction of Model Footing			X			X			X			
6. Monitor Field Vibrations and Footing Settlements			X	X		X	X		X	X		
7. Interpretation of Field Data			X	X	X	X	X	X	X	X		
8. Evaluation of Model Performance					X			X			X	
9. Draft Final Report											X	
10. Final Report Submission												X

\* Schedule is conceptual in nature, as actual schedule will need to be developed in conjunction with available drilling equipment, construction schedules, etc.

Table 2 Budget  
**CENTER FOR TRANSPORTATION ENGINEERING STUDIES**

**CONSTRUCTION RELATED VIBRATIONS:  
 FIELD VERIFICATION OF VIBRATION INDUCED SETTLEMENT MODEL**

**1994 - 1995 BUDGET AUTHORIZATION**

Project: \_\_\_\_\_

Federal Aid Funding

Budget Line Items	<u>7/1/94-6/30/95</u>
<b>1. PERSONNEL</b>	
1-A Salaries and Wages	
(a) R. H. Borden (PI) Summer, 1 mo.	\$ 6,969
(b) Grad. Res. Asst. Aca. Yr., Half-time	16,100
Summer, 2-1/2 mos. full-time	
(c) Grad. Res. Asst. Summer, 2-1/2 mos.	5,750
full-time	
1-B Fringe Benefits (22.05% of PI)	1,537
1-C Fringe Benefits (0.4% of GRA)	87
1-D Overhead (15% of total personnel)	<u>4,323</u>
<b>TOTAL PERSONNEL BUDGET</b>	<b>\$34,766</b>
<b>2. TRAVEL</b>	
2-A Mileage (1000 miles @ \$0.21/mile)	210
2-B Subsistence	<u>0</u>
<b>TOTAL TRAVEL BUDGET</b>	<b>\$ 210</b>
<b>3. LABORATORY AND FIELD MATERIAL AND GENERAL SUPPLIES</b>	<b>2,500</b>
<b>4. INSTRUMENTATION RENTAL</b>	<b>1,500</b>
<b>5. PRINTING</b>	<b>200</b>
<b>6. COMPUTING COSTS</b>	<b>0</b>
<b>7. COMMUNICATIONS (Telephone and Mail)</b>	<b><u>95</u></b>
<b>TOTAL BUDGET AUTHORIZATION FOR PROJECT (1994 - 1995)</b>	<b>\$39,271</b>

Specimen No.	RC/TS Test Pressure (Kpa)	Water Content (%)	Specific Gravity	Void Ratio	Degree of Saturation (%)
2ST#3	25,50,100	38.9	2.79	1.64	66.2
2ST#5	50,100	14.8	2.60	0.79	48.4
2ST#7	25,50,100	12.6	2.60	0.84	39.1
2ST#8	100,50	15.0	2.60	0.87	45.0
2ST#9	25,50,100	26.2	2.69	1.01	69.8
2ST#10	100	29.6	2.75	1.12	72.9
2ST#11	50	29.6	2.71	1.14	70.6

Site		
2ST#3	2ST#5, 7&8	2ST#9, 10&11
Project: NCDOT 4 6321302	Project: NCDOT 4.6321302	Project: NCDOT 4.6321302
Location: Centennial Parkway, Raleigh	Location: Centennial Parkway, Raleigh	Location: Centennial Parkway, Raleigh
Station: 22+95, 30' LT	Station: 81+00, -L-	Station: 22+95, 31-33' LT
Depth: 3 - 5 ft	Depth: 5 - 9 ft	Depth: 3 - 5 ft
Groundwater: N/A	Groundwater: N/A	Groundwater: N/A
Samples Obtained: 12/17/92	Samples Obtained: 12/17/92	Samples Obtained: 2/15/93

Specimen No.	RC/TS Test Pressure (Kpa)	Water Content (%)	Specific Gravity	Void Ratio	Degree of Saturation (%)
3ST#2	25,50,100	23.91	2.75	1.322	49.72
3ST#2L	25	22.9	2.75	1.244	50.63
3ST#3	50,100	26.82	2.67	1.136	63.04
3ST#4	25,50,100	23.55	2.657	1.167	53.6
3ST#5L	25	18.42	2.694	1.162	42.69
3ST#6	50,100	19.5	2.746	0.931	57.54
3ST#8	25,50,100	22.79	2.72	1.236	50.16
3ST#9	50,100	15.31	2.738	0.859	48.75
3ST#10L	25	34.78	2.759	1.423	67.45
3ST#12	25,50,100,50	35.62	2.723	1.432	67.72
4ST#1	50,100	16.65			

Site		
3ST#1, 2, 3 & 4	3ST#5, 6, 7, 8, 9, 10, 11&12	4ST#1
Project: NCDOT 6.409003T	Project: NCDOT 6.409003T	Project: NCDOT 8.T401704
Location: US 64, Raleigh	Location: US 64, Raleigh	Location: US 64, Raleigh
Station: 4+50, 70-75' LT	Station: 4+00, 60' LT	Station: 143+00, 250' LT
Depth: 4.9 - 9.0 ft	Depth: 2.9 - 8.0 ft	Depth: 13.2 - 15.2 ft
Groundwater: N/A	Groundwater: N/A	Groundwater: N/A
Samples Obtained: 5/28/93	Samples Obtained: 7/2/93	Samples Obtained: 11/22/93

Table 3 Basic soil properties of the specimens analyzed

11-7

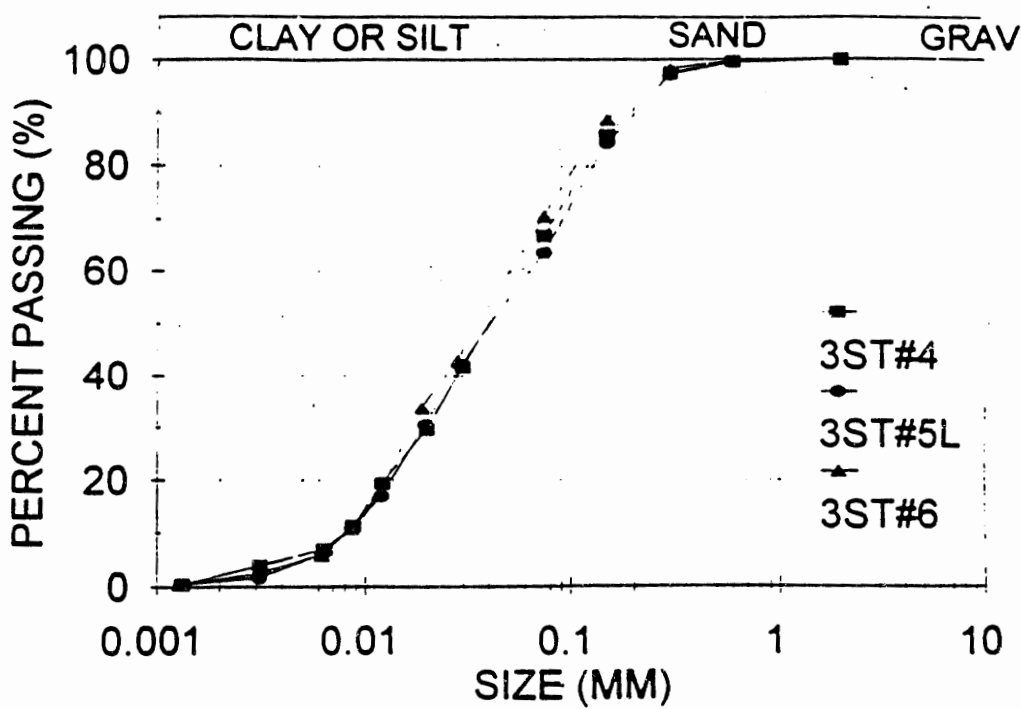
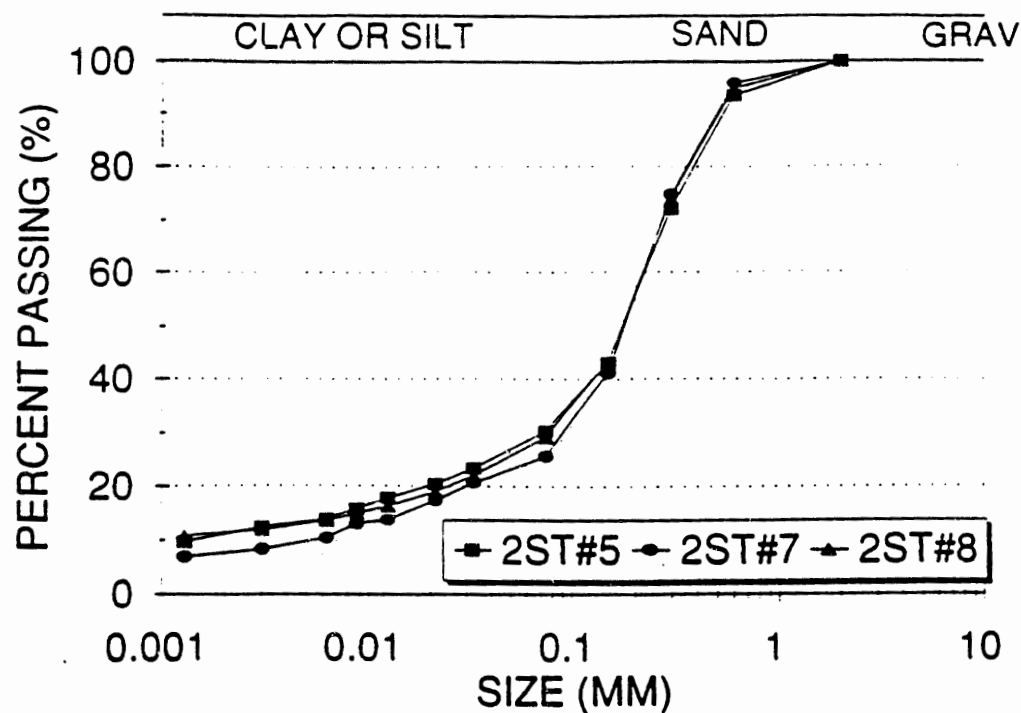


Fig. 1 Grain size distributions of the specimens analyzed

11/29/12

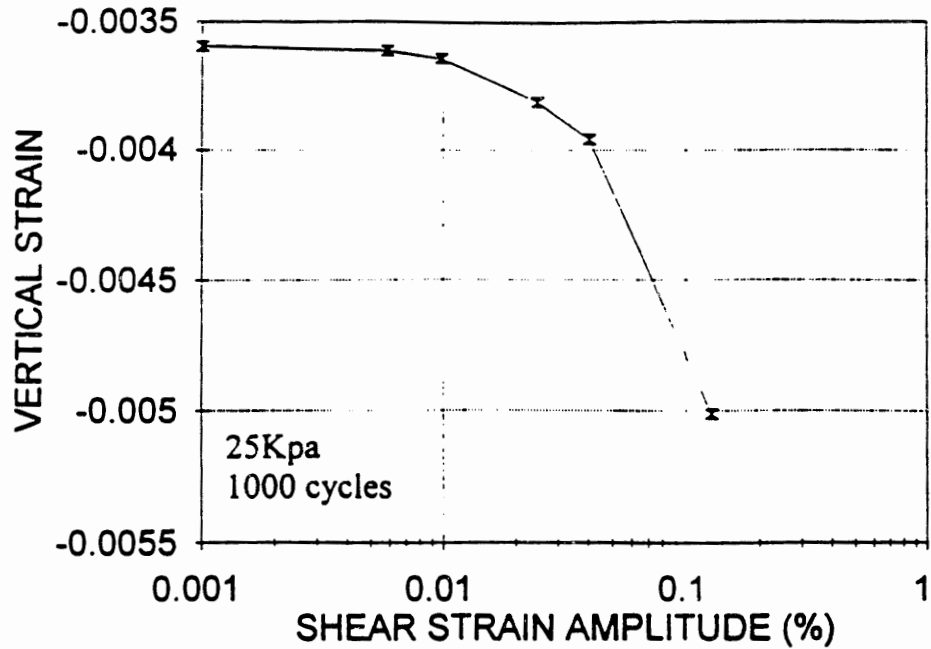


Fig. 2 Vertical strain in 1000 cycles versus shear strain amplitude (3ST#8)  
 There is no settlement when the shear strain amplitude is less than 0.005%.

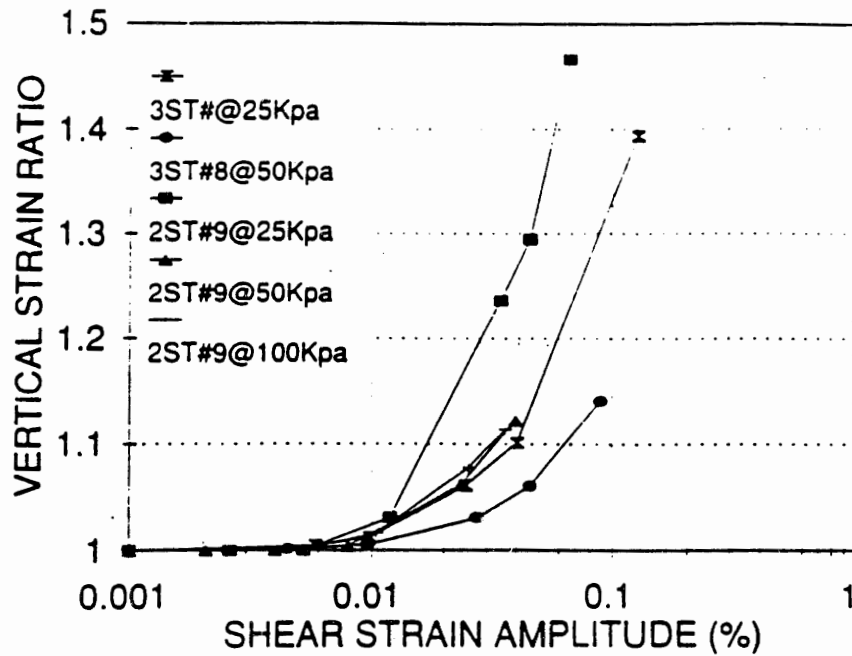


Fig. 3 Vertical strain ratio versus shear strain amplitudes (3ST#8 and 2ST#9)  
 The threshold shear strain amplitude for the dynamic settlement depends on soil type and confining pressure.

Handwritten signature or initials.

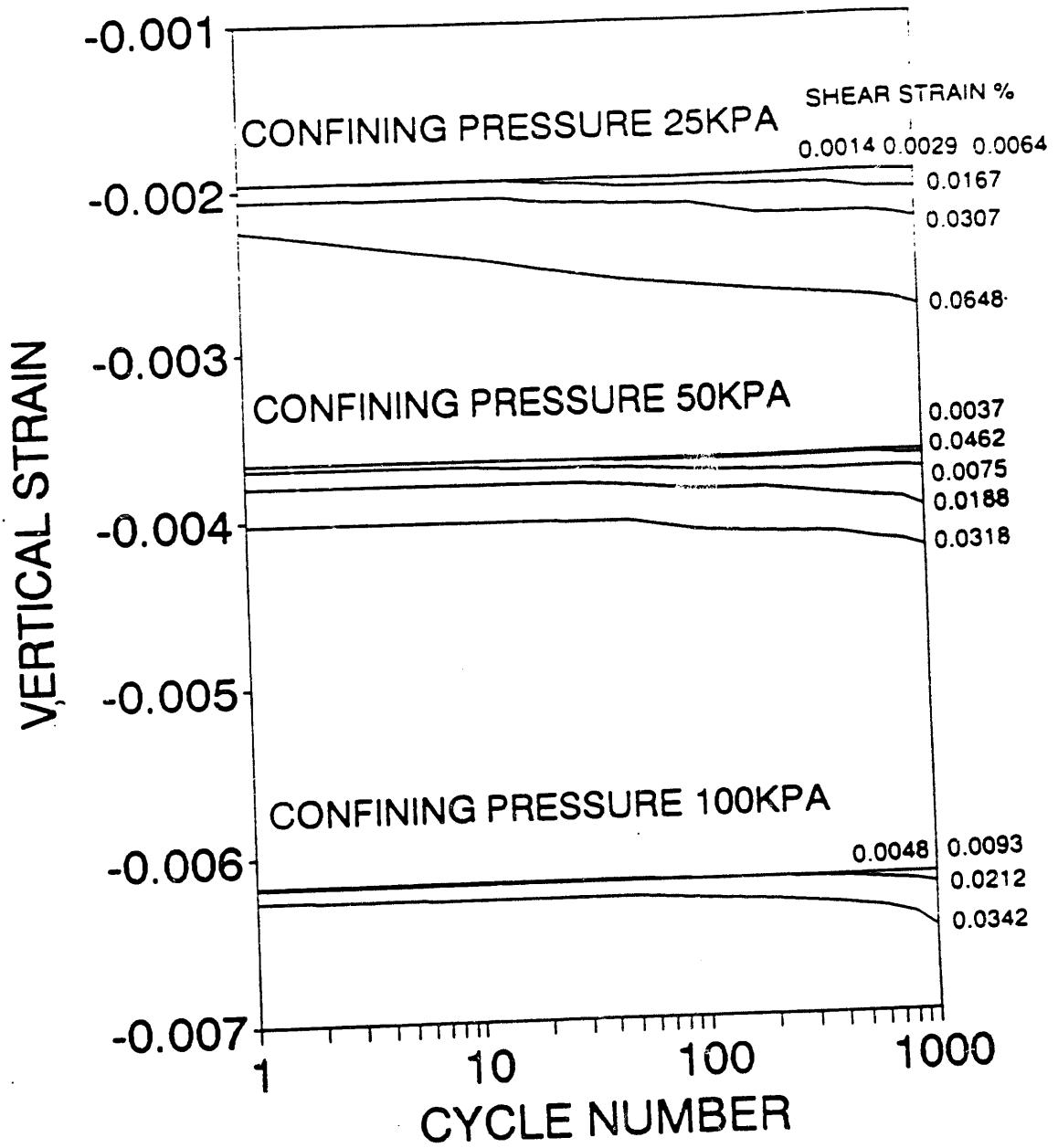


Fig. 4 Vertical strain versus number of cycles for different shear strain amplitudes and confining pressures (2ST#3)

417

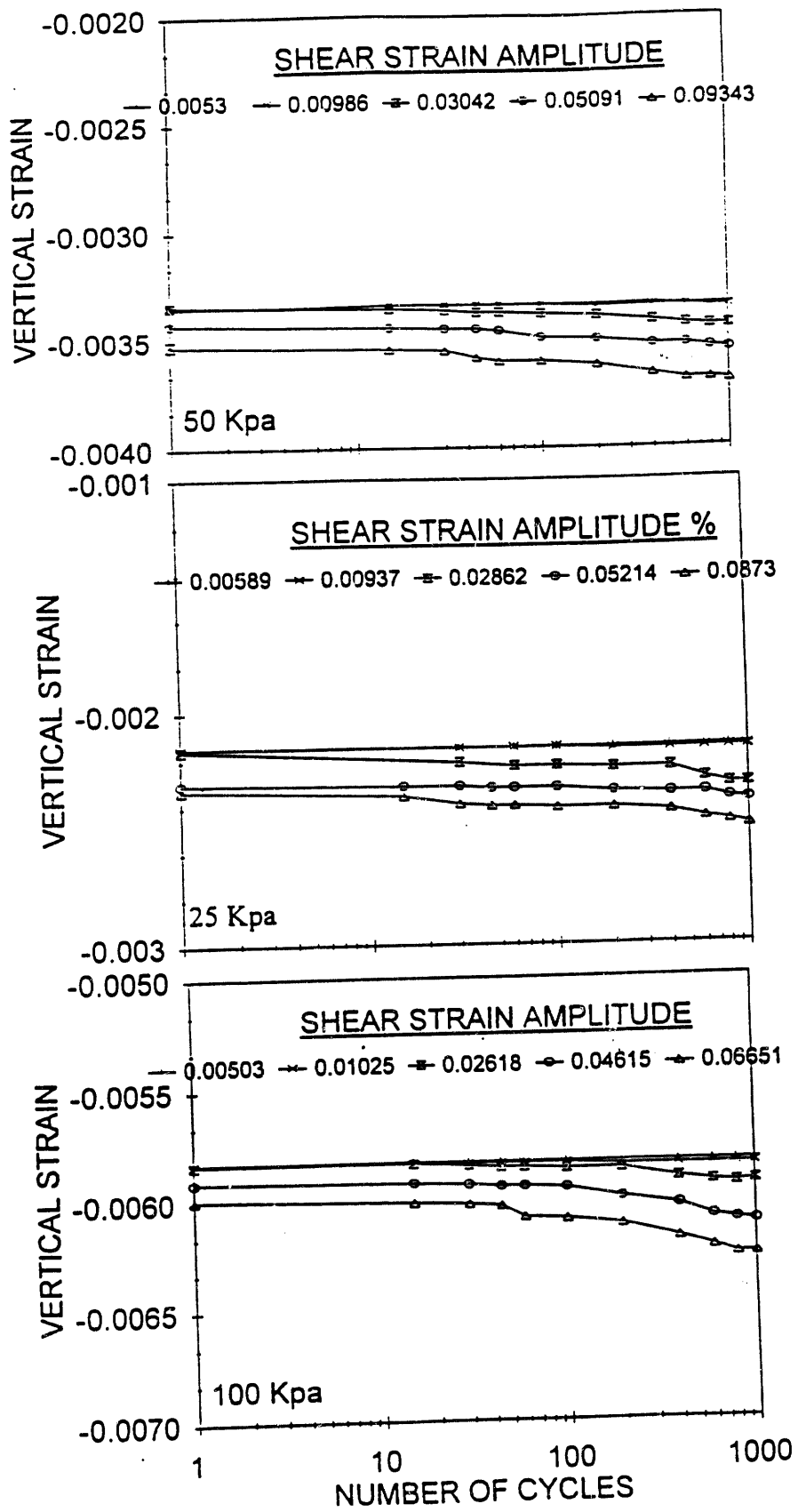


Fig. 5 Vertical strain versus number of cycles at different shear strain amplitude and confining pressure (3ST#12)

Handwritten signature or initials.



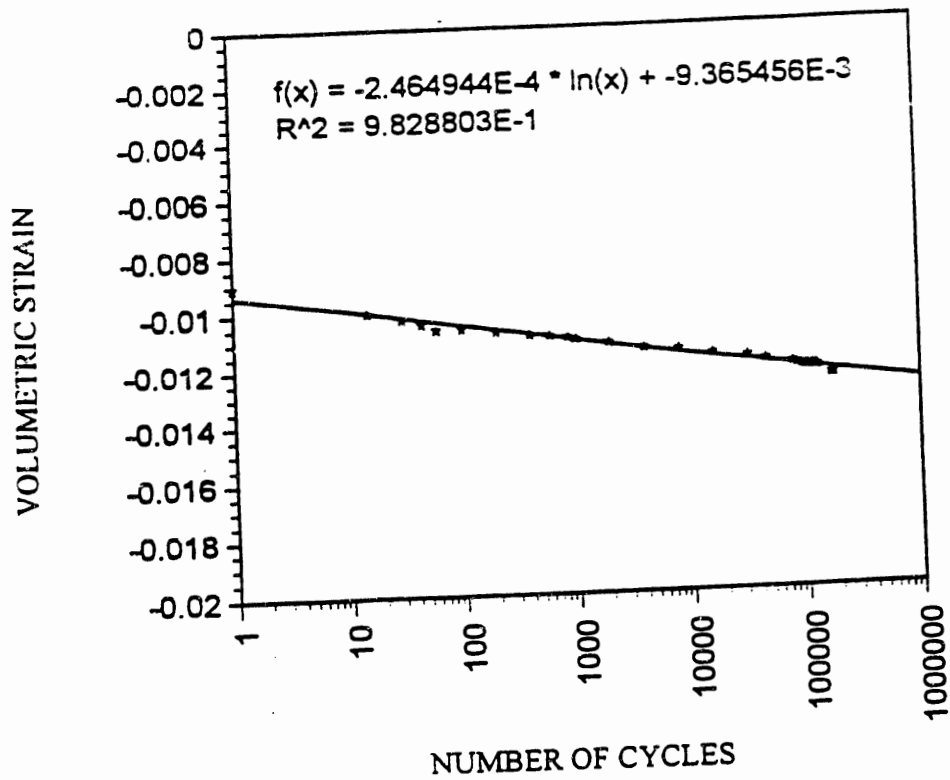


Fig. 6 Volumetric strain versus number of cycles under 25 Kpa confining pressure.

15/1/11



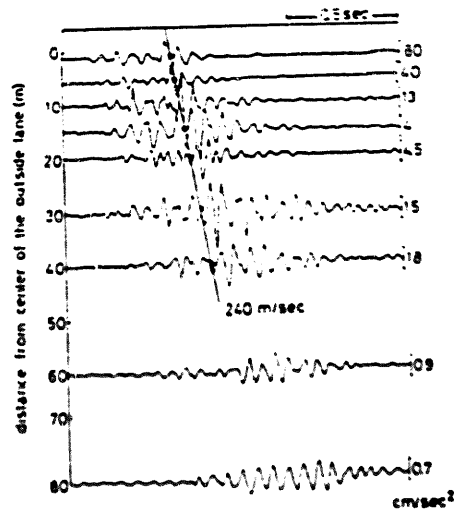


Fig. 8 Wave Motion Record ( 10 Mg truck, speed 60 km/hour, 18-mm block, vertical component) (Taniguchi, 1979)

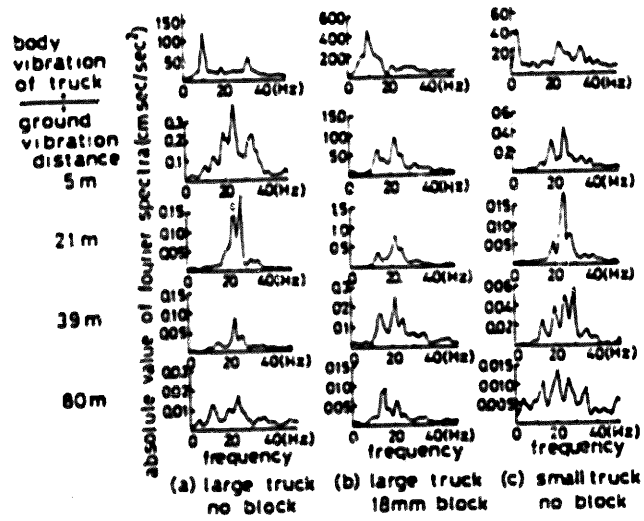


Fig. 9 Fourier Spectra (truck running speed 60 km/hour) (Taniguchi, 1979)

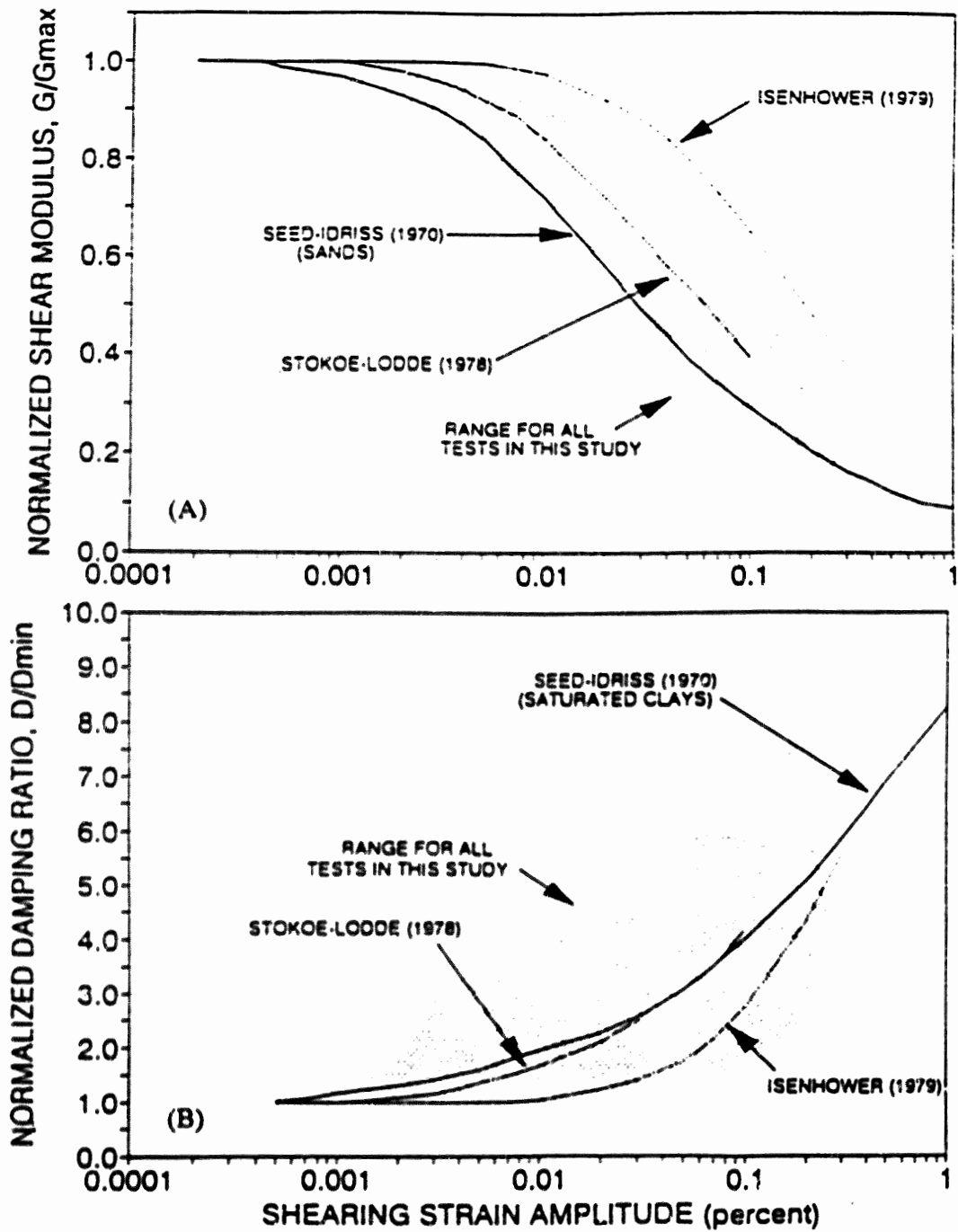


Fig. 10 (A) Normalized shear modulus, and (B) normalized damping ratio as a function of shear strain amplitude for the results of this study versus results from Seed and Idriss (1970), Stokoe and Loddle (1978), and Isenhower (1979).

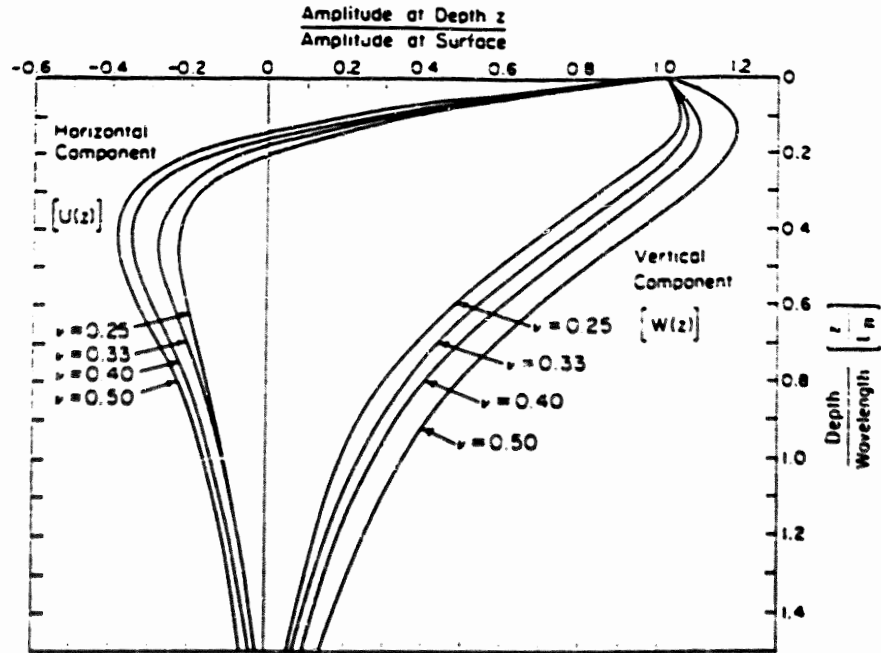


Fig. 11 Amplitude ratio versus dimensionless depth for Rayleigh wave (from Richard, 1968)

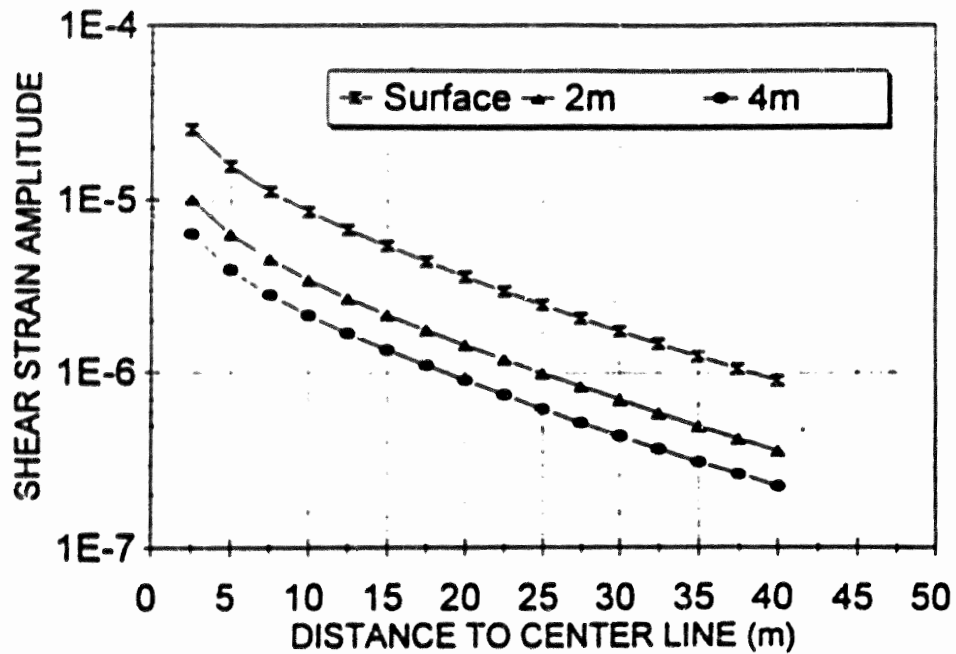


Fig. 12 Wave attenuation profile for a loaded truck (20 Mg) over a 18 mm plank at 60 km/hour (calculated from field test data reported by Taniguchi, 1979)

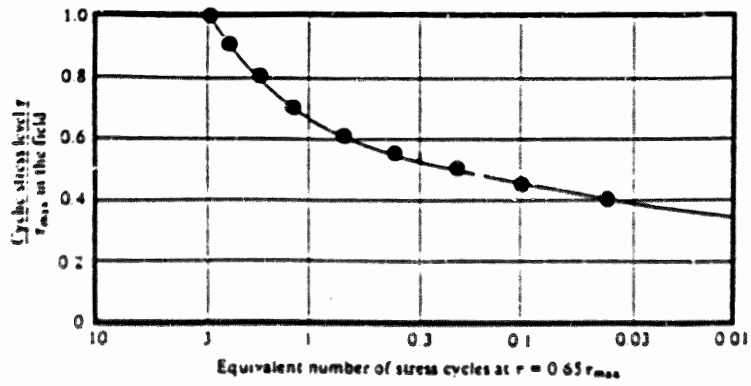


Fig. 13 Plot of  $\tau/\tau_{max}$  vs  $N$  at  $\tau=0.65\tau_{max}$  (Seed, et al. 1975)

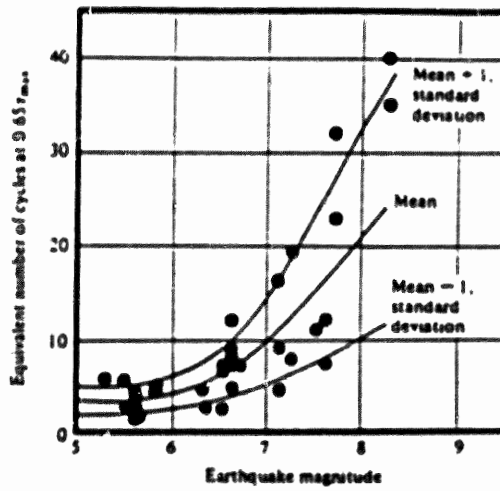


Fig. 14 Equivalent number of uniform stress cycles based on strong component of ground motion (Seed, et al. 1975)

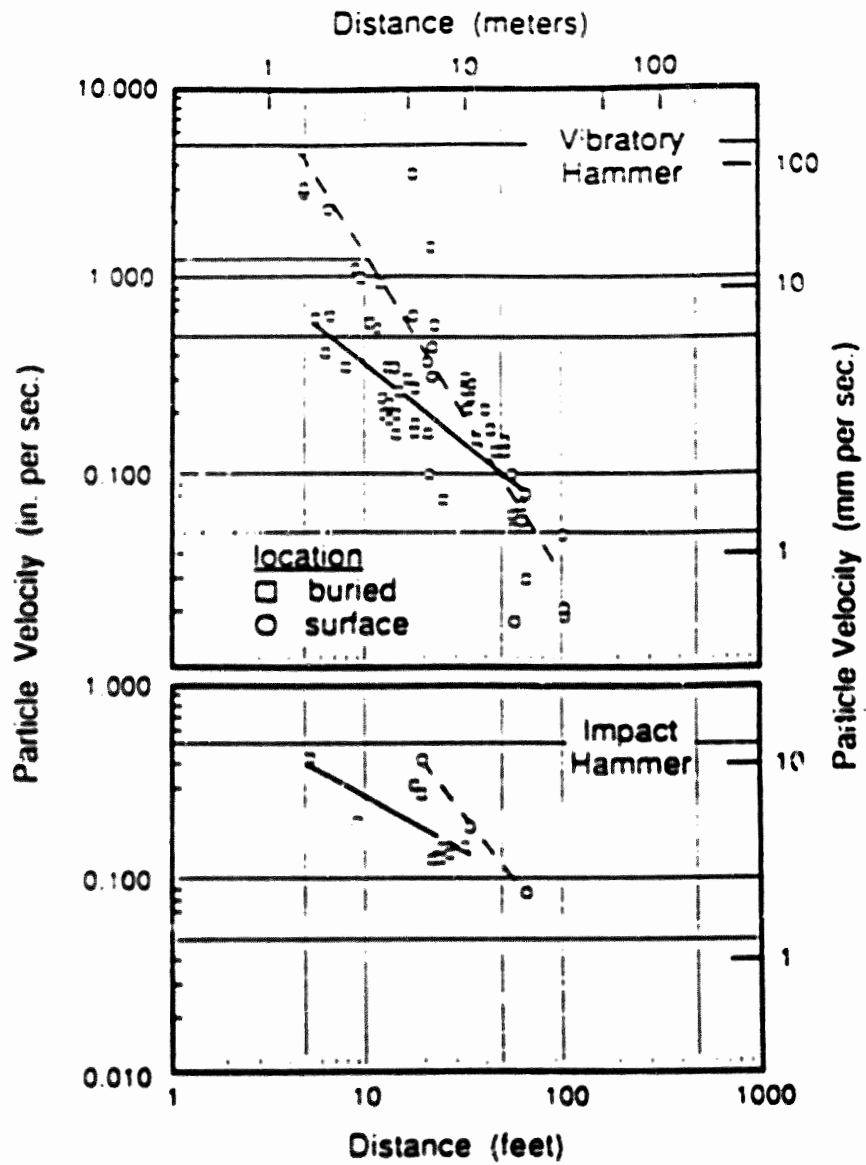


Fig. 15 Comparison of motions measured at the ground surface and on buried pipe line shows that both impact and vibratory motion are lower at depth (Dowding, 1991)

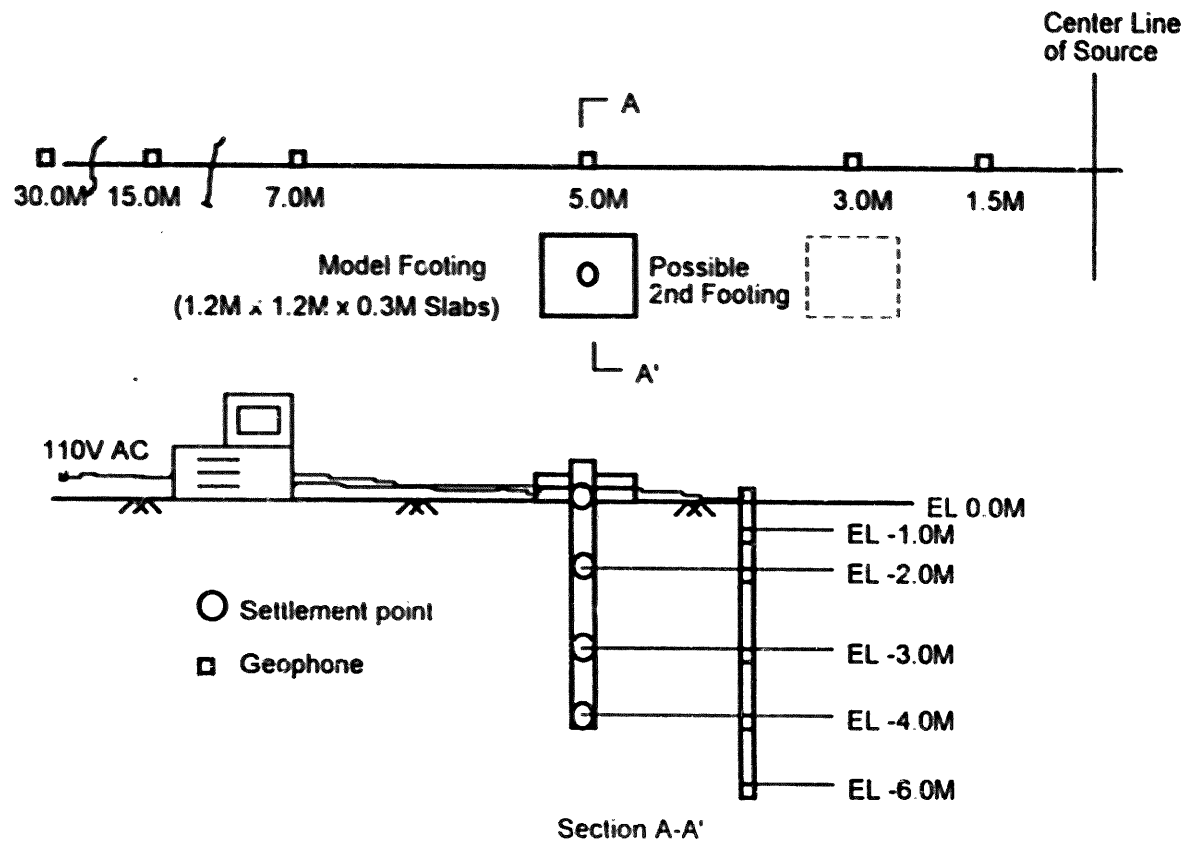


Fig 16 Field verification site design



**CENTER FOR TRANSPORTATION ENGINEERING STUDIES**  
**CONSTRUCTION RELATED VIBRATIONS:**  
**FIELD VERIFICATION OF VIBRATION INDUCED SETTLEMENT MODEL**

**1994-1995 BUDGET AUTHORIZATION**

Project 23241-95 - 5  
 Federal Aid Funding  
7/1/94-6/30/95

**Budget Line Items**

1.	PERSONNEL		
	1-A	Salaries and Wages	\$ 6,969
		a) R. H. Borden (PI)	16,100
		b) Grad. Res. Asst.	
		Summer, 1 mo.	
		Aca. Yr., half-time	
		Summer, 2-1/2 mos.	
		full-time	5,750
		c) Grad. Res. Asst.	
		Summer, 2-1/2 mos.	
		full-time	
			1,537
	1-B	Fringe Benefits (22.05% of PI)	87
	1-C	Fringe Benefits (0.4% of GRA)	
2.	TRAVEL		210
	2-A	Mileage (1000 miles @ \$0.21/mile)	<u>0</u>
	2-B	Subsistence	
			\$ 210
		TOTAL TRAVEL BUDGET	2,500
3.	LABORATORY AND FIELD MATERIAL AND GENERAL SUPPLIES		1,500
4.	INSTRUMENTATION RENTAL		200
5.	PRINTING		0
6.	COMPUTING COSTS		95
7.	COMMUNICATIONS (Telephone and Mail)		<u>5,243</u>
8.	OVERHEAD (15% of total budget)		\$40,191

**TOTAL BUDGET AUTHORIZATION FOR PROJECT 1994-1995**

*[Signature]*  
 Principal Investigator

6/13/94  
 Date

*[Signature]*  
 Director of CTES

6/23/94  
 Date

*[Signature]*  
 Director of TIRE

7-5-94  
 Date

*[Signature]*  
 State Highway Administrator

7-1-94  
 Date

*[Signature]*  
 Federal Highway Administrator

7/1/94  
 Date

*[Signature]*

JUL 5 1994



# North Carolina State University

College of Engineering  
Research Programs

Office of the Dean  
Box 7903  
Raleigh, NC 27695-7903  
(919) 515-2345  
FAX: (919) 515-2463



## MEMORANDUM

TO: Sponsored Programs  
FROM: Emily Tate *Emily Tate*  
SUBJECT: ITRE Contracts  
DATE: July 15, 1994

Please process awards for the attached signed contracts from ITRE as follows:

### Continuing Research Projects

Log 46-0011	Center for Transportation Engineering Studies and Technical Services
Log 46-0016	A Comparative Study of Performance of Different Designs for Flexible Pavements
Log 46-0042	Automation in Applying Reflective Pavement Markers
Log 46-0040	Jointless Bridge Decks
Log 46-0041	Use of Large Stone Asphaltic Concrete in Overlays of Flexible Pavements
Log 46-0043	Capacity and Delay in Major Freeway Construction Zones

Memo to Sponsored Programs  
Page 2  
July 15, 1994

New Research Projects

Log 43-0001	Robotic Systems for Bridge Maintenance
Log 43-0002	Design and Evaluation of Cold-Mix Recycled Pavements
Log 43-0003	Development of Methodology for Testing Analysis and Validation of the Performance Based SHRP Asphalt Binder Specifications for North Carolina Asphalt Cements
Log 43-0004	Statewide Calibration of Asphalt Temperature Study from 1992 and 1993
Log 43-0007	Construction Related Vibration: Field Verification of Vibration Induced Settlement Model
Log 43-0009	Determination of Effects of Fine Content from Crushed Concrete
Log 43-0010	Procedure for Establishing No Passing Zones

If you have any questions concerning these awards, please contact me.

Attachments

Enclosure

**END  
FILMED**

DATE:

**4-9-96**

**NTIS**